POLITEKNIK NEGERI BALI

Journal of Engineering Design and Technology

logic

Vol. 25 No. 2 July 2025

LOGIC

Jurnal Rancang Bangun dan Teknologi

p-ISSN. 1412-114X

e-ISSN. 2580-5649

LOGIC

Jurnal Rancang Bangun dan Teknologi

Journal of Engineering Design and Technology

Gedung P3M, lt.1 Politeknik Negeri Bali, Bukit Jimbaran
PO BOX 1064 Kuta Selatan, Badung, Bali - Indonesia
Telp. (+62)361 701981 Fax. (+62)361 701128
Email: logic@pnb.ac.id

LOGIC JOURNAL TEAM

PREFACE

Logic: Jurnal Rancang Bangun dan Teknologi (Journal of Engineering Design and Technology) is a peer-reviewed research journal aiming at promoting and publishing original high quality research in all disciplines of engineering and applied technology. All research articles submitted to Logic should be original in nature, never previously published in any journal or presented in a conference or undergoing such process across the world. All the submissions will be peer-reviewed by the panel of experts associated with particular field. Submitted papers should meet the internationally accepted criteria and manuscripts should follow the style of the journal for the purpose of both reviewing and editing.

Logic is a journal covering articles in the field of civil and mechanical engineering, design, and technology published 3 times a year in March, July, and November. Language used in this journal is English.

LOGIC. P-ISSN 1412-114X
LOGIC. E-ISSN 2580-5649
Indexing : GOOGLE SCHOLAR, DOAJ, EBSCO OPEN SCIENCE DIRECTORY, SINTA, GARUDA

Best Regard,

LOGIC Editorial Team

TABLE OF CONTENTS

LOGIC
Journal of Engineering Design and Technology
Vol. 25 No. 2 July; p. 78-84

p-ISSN : 1412-114X
e-ISSN : 2580-5649
http://ojs2.pnb.ac.id/index.php/LOGIC

CHARACTERISTICS OF PEAT WATER AND COCONUT WATER MOLECULES IN THE ELECTROLYSIS PROCESS TO PRODUCE HYDROGEN GAS

Imron Musthofa[1)*], Reza Taufiqi Ivana [1)], Hajar Isworo[1)], Adhiela Noer Syaief [1)], Rusuminto Syahyuniar[1)], Muhammad Rezki Fitri Putra[2)]

1) Heavy Equipment Department Technology. Politeknik Negeri Tanah Laut, Kalimantan Selatan
2) Automotive Technology Department. Politeknik Negeri Tanah Laut, Kalimantan Selatan

Corresponding email [1)] : imron@politala.ac.id

Abstract. Hydrogen energy is one of the alternative energy sources that will help overcome the scarcity of fossil fuels. One of the steps to produce hydrogen energy is by the electrolysis method. In this study, the electrolysis process was carried out with a combination of peat water and coconut water. Given that there are extensive areas of peat land and also many coconut trees in South Kalimantan, a combination of peat and coconut water is used for the electrolysis to promote a sustainable process. In addition, the presence of metallic compounds containing Na, Mg, Al, Fe, Ca, K, and others in peat water may also be beneficial in the electrolysis process. These mineral compounds help in accelerating the formation of hydrogen gas by indirectly producing electrolyte properties and acting as a catalyst. From the results of the research conducted, as much as 155 ml of hydrogen was produced. Hydrogen gas production, 0.6 A of electric current, and 7.3 Watts of electric power in the 30-minute electrolysis process were found in sample F (1.5 L of pure coconut water). In the electrolysis process, peat water and coconut water, the voltage used during the electrolysis process was 12 V, which flowed through the cathode and anode.

Keywords: Coconut Water, Electrolysis, Hydrogen, Mineral, Peat Water

1. INTRODUCTION

The electrolysis process is a technique for separating water (H_2O) into hydrogen gas (H_2) and oxygen (O_2) using an electric current through electrodes in an electrolyte liquid medium [1]. This technology is being increasingly developed as an environmentally friendly method for hydrogen production, supporting the transition to renewable energy [2]. Recent studies have shown that the choice of electrolyte fluid greatly affects the efficiency and success of the electrolysis process [3]. Conventional electrolytes such as acid solutions (H_2SO_4) [4], bases (KOH), or salt (NaCl) have high conductivity but hurt the environment [5]. As an alternative, researchers have begun to develop natural electrolyte fluids such as coconut water and peat water [6]. Coconut water has a high mineral content, such as potassium, sodium, and magnesium, which can increase electrical conductivity and support the formation of hydrogen gas bubbles on the cathode [7]. Meanwhile, peat water contains complex organic compounds such as humic and fulvic acids, which can act as current-conducting ions although their efficiency is lower [8]. With additional processing, such as filtration or the addition of external electrolytes, peat water still has the potential to be used as a cheap and abundant local electrolyte in tropical regions. Therefore, the use of coconut water and peat water as electrolysis fluids is part of a green technology innovation to produce clean hydrogen sustainably [9].

Energy has become an essential component of all activities and plays a vital role in the economic development of any country. The demand for energy in all sectors is continuously increasing due to increasing

consumption, population growth, changing lifestyles, and technological advancements [10]. Almost every industry relies on energy, most of which comes from fossil fuels. Renewable energy plays a vital role in addressing all these issues. For this reason, the world and governments are developing new policies, especially in major industrialized countries, seeking to reduce their dependence on fossil fuels [11]. In an effort to boost the share of energy generated from renewable sources, researchers and scientists have proposed "hydrogen" for its advantageous properties. Hydrogen's density is lower than that of air. The gravimetric density of hydrogen is roughly double that of fossil fuels [12]. Hydrogen serves as a fuel that can act as an alternative to conventional fossil fuels like natural gas. Hydrogen is an encouraging energy carrier as it has the ability to store and provide energy in a usable format [13]. The energy density of hydrogen varies from 120 MJ/kg (LHV) to 142 MJ/kg (HHV) [14]. Depending on the method of production, hydrogen exhibits a fairly high power density and low carbon emissions throughout its life cycle. Hydrogen can additionally be mixed with natural gas to satisfy the fuel requirements of different energy systems [15]. However, hydrogen production must be environmentally and economically competitive, which has triggered significant research and development efforts. As an important part of the energy system, fossil fuels not only meet human demand but also cause ecological damage and pollution [16].

The development and use of alternative fuels are becoming increasingly important in global efforts to reduce greenhouse gas emissions [18], improve energy security, and promote environmental sustainability [19]. Although there are still challenges in terms of cost, infrastructure, and technology, progress continues to expand the use of alternative fuels in various economic sectors.

To produce hydrogen gas as a need for self-sufficiency in new renewable energy, a method is needed to produce hydrogen gas in the long term [20], and an electrolyte solution that is environmentally friendly and easy to obtain is needed. Of the many electrolyte fluids that use chemical additives, in the research that we developed, the use of natural electrolyte fluids that are easy to obtain in tropical areas, namely, coconut water, as a substitute for the electrolyte fluid used to produce hydrogen gas. There are several studies in producing hydrogen gas that still use chemical additives, namely research on the productivity of hydrogen gas with a catalyst in the form of KOH, then with a baking soda catalyst, NaCl, and so on.

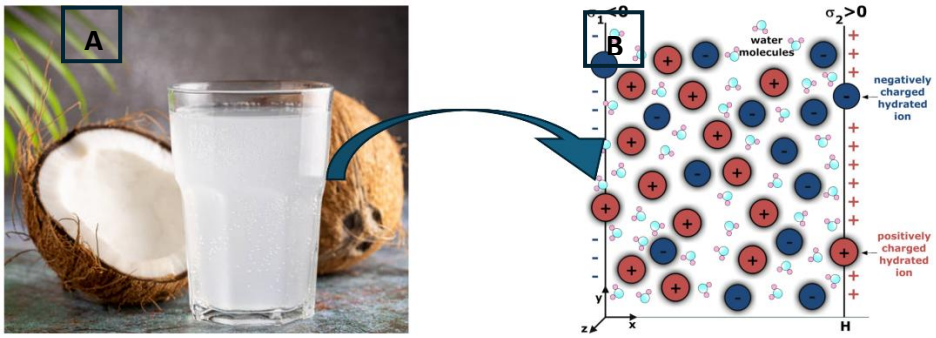

Figure 1. a. Coconut water, b. electrolyte properties of coconut water [21]

Pure coconut water without additional chemicals contains mineral compounds. These mineral compounds consist of Mg, Na, Cl, Al, K, Ca, and so on. These mineral compounds found in coconut water have electrolyte properties; in the world of health, this electrolyte fluid functions to replace sweat fluid after exercise. However, the electrolyte fluid contained in coconut water can function as a conductor of electric current. In addition to coconut water, which is used as an electrolyte medium, in this study, coconut water is also combined with peat water as a combination of electrolyte fluid because peat water found in swamp land has electrolyte properties. In research on swamp water in the laboratory, peat water also has a mineral composition including Mg, K, Na, Ca, Al, Fe, and fulvic acid. Fulvic acid found in peat water has a magnetic field found in the aromatic ring. Aromatic rings that are magnetic can interfere with hydrogen bonds in water, so that they can facilitate the reduction of H_2O bonds.

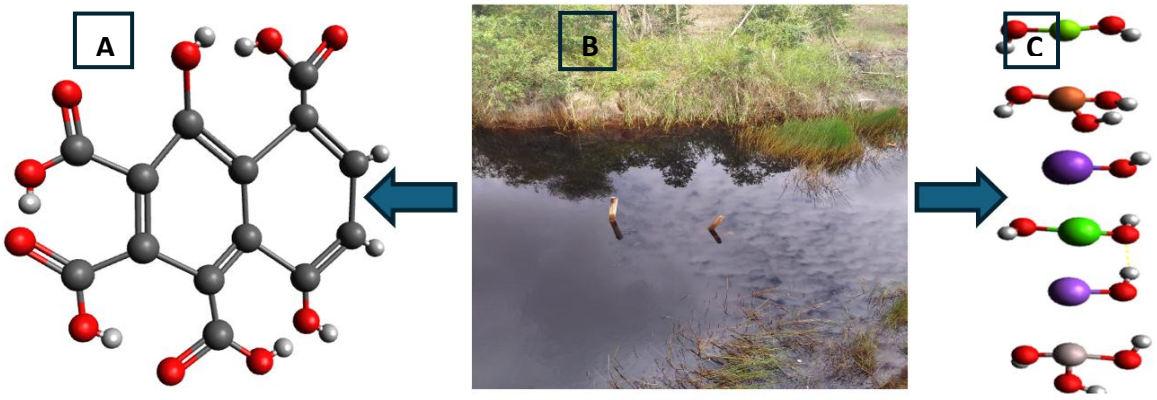

Figure 2. a. Peat fulvic acid structure, b Peat water, c. Peat mineral compounds structure

Thus, the combination of electrolyte fluid from coconut water and electrolyte fluid from peat water can provide a positive impact to obtain maximum results through hydrogen gas production by the electrolysis method. Electrolysis of hydrogen gas requires electrolyte fluid to carry out the separation reaction between hydrogen gas at the cathode and oxygen at the anode through water media that has electrolyte properties. Water that has electrolyte properties can easily reduce H_2O to produce hydrogen gas.

2. METHODS

2.1. Research Variables

Thus, this research process uses an experimental method to obtain hydrogen gas from coconut water and peat water. There are 6 sets of samples listed in Table 2.1. The results of the analysis of the content of peat water with a coconut water catalyst and pure coconut water were obtained by testing at the Balitra Banjarbaru Laboratory, South Kalimantan and are shown in Table 2.2.

Table 2.1 Formulation of Electrolyte Mixture in Experiments

Water Mixture Formulation		
Variable	Peat Water (mL)	Coconut Water (mL)
Sample A	1300	200
Sample B	1200	300
Sample C	1100	400
Sample D	1000	500
Sample E	900	600
Sample F	0	1500

Table 2.2 Results of Peat Water + Coconut Water Composition Analysis

Number	Parameters	Unit	Variable					
			Sample A	Sample B	Sample C	Sample D	Sample E	Sample F
	Code		1	2	3	4	5	6
1	K	m.e L^{-1}	3,49	4,86	5,66	7,17	8,58	24,41
2	Na	m.e L^{-1}	0,94	0,87	0,95	1,11	1,22	4,21
3	Ca	m.e L^{-1}	2,53	2,34	2,50	3,37	3,82	12,93
4	Mg	m.e L^{-1}	2,64	2,01	2,53	3,21	3,50	6,91
5	Fe	m.e L^{-1}	0,06	0,06	0,07	0,04	0,09	0,02
6	Al	m.e L^{-1}	0,06	0,08	0,07	0,04	0,06	0,06

The results of laboratory tests on the sample solution between peat water and coconut water showed that the higher the concentration of coconut water, the higher the overall mineral content produced at the solution concentration, such as K, Na, Ca, and Mg found in sample F compared to other sample concentrations. However, the values of Fe and Al are still relatively the same, and the smallest value is in Fe. Overall, from the results of laboratory tests, sample F can be categorized as the best electrolyte for the electrolysis process and can contribute the most to producing hydrogen gas through the electrolysis process.

Table 2.1 shows the composition of the peat water and coconut water mixture used as the electrolyte variable in the electrolysis process for hydrogen gas production. In each sample, the total volume of the

electrolyte fluid was maintained at 1,500 mL, but with different mixture proportions between peat water and coconut water. By increasing the proportion of coconut water, it is expected to increase the conductivity of the solution and the efficiency of hydrogen production. Sample F (100% coconut water) likely demonstrated the highest performance in terms of gas productivity and energy efficiency.

2.2. Research Mechanism

In the research process using water electrolysis, the main thing to do is to determine the concentration of mineral content in coconut water and peat samples. This is done in order to find out the variables used to collect data accurately. After knowing the concentration of mineral content, then one by one the samples are electrolyzed by flowing 12 V DC electric current through the cathode and anode electrodes. From the electrolysis process, hydrogen and oxygen gases are obtained, which are collected in the tube. The method for measuring the volume of hydrogen gas is by observing the decrease in the water level in the tube, which has previously been marked with a measuring instrument in the form of milliliters. The decrease in water pressure is caused by the pressure of the hydrogen gas produced. The amount of water reduction is interpreted as the amount of hydrogen gas produced in mL units. In addition to measuring hydrogen gas productivity, this study also measured the pH of the solution before and after the electrolysis process and changes in current and power during the electrolysis process.

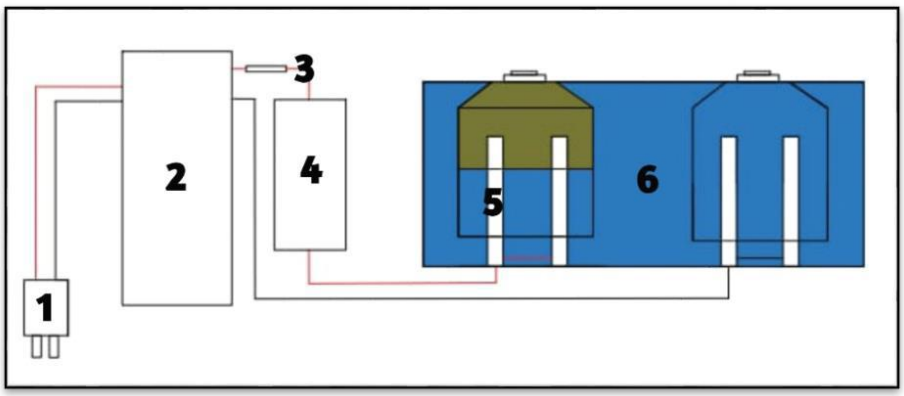

1. Socket
2. Power supply
3. Wiring
4. Multimeter
5. Electrode
6. Reactor

Figure 3. Research installations

3. RESULTS AND DISCUSSION

3.1. Hydrogen Production

The results of hydrogen gas production tests from six different samples, tested at different times, are as follows:

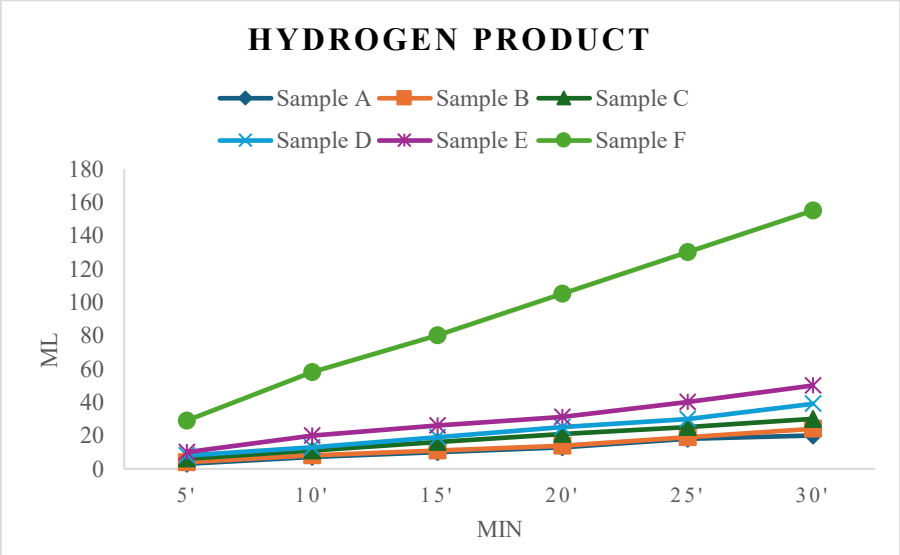

Figure 4. Hydrogen gas production results

Figure 4 shows the highest hydrogen gas production results in sample F with 155 ml of hydrogen gas production in a 30-minute electrolysis process, compared to sample A, which produces 20 ml of hydrogen gas; sample B, which produces 24 ml of hydrogen gas; sample C, which produces 30 ml of hydrogen gas; sample D, which produces 39 ml of hydrogen gas; and sample E, which produces 50 ml of hydrogen gas using peat water with the addition of a coconut water catalyst. The difference in the ability of pure coconut water with peat water with the addition of a coconut water catalyst to produce hydrogen gas is influenced by the electrolyte content in it, thus affecting the productivity of hydrogen gas. Pure coconut water naturally contains potassium, sodium, chloride, magnesium, and so on, while peat water, with the addition of a catalyst, contains lower electrolytes compared to pure coconut water. When coconut water is electrolyzed, the dissolved ions increase the electrical conductivity, allowing electric current to flow more easily [22]. This results in a more efficient electrolysis process where more ions can react and produce more hydrogen and oxygen gas. In contrast, samples A, B, C, D, and E, containing peat water with the addition of a coconut water catalyst, have lower electrolyte content than sample F, which is only pure coconut water, so the electrical conductivity is lower and the electrolysis process is less efficient, resulting in less hydrogen gas. Therefore, pure coconut water tends to produce more hydrogen gas because of its ability to carry an electric current better due to its higher electrolyte content [23].

3.2. Electric Current

The flowing current varies in each sample. In sample A, the flowing current is 0.11 A after electrolysis for 30 minutes; in sample B, the flowing current is 0.14 A after electrolysis for 30 minutes; in sample C, the flowing current is 0.21 A after electrolysis for 30 minutes; in sample D, the flowing current is 0.23 A after electrolysis for 30 minutes; in sample E, the flowing current is 0.25 A after electrolysis for 30 minutes; and in sample F, the flowing current is 0.60 A after electrolysis for 30 minutes. This difference is due to the content of electrolyte concentration in it. Sample F only uses pure coconut water without any mixture, while the other samples use a mixture of peat water and coconut water. It can be seen in the graph above that the more coconut water is mixed, the higher the current flows. This is due to the high concentration of natural electrolytes in coconut water, such as potassium, sodium, and chloride [24]. These electrolytes can increase the conductivity of the solution, allowing electric current to flow more easily through the solution. This makes coconut water usable as a natural catalyst or directly electrolyzable to produce hydrogen gas. During electrolysis, the current flowing for 5 minutes, 10 minutes, 15 minutes, 20 minutes, 25 minutes, and 30 minutes varies due to the influence of the solution reaction.

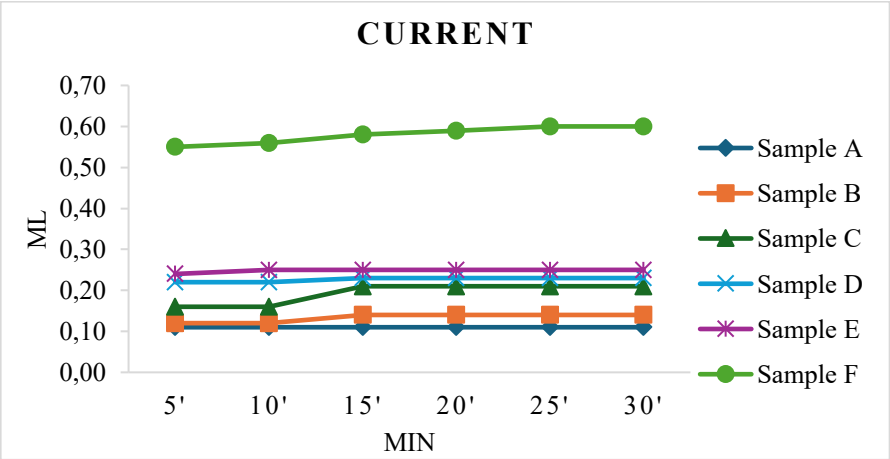

Figure 5. Comparison of electrolysis currents

3.2. Power

Figure 4.2 It can be seen that the power produced varies in each sample. In sample A, the power produced is 1.3 watts after electrolysis for 30 minutes; in sample B, the power produced is 1.7 watts after electrolysis for 30 minutes; in sample C, the power produced is 2.5 watts after electrolysis for 30 minutes; in sample D, the power produced is 2.8 watts after electrolysis for 30 minutes; in sample E, the power produced is 3.0 watts after electrolysis for 30 minutes; and in sample F, the power produced is 7.3 watts after electrolysis for 30 minutes. This difference is due to the content of electrolyte concentration in it. Sample F only uses pure coconut water without any mixture, while the other samples use a mixture of peat water and coconut water. It can be seen in the graph above that the more coconut water is mixed, the higher the power produced. This is due to the high concentration of natural electrolytes in coconut water, such as potassium, sodium, and chloride. These electrolytes can increase the conductivity of the solution, allowing electric current to flow more easily through the solution [25]. This makes

coconut water usable as a natural catalyst or directly electrolyzable to produce hydrogen gas. During electrolysis, the power generated from 5 minutes, 10 minutes, 15 minutes, 20 minutes, 25 minutes, and 30 minutes varies due to the influence of the solution reaction.

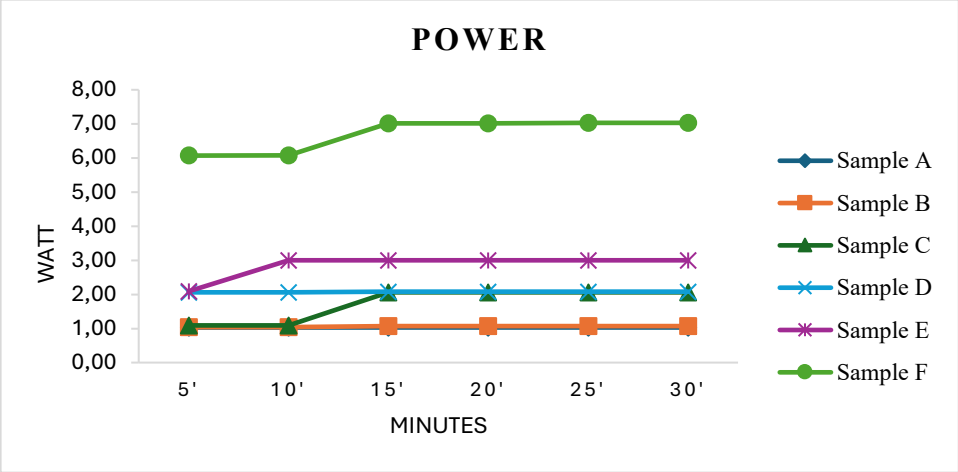

Figure 6. Comparison of electrolysis process power

4. CONCLUSION

Although the electrolysis results showed that coconut water performed better in terms of current, voltage, and gas productivity, the use of peat water still produced measurable electrolysis results. This evidence indicates that peat water has limited electrolyte potential. The organic and mineral content of peat water allows for electrochemical reactions, but not as efficiently as coconut water. Therefore, peat water has the potential to be used as an alternative, inexpensive, and abundant local electrolyte solution. However, further optimization, such as the addition of external electrolytes or pretreatment, is needed to increase its efficiency in the electrolysis process. Therefore, coconut water plays a significant role as an electrolyte supplement to produce hydrogen gas in the electrolysis process when combined with peat water.

5. REFERENCES

[1] K. Scoot, "Introduction to electrolysis, electrolysers and hydrogen production," Electrochem. Methods Hydrog. Prod., no. 25, pp. 1–27, 2019, [Online]. Available: www.rsc.org

[2] C. Acar, Y. Bicer, M. E. Demir, and I. Dincer, "Transition to a new era with light-based hydrogen production for a carbon-free society: An overview," Int. J. Hydrogen Energy, vol. 44, no. 47, pp. 25347–25364, 2019, doi: 10.1016/j.ijhydene.2019.08.010.

[3] A. O. O. Bahdad, Y. Li, and T. Van Nguyen, " Characterization of the electrochemical behavior of $MnSO_4$ with and without $TiOSO_4$ in H_2SO_4 Solution ," J. Electrochem. Soc., vol. 168, no. 7, p. 070524, 2021, doi: 10.1149/1945-7111/ac0e4e.

[4] A. Bazarah, E. H. Majlan, T. Husaini, A. M. Zainoodin, I. Alshami, J. Goh, and M. S. Masdar, Factors influencing the performance and durability of polymer electrolyte membrane water electrolyzer: A review, International Journal of Hydrogen Energy , vol. 47, pp. 35976-35989, 2022 https://doi.org/10.1016/j.ijhydene.2022.08.180.

[5] T. P. Shannon, S. J. Ahler, A. Mathers, C. D. Ziter, and H. A. Dugan, "Road salt impact on soil electrical conductivity across an urban landscape," J. Urban Ecol., vol. 6, no. 1, pp. 1–8, 2020, doi: 10.1093/jue/juaa006.

[6] M. S. El Halimi, A. Zanelli, F. Soavi, and T. Chafik, "Building towards Supercapacitors with Safer Electrolytes and Carbon Electrodes from Natural Resources," World, vol. 4, no. 3, pp. 431–449, 2023, doi: 10.3390/world4030027.

[7] H. H. Halim et al., "Ergogenic attributes of young and mature coconut (Cocos nucifera l.) water based on physical properties, sugars and electrolytes contents," Int. J. Food Prop., vol. 21, no. 1, pp. 2378–2389, 2018, doi: 10.1080/10942912.2018.1522329.

[8] D. Wu, Y. Lu, L. Ma, J. Cheng, and X. Wang, "Preparation and molecular structural characterization of fulvic acid extracted from different types of peat," Molecules, vol. 28, no. 19, 2023, doi: 10.3390/molecules28196780.

[9] A. Franco and C. Giovannini, "Recent and future advances in water electrolysis for green hydrogen generation: critical analysis and perspectives," Sustain., vol. 15, no. 24, 2023, doi: 10.3390/su152416917.

[10] N. Abas, A. Kalair, and N. Khan, "Review of fossil fuels and future energy technologies," Futures, vol. 69, pp. 31–49, 2015, doi: 10.1016/j.futures.2015.03.003.

[11] A. Månberger, "Reduced use of fossil fuels can reduce supply of critical resources," Biophys. Econ. Sustain., vol. 6, no. 2, pp. 1–15, 2021, doi: 10.1007/s41247-021-00088-5.
[12] C. J. Winter, "Hydrogen energy - abundant, efficient, clean: a debate over the energy-system-of-change," Int. J. Hydrogen Energy, vol. 34, no. 14 SUPPL. 1, pp. 1–52, 2009, doi: 10.1016/j.ijhydene.2009.05.063.
[13] M. H. McCay and S. Shafiee, "Hydrogen: an energy carrier," Futur. Energy Improv. Sustain. Clean Options Our Planet, pp. 475–493, 2020, doi: 10.1016/B978-0-08-102886-5.00022-0.
[14] A. G. Olabi et al., "Large-vscale hydrogen production and storage technologies: Current status and future directions," Int. J. Hydrogen Energy, vol. 46, no. 45, pp. 23498–23528, 2021, doi: 10.1016/j.ijhydene.2020.10.110.
[15] M. Yue, H. Lambert, E. Pahon, R. Roche, S. Jemei, and D. Hissel, "Hydrogen energy systems: A critical review of technologies, applications, trends and challenges," Renew. Sustain. Energy Rev., vol. 146, no. June 2020, p. 111180, 2021, doi: 10.1016/j.rser.2021.111180.
[16] U. Politechnica, D. Marche, and F. O. F. Engineering, "Master ' S Degree in Environmental Engineering Analysis of Performance and Features of Hydrogen," 2022.
[17] O. Litvak and S. Litvak, "Some aspects of reducing greenhouse gas emissions by using biofuels," J. Ecol. Eng., vol. 21, no. 8, pp. 198–206, 2020, doi: 10.12911/22998993/126967.
[18] J. Wang and W. Azam, "Geoscience frontiers natural resource scarcity , fossil fuel energy consumption , and total greenhouse gas emissions in top emitting countries," Geosci. Front., vol. 15, no. 2, p. 101757, 2024, doi: 10.1016/j.gsf.2023.101757.
[19] L. Proskuryakova, "Updating energy security and environmental policy: Energy security theories revisited," J. Environ. Manage., vol. 223, no. May, pp. 203–214, 2018, doi: 10.1016/j.jenvman.2018.06.016.
[20] S. K. Dash, S. Chakraborty, and D. Elangovan, "A brief review of hydrogen production methods and their challenges," Energies, vol. 16, no. 3, 2023, doi: 10.3390/en16031141.
[21] E. Gongadze et al., "Ions and water molecules in an electrolyte solution in contact with charged and dipolar surfaces," Electrochim. Acta, vol. 126, pp. 42–60, 2014, doi: 10.1016/j.electacta.2013.07.147.
[22] C. Averion, F. C. Mendoza, F. Joe Ortiz, and F. J. Balinado, "Development of an electrolytic cell using coconut (Cocos Nucifera) water as an electrolyte for perimeter lighting," J. Eng. Comput. Stud., vol. 4, no. 2, pp. 28–33, 2019.
[23] S. P. G. G. Tista, I. G. N. N. Santhiarsa, M. R. Murti, P. W. Sunu, and W. Wardoyo, "Utilization of coconut shell activated carbon to generate electrical energy using sodium chloride electrolyte," EUREKA, Phys. Eng., vol. 2024-July, no. 4, pp. 28–39, 2024, doi: 10.21303/2461-4262.2024.003281.
[24] A. C. Kannangara, V. Chandrajith, and K. Ranaweera, "Comparative analysis of coconut water in four different maturity stages" J. Pharmacogn. Phytochem., vol. 7, no. 3, pp. 1814–1817, 2018.
[25] M. Li, C. Wang, Z. Chen, K. Xu, and J. Lu, "New concepts in electrolytes," Chem. Rev., vol. 120, no. 14, pp. 6783–6819, 2020, doi: 10.1021/acs.chemrev.9b00531.

LOGIC
Journal of Engineering Design and Technology
Vol. 25 No. 2 July 2025 ; p. 85-92

p-ISSN : 1412-114X
e-ISSN : 2580-5649
http://ojs2.pnb.ac.id/index.php/LOGIC

THE EFFECT OF VOLUME FRACTION VARIATION ON THE MECHANICAL PROPERTIES OF EPOXY-BASED SUGARCANE FIBER COMPOSITES

Anisa Fitri [1)*], Ahmad Andryan Prakoso[1)], Bayu Prasetya[1)], Mhd. Yasin Siregar[1)], Wahyu Solafide Sipahutar[1)]

1) Department of Materials Engineering, Faculty of Industrial Technology, Institut Teknologi Sumatera

Corresponding email : anisa.fitri@mt.itera.ac.id

Abstract. The use of natural fibers as reinforcement in composite materials offers an environmentally friendly alternative to synthetic fibers. Among them, sugarcane fiber (bagasse), an agro-industrial byproduct rich in cellulose, hemicellulose, and lignin, holds considerable potential but remains underutilized. This study aims to evaluate the effect of varying sugarcane fiber volume fractions (50%, 60%, and 70%) on the mechanical properties of epoxy resin-based composites. The composites were fabricated using the hand lay-up method, followed by mechanical testing including tensile tests (ASTM D3039) and bending tests (ASTM D790). The results showed that the highest tensile strength of 26.43 MPa was achieved by the E70 sample, while the E50 sample exhibited the highest bending strength at 142.53 MPa. Fractographic analysis revealed that structural defects such as voids, fiber pull-out, and debonding significantly influenced the mechanical performance of the composites. While fiber volume fraction has a notable impact on tensile and bending strengths, the relationship is not strictly linear due to variations in fiber-resin distribution and interfacial bonding quality. These findings suggest that sugarcane fiber-based epoxy composites, particularly with a 50% volume fraction, have strong potential for application in lightweight structural components, furniture panels, or automotive interior parts. Future research may focus on improving interfacial bonding through chemical treatments or hybridization with other natural fibers to further enhance performance

Keywords:Bending Composite, Epoxy, Sugarcane, Fiber

1. INTRODUCTION

The advancement of material technology in recent decades has increasingly driven the search for materials that not only exhibit high mechanical performance but are also environmentally friendly and sustainable. One promising innovation is the development of natural fiber-reinforced composites, which are considered an ideal alternative to synthetic fibers that are difficult to decompose and potentially harmful to the environment. Previous studies by Liu et al. [1] and Ismail et al. [2],[3] demonstrated that sugarcane fiber composites with epoxy matrices exhibit promising mechanical properties, but optimal fiber content and distribution remain a challenge. Moreover, research on the influence of high-volume fractions (above 50%) is still limited, particularly regarding their behavior under combined tensile and bending loads. This study aims to fill this gap by systematically evaluating the effect of 50%, 60%, and 70% fiber volume fractions on the mechanical response of the composites. The use of natural fibers in composites not only reduces reliance on synthetic materials but also promotes the utilization of organic waste from the agricultural and industrial sectors [4], [5].

Among the various types of natural fibers, sugarcane bagasse, an agro-industrial byproduct of sugarcane processing, holds significant potential yet remains underutilized. This fiber contains cellulose, hemicellulose, and lignin, which are the primary constituents responsible for its inherent strength [6],[7]. Sugarcane fiber is lightweight, biodegradable, abundantly available, and cost-effective, making it a promising candidate as a reinforcement material in environmentally friendly composites.

In composite structures, the fiber acts as the reinforcement that contributes to mechanical strength, while

the resin matrix binds the fibers together and distributes the applied loads. In this study, epoxy resin was selected as the matrix due to its excellent adhesion, high mechanical strength, and resistance to environmental and chemical degradation. The combination of sugarcane fiber and epoxy resin is expected to yield composite materials with competitive mechanical properties [8],[9].

However, one of the main challenges in fabricating natural fiber composites lies in determining the optimal fiber volume fraction. A fiber ratio that is too low may result in insufficient mechanical strength, whereas an excessively high fiber content can lead to structural defects such as voids, debonding, and fiber pull-out due to inadequate resin impregnation[10]. These defects can significantly compromise the quality and durability of the composite under tensile and bending loads.

To address these challenges, this study investigates the effects of varying sugarcane fiber volume fractions (50%, 60%, and 70%) on the mechanical properties of epoxy-based composites. The research focuses on evaluating tensile and bending strength and includes macroscopic analyses of fracture surfaces to better understand the failure mechanisms involved.

2. METHODS

This study was conducted to fabricate a composite material using natural fibers derived from sugarcane bagasse, with fiber volume fractions of 50%, 60%, and 70%. The process began with fiber preparation, where dry sugarcane fibers were combed using a wire brush to remove any residual cork or surface impurities. The fibers were then thoroughly washed and sun-dried until completely dry.

Subsequently, the fibers underwent an alkali treatment by soaking them in a 5% sodium hydroxide (NaOH) solution for 2 hours [11]. This surface modification process aims to remove components such as hemicellulose, lignin, and pectin, which are less effective in promoting interfacial bonding. Reducing these components increases the cellulose content, thereby enhancing fiber stiffness and strength, while also improving surface roughness to facilitate better wetting and adhesion with the resin. After soaking, the fibers were rinsed with water until a neutral pH was achieved.

The composite fabrication employed the hand lay-up method, which is suitable for producing simple components with smooth mold surfaces [12]. The mold was first coated with wax, and a layer of waxed Teflon paper was placed at the base. A mixture of epoxy resin and hardener was then poured slowly into the mold to fill it halfway. Sugarcane fibers were placed onto the resin layer, followed by another layer of resin to fully encapsulate the fibers. The top was covered with another sheet of waxed Teflon paper, and pressure was applied to the mold to eliminate air entrapment and ensure proper impregnation of the fibers.

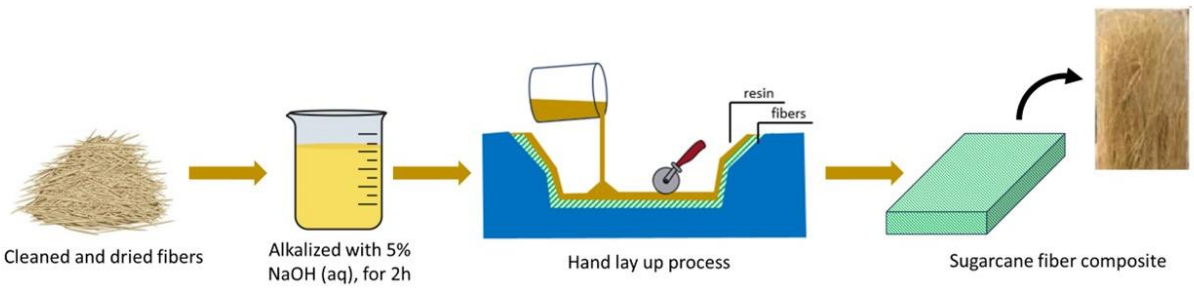

Figure 1. Research procedure for producing sugarcane fiber composites using the hand lay-up method.

Tensile and bending tests were conducted following ASTM D3039 and ASTM D790 standards, respectively [13]. The tensile test was performed to determine key mechanical properties of the composite, including tensile strength, elongation, and modulus of elasticity. The test specimens measured 175 mm × 25 mm × 3 mm and were tested using a Universal Testing Machine (UTM) at a crosshead speed of 2 mm/min (0.05 in/min). The testing was carried out in the Materials Engineering Laboratory at the Sumatra Institute of Technology (ITERA).

The results included the calculated values of maximum tensile strength (σ), strain (ε), and modulus of elasticity (E). In addition, a bending test is also carried out to measure the strength of the material due to loading and elasticity of the sample. The bending test was carried out using a Universal Testing Machine (Zwick/Roell Z250, capacity 250 kN), this test uses a specimen measuring 127 mm x 12.7 mm x 3.5 mm, equipped with a three-point bending fixture and operated at a crosshead speed of 1.4 mm/min, in accordance with ASTM D790.

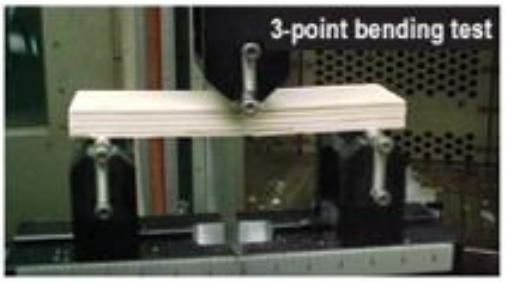

Figure 2. Three-Point Bending

To find the bending stress (σb), bending strain (εb), and bending modulus of elasticity (Eb), use the following equations:

$$\sigma b = \frac{3FL}{2db^2} \quad (1)$$

$$Eb = \frac{L^3 m}{4bd^3} \quad (2)$$

$$Eb = \frac{L^3 m}{4bd^3} \quad (3)$$

Description:
F = load applied at the midpoint (N)
L = span length (distance between two supports) (mm)
b = specimen width (mm)
d = specimen thickness (mm)
D = deflection (displacement) at the midpoint of the specimen (mm)
m = slope of the load-deflection curve in the linear section (N/mm)

3. RESULTS AND DISCUSSION

3.1 Composite Tensile Test Results

The strain versus stress graph of sugarcane fiber composites with fiber volume fractions of 50%, 60%, and 70% is shown in Figure 3.

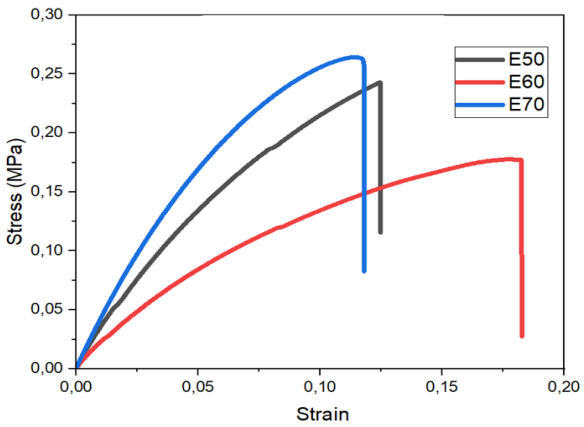

Figure 3. Stress–strain curves of sugarcane fiber-reinforced composites with varying fiber volume fractions.

Based on the graph above, the highest tensile stress is observed in sample E70 (with a 70% fiber volume fraction), reaching 26.43 MPa. This result is attributed to the higher fiber content in sample E70, which allows the applied load to be more evenly distributed. Since fibers generally possess higher tensile strength than the epoxy resin matrix, the increased fiber content enhances the overall tensile strength of the composite. As a result, sample E70 exhibits greater tensile strength compared to the samples with 60% and 50% fiber content.

However, an increase in fiber volume fraction does not always lead to a linear improvement in tensile strength. The effectiveness of load transfer is also influenced by the fabrication process and the uniformity of fiber–resin distribution. In the E60 sample (60% fiber volume), an imbalance in fiber and resin distribution likely created structural weak points, which served as initiation sites for failure under tensile loading. This is supported by both macroscopic analyses of the fracture surface, which revealed significant voids and fiber pull-outs. These defects, such as voids and debonding, reduce the interfacial bonding and compactness of the composite, preventing effective stress transfer from the matrix to the fibers. Consequently, the E60 sample exhibited the lowest tensile strength value of 17.79 MPa. The tensile test results for each sample are summarized in Table 1 below.

Table 1. Mechanical Properties Of Sugarcane Fiber Composite Samples From Tensile Testing.

Sample	UTS (Ultimate Tensile Strength) (MPa)	Yield Strength (MPa)	Young's Modulus (MPa)	Strain
E50	24.30 ± 1.91	23.5± 6.3	2.609 ± 68.51	0.12 ± 0.04
E60	17.79 ± 2.34	17.5 ± 2.68	1.844 ± 24.03	0.18 ± 0.05
E70	26.43 ± 0.75	22.5 ± 1.59	2.375 ± 84.55	0.17 ± 0.03

Based on the tensile test results, the highest Young's modulus was recorded in sample E50 at 2.609 ± 68.51 MPa, followed by sample E70 at 2.375 ± 84.55 MPa, and the lowest in sample E60 at 1.844 ± 24.03 MPa. Theoretically, an increase in fiber volume fraction should correlate positively with an increase in elastic modulus, since natural fibers possess greater stiffness than the resin matrix[14]. However, the experimental findings revealed discrepancies from this expectation, primarily due to the presence of different types and levels of defects in each sample.

Sample E50, with a 50% fiber volume fraction, exhibited a relatively uniform distribution of fiber and resin. Although minor defects such as voids and matrix-rich zones were present, they occurred in minimal amounts. This favorable distribution allowed for effective elastic load transfer from the matrix to the fiber, resulting in the highest elastic modulus among the samples.

In contrast, sample E60 exhibited the highest concentration of defects, including voids, fiber pull-out, and debonding, indicating poor interfacial bonding between the fiber and matrix. These imperfections hindered uniform stress transfer, leading to a significant reduction in the composite's stiffness. In sample E70, although the fiber content was higher, defects such as voids and crack deflection were also observed. These defects were primarily caused by suboptimal fiber arrangement and insufficient resin coverage, which impeded the fiber's ability to effectively resist elastic deformation.

This behavior aligns with the chemical characteristics of the epoxy resin used. Epoxy is a thermosetting polymer formed through the polymerization of epoxide groups (−C−O−C−), which are highly reactive and capable of forming strong covalent bonds with the hydroxyl groups found in natural fibers such as cellulose[15][16]. These chemical bonds enhance interfacial adhesion and reinforce the interaction between the matrix and the fiber. When the resin is properly distributed, epoxy functions optimally as a binder, improving the mechanical integrity of the composite[17].

3.2 Fracture Pattern Analysis of Composite Tensile Test Results

Fracture pattern analysis of the tensile-tested composites was carried out to examine how variations in fiber volume fraction influence fracture mechanisms. Figure 4 illustrates the fracture patterns observed in samples with fiber volume fractions of 50%, 60%, and 70%.

In Figure 4, the composite sample with a 50% fiber volume fraction (E50) exhibits a fracture located at the center of the specimen, classified as an LGM (Lateral Gage Middle) fracture. A midsection fracture indicates that the applied load was evenly distributed and that failure occurred at the region with the highest stress concentration.

In contrast, the E60 and E70 samples show fractures occurring near the top of the specimens, classified as LGT (Lateral Gage Top) fractures. This pattern suggests irregularities in fiber and resin distribution or the presence of localized defects, such as voids or debonding, near the top region. At higher fiber volume fractions, the resin may not sufficiently wet and bond with all fiber surfaces, leading to poor interfacial adhesion. As a result, stress distribution becomes uneven, and the specimen is more prone to early failure.

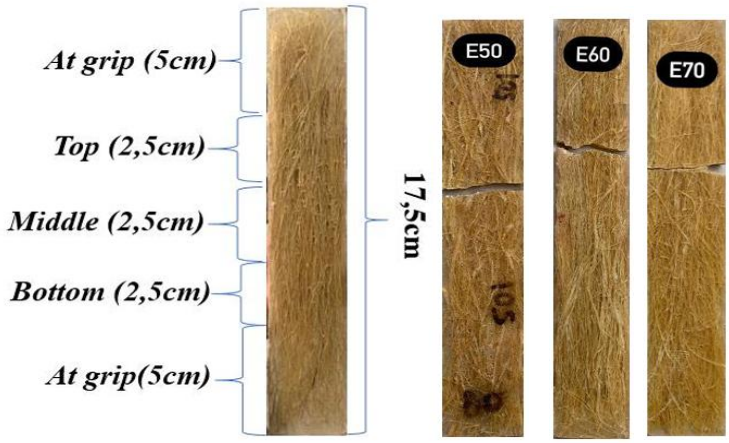

Figure 4. Fracture patterns of tensile test specimens with varying fiber volume fractions (E50, E60, E70).

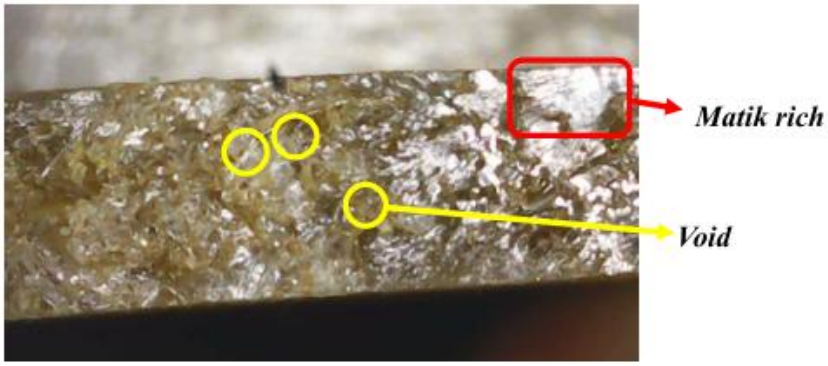

Figure 5. Macroscopic image of tensile fracture surface in sample E50.

Figure 5 shows the fracture surface of the E50 composite sample. The image reveals a failure mode characterized by matrix-rich regions, where the composite is dominated by resin with little to no presence of reinforcing fibers. This condition typically results from uneven fiber distribution during the fabrication process, leading to zones composed primarily of the matrix without adequate fiber reinforcement. In addition, void defects were also observed, which are attributed to air entrapment within the resin during molding. These trapped air pockets form cavities as the resin cures. However, the voids in this sample appear to be minimal and randomly distributed, thus having a negligible effect on the overall structural integrity and mechanical performance of the composite.

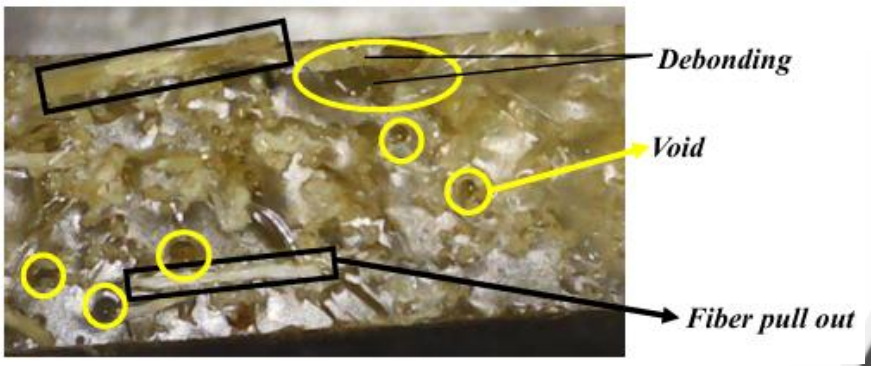

Figure 6. Macroscopic image of tensile fracture surface in sample E60.

Figure 6 displays the fracture surface of the E60 composite sample. The image reveals a LGT (Lateral Gap Top) fracture pattern, where the failure occurs near the upper section of the specimen. This indicates an uneven distribution of fiber and resin within the composite, resulting in non-uniform load transfer during tensile testing.

Compared to the E50 and E70 samples, the E60 sample exhibits a higher concentration of void defects, which are likely caused by trapped air during the fabrication process. Additionally, the fracture surface shows

evidence of fiber pull-out, where fibers are detached from the resin matrix. This phenomenon is indicative of debonding at the fiber–matrix interface, reflecting poor adhesion and contributing to the reduced mechanical performance of the sample.

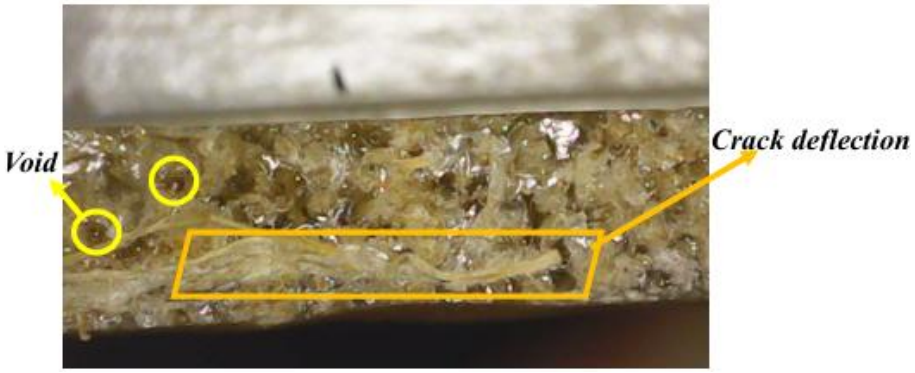

Figure 7. Macroscopic image of tensile fracture surface in sample E70.

Figure 7 shows that the failure type observed is also LGT (Lateral Gage Top), where the fracture initiates at the upper region of the specimen. In this sample, a crack deflection defect is evident, which is caused by the misaligned or tilted orientation of the fibers. When subjected to loading, the crack propagates along the path of the inclined fibers rather than perpendicular to the applied stress. This condition is likely the result of improper fiber alignment during the molding process, indicating a fabrication error that affects the structural integrity of the composite.

3.3 Composite Bending Test Results

The force–deformation curves resulting from the bending test of sugarcane fiber composites with varying fiber volume fractions (50%, 60%, and 70%) are shown in Figure 8.

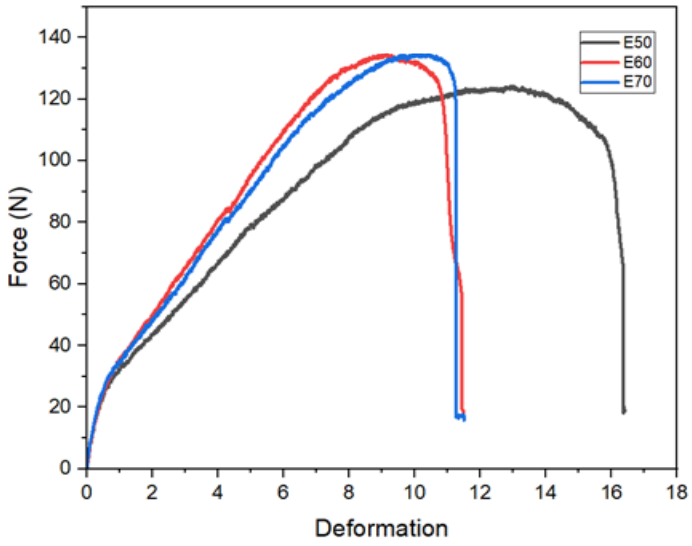

Figure 8. Force deformation graph of sugarcane fiber composite samples under bending test.

Table 2. Mechanical Properties Of Sugarcane Fiber Composites From Bending Tests

Sample	Max Force (N)	Bending Strength (MPa)	strain (mm)	Modulus of Elasticity (MPa)
E50	134.45	142.53 ± 8.73	9.73	1.57 ± 0.41
E60	133.75	119.15 ± 13.83	11.73	1.09 ± 0.08
E70	109.79	89.53 ± 10.38	11.70	2.10 ± 0.70

Based on Figure 8 (force deformation graph) and Table 2, which present the results of the bending test on sugarcane fiber-reinforced epoxy composites with fiber volume fractions of 50%, 60%, and 70%, the highest force and bending strength values were recorded in the E50 sample, at 134.45 N and 142.53 MPa, respectively. The E50

sample demonstrates an optimal ratio between fiber and resin, where the resin adequately coats the fibers, ensuring strong interfacial adhesion and effective mechanical interlocking. This optimal bonding allows the composite to withstand higher bending loads before failure occurs.

In contrast, the lowest force and bending strength values 109.79 N and 89.53 MPa were observed in the E70 sample. The high fiber content in this sample resulted in insufficient resin to fully impregnate all fibers, leading to poor fiber–matrix bonding. Additionally, the uneven resin distribution contributed to the formation of voids and inconsistent load transfer during testing. Despite having the highest elastic modulus (2.10 MPa), which indicates greater stiffness, the E70 sample exhibited low resistance to deformation and failed more quickly under bending loads.

4. CONCLUSION

Based on the mechanical testing results, variations in sugarcane fiber volume fraction significantly affect the tensile and flexural properties of the epoxy-based composites. The sample with a 70% fiber volume fraction (E70) achieved the highest tensile strength of 26.43 MPa, while the sample with a 50% fiber volume fraction (E50) exhibited the highest flexural strength of 142.53 MPa. However, increasing the fiber content does not always lead to a proportional improvement in all mechanical properties. For applications requiring a balance between tensile and flexural strength, a 50% fiber volume fraction is recommended as the optimal composition. At this level, the fiber and resin distribution is more uniform, resulting in better interfacial bonding and minimal defects such as voids and delamination. Therefore, the 50% fiber volume fraction offers well-balanced mechanical performance and can serve as a practical guideline for material selection in future lightweight structural composite applications

5. REFERENCES

[1] K.-L. Liu, K. Hsieh, S. Lai, and J. Han, “Properties of sugarcane fiber/polyurethane-crosslinked epoxy composites under different interfacial treatments,” Polym. Compos., vol. 41, no. 3, pp. 511–519, 2020, doi: 10.1002/pc.25710.

[2] I. Ismail, Q. Aini, Zulfalina, Z. Jalil, and S. H. S. Md Fadzullah, “Mechanical and physical properties of the rice straw particleboard with various compositions of the epoxy resin matrix,” J. Phys. Conf. Ser., vol. 1120, no. 1, pp. 1–7, 2018, doi: 10.1088/1742-6596/1120/1/012014.

[3] I. Ismail et al., “Properties enhancement of nano coconut shell filled in packaging plastic waste bionanocomposite,” Polymers, vol. 14, no. 4, p. 772, 2022, doi: 10.3390/polym14040772.

[4] S. Huo, M. Fuqua, and C. Ulven, “Natural fiber reinforced composites,” Polym. Rev., vol. 52, no. 3, pp. 259–320, 2012, doi: 10.1080/15583724.2012.705409.

[5] H. Fink, A. Bledzki, M. Sain, and O. Faruk, “Progress report on natural fiber reinforced composites,” Macromol. Mater. Eng., vol. 299, no. 1, pp. 9–26, 2014, doi: 10.1002/mame.201300008.

[6] S. Mazumder and N. Zhang, “Cellulose–hemicellulose–lignin interaction in the secondary cell wall of coconut endocarp,” Biomimetics, vol. 8, no. 2, p. 188, 2023, doi: 10.3390/biomimetics8020188.

[7] B. Prasetya, A. A. Prakoso, A. Rianjanu, W. S. Sipahutar, and A. Fitri, “Mechanical properties of sugarcane bagasse fiber composites: Epoxy vs polyester resin matrices,” J. Perancangan, Manufaktur, Material, dan Energi (PERMADI), vol. 7, no. 1, pp. 95–104, 2025.

[8] A. Fitri, F. F. Mubina, B. Prasetya, M. Y. Siregar, Q. Ainia, and W. S. Sipahutar, “Effect of coconut and sugarcane fiber volume fraction variations on the tensile properties of epoxy matrix composites,” J. Perancangan, Manufaktur, Material, dan Energi (PERMADI), vol. 7, no. 1, pp. 105–113, 2025.

[9] M. Y. Siregar, F. F. Mubina, W. S. Sipahutar, A. Fitri, and M. G. I. Khan, “Tensile strength of epoxy hybrid composites reinforced with coconut and sugarcane fibers,” J. Perancangan, Manufaktur, Material, dan Energi (PERMADI), vol. 7, no. 2, pp. 155–162, 2025.

[10] P. Banakar, J. Katiyar, R. Sailaja, P. Sampathkumaran, and H. Jagadeesh, “Influence of varying matrix/fiber concentration on mechanical properties of bi-directional carbon fiber reinforced polymer composite,” J. Reinf. Plast. Compos., 2024, doi: 10.1177/07316844241263188.

[11] T. Zhong et al., “Effect of alkali treatment on microstructure and mechanical properties of individual bamboo fibers,” Cellulose, vol. 24, pp. 333–347, 2016, doi: 10.1007/s10570-016-1116-6.

[12] Y. Gawali, S. Tambe, P. S. Kanade, C. Mate, and S. Nimse, “Fabrication of fiber reinforced composite material like bamboo flex, glass fiber and epoxy resin,” Int. J. Sci. Technol., vol. 16, no. 2, 2025, doi: 10.71097/ijsat.v16.i2.3146.

[13] T. Batu and H. G. Lemu, “Investigation of mechanical properties of false banana/glass fiber reinforced hybrid composite materials,” Results Mater., vol. 8, p. 100152, 2020, doi: 10.1016/j.rinma.2020.100152.

[14] M. Arifuzzaman, M. S. Hossain, M. S. Islam, and M. S. Anwar, “Effect of fiber orientation and volume fraction on Young’s modulus for unidirectional carbon fiber reinforced composites: A numerical investigation,” Malaysian J. Compos. Sci. Manuf., vol. 13, no. 1, pp. 45–54, 2024, doi: 10.37934/mjcsm.13.1.4554.

[15] K. Tanaka, A. Shundo, and S. Yamamoto, "Network formation and physical properties of epoxy resins for future practical applications," JACS Au, vol. 2, pp. 1522–1542, 2022, doi: 10.1021/jacsau.2c00120.
[16] S. Jodeh et al., "Viscosity of epoxy resins based on aromatic diamines, glucose, bisphenolic and bio-based derivatives: A comprehensive review," J. Polym. Res., vol. 29, no. 1, pp. 1–29, 2022, doi: 10.1007/s10965-022-03040-3.
[17] M. A. S. Anam, P. Manik, and G. Rindo, "Analisis pengaruh material abrasif pada blasting dengan variasi metode coating terhadap prediksi laju korosi dan daya rekat adhesi," J. Tek. Perkapalan, vol. 12, no. 2, pp. 65–72, Jun. 2024.

LOGIC
Journal of Engineering Design and Technology
Vol. 25 No. 2 July 2025 ; p. 93-99

p-ISSN : 1412-114X
e-ISSN : 2580-5649
http://ojs2.pnb.ac.id/index.php/LOGIC

PERFORMANCE ANALYSIS OF THERMOELECTRIC COOLER BOX WITH WATER COOLING BLOCK (WCB) AND HEAT SINK FAN

I Wayan Sutina [1)*], Adi Winarta [1)], I Nyoman Agus Adi Saputra [1)]

1) Mechanical Engineering, Politeknik Negeri Bali, Jl. Kampus Bukit Jimbaran, Badung, Bali 80362

Corresponding email : sutina@pnb.ac.id

Abstract. Thermoelectric cooler boxes offer an environmentally friendly, energy-efficient, and portable cooling solution. However, the performance of thermoelectric cooling systems is highly dependent on the effectiveness of heat dissipation on the hot side of the Peltier module (TEC). This study aims to experimentally investigate the impact of using a Water Cooling Block (WCB) compared to a conventional heat sink fan on the cooling performance of a thermoelectric-based cooler box. The experimental setup involved two configurations for the hot side cooling system, where parameters such as hot-side temperature, cabin temperature, and Coefficient of Performance (COP) were measured and analyzed. The experimental results showed that the use of WCB was able to significantly reduce the temperature on the hot side, with a temperature reduction in the cabin reaching 20.35 °C and an average COP of 0.09687. Meanwhile, the TEC-fan temperature in the cabin cooler box was lower at 21.45 °C, with an average COP value of 0.04718. Therefore, the Water Cooling Block demonstrates superior efficiency and thermal management compared to the heat sink fan, offering enhanced performance for thermoelectric cooler box applications in various low-temperature storage needs.

Keywords : Thermoelectric, Cooler box, Water cooling block, Heat sink fan, COP, Peltier module.

1. INTRODUCTION

Refrigeration machines have become an essential part of modern life. Refrigeration machines with vapor compression systems are the most commonly used type of refrigeration machine in industries such as hospitality, power generation, pharmaceuticals, and food storage industries, such as meat, fruit, and vegetables [1]. However, the use of vapor compression refrigeration systems carries several risks that can cause environmental damage, such as the use of chlorofluorocarbons (CFCs) and hydrochlorofluorocarbons (HCFCs) as refrigerants, which can cause global warming and damage the ozone layer. For this reason, the use of these types of refrigerants has been widely banned around the world [2]. One system that can be used as an alternative to environmentally friendly cooling machines is the Thermoelectric (TEC) system. Cooling machines with thermoelectric systems have lower noise levels because they have fewer moving mechanical components and more accurate temperature control [3]. Thermoelectric cooler boxes are becoming a replacement for conventional refrigerators, with a compact and lightweight design that makes them easy to place anywhere. These cooler boxes do not require a lot of electricity and can be powered by DC current, so their energy consumption is relatively low and they are more flexible and easier to move [4].

The Thermoelectric Module (TEC) is an integrated circuit with a solid form that works with three thermodynamic principles known as the Seebeck, Peltier, and Thomson effects [5]. Peltier elements can be used as coolers or heaters depending on the direction of the current supplied. Peltier elements are commonly used in car air conditioning systems [6] and water temperature control systems [7]. Peltier elements become cold due to the flow of electrons from P-type semiconductor components to higher electron levels in N-type semiconductors [8]. The effectiveness of thermoelectric cooling systems depends heavily on the ability to dissipate heat from the hot

side of the module. One important component that supports this process is the heat sink, which serves to conduct and dissipate heat to the environment [9]. The effectiveness and performance improvement of thermoelectric modules are influenced by the heat transfer cross-sectional area on the heat sink [10]. The use of thermoelectric modules as a 34-liter beverage cooler has been carried out with two or three TEC modules by Azridjal Aziz et al. The results show that heat absorption in a cooler box with three TEC modules is more effective than with two TEC modules [11]. Previous research has shown how the use of a water cooling block (WCB) system in TEG modules can improve the performance of thermoelectric generators (TEG) [12]. Improvements in cooling performance with thermoelectric modules still depend on the effectiveness of heat dissipation on the hot sink side.

Due to these issues, this study was conducted to experimentally examine the effect of using a water cooling block on the heat sink on the cooling performance of a thermoelectric cooler box. By conducting direct testing, this study is expected to provide important information regarding the optimization of the use of water cooling block (WCB) heat sinks that support the overall efficiency of thermoelectric cooling systems.

2. METHODS

2.1 Research Design

This cooling system consists of a main component in the form of a thermal insulation box equipped with a thermoelectric module. The cooling box is made of 40 mm thick polyurethane board. The internal dimensions of the box are 240 mm × 240 mm × 270 mm. As the cooling element, a double-deck thermoelectric module of type TEC2-25408 is used, measuring approximately 40 mm × 40 mm × 6 mm. This module operates at a current of 4.5 amperes and a voltage of 12 volts.

Table 1. Thermoelectric Specification

TEC specification	
Type	Double Deck Thermoelectric Cooler
Model	TEC2-25408
Voltage	12 V
Current Max.	8 A
Power Max.	70 watt
ΔT Max	80°C
Dimension	40mm x 40mm x 6mm

Cooling on the cold sink side is carried out using a finned aluminum heat sink equipped with a fan to increase heat transfer from the cooling chamber. Conversely, the hot sink side is used as a heat extraction point through the installation of an 80 mm × 80 mm water cooler block, which functions to transfer heat to the cooling water fluid. The pump used has a power of 2.52 watts with a current of 0.21 A and a voltage of 12 volts. A condenser is used to cool the water from the WCB with the help of a fan. This experimental configuration can be seen visually in Figure 1.

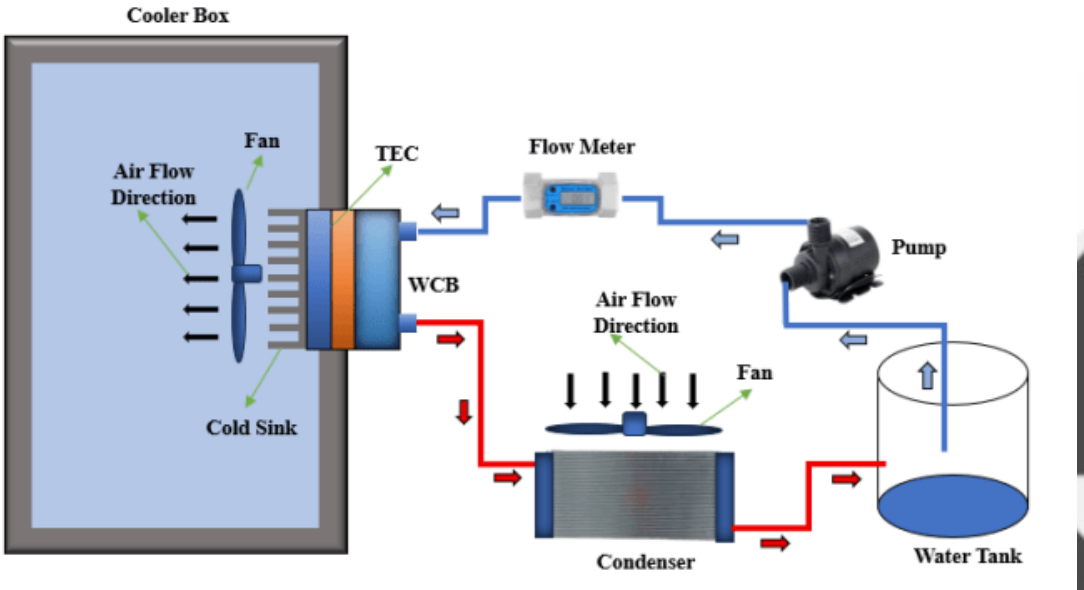

Figure 1. WCB thermoelectric experimental scheme

The initial step in the operation of the thermoelectric system with a heat sink-fan and water cooling block involves the cold side, where the heat sink absorbs heat from the cooling chamber, assisted by a fan to accelerate heat absorption. On the hot side, the TEC module is fitted with a water cooling block, where water from the reservoir tank is pumped to the flow meter for checking the water flow rate, then the water flows to the water cooling block to help dissipate heat from the TEC on the hot side. The water exiting the water cooling block flows to the radiator, which functions to release the heat from the water generated by heat absorption on the hot side with the assistance of a fan. The water then returns to the reservoir tank and the cycle continues.

The performance calculation of this cooler box was carried out by analyzing the data obtained and then calculating the COP value using equation (1) as follows:

$$COP = \frac{Q_t}{Pt} \quad (1)$$

$$Q_C = Q_w + Q_a + Q_{tr} \quad (2)$$

$$P_t = P_1 + P_2 \quad (3)$$

Where Q_t (watts) is the total cooling load on the cooler box cabin, which can be calculated using equation (2), consisting of heat transfer within the box cabin Qa and heat lost through the box walls Qw to the environment. Meanwhile, P_t (watts) is the total power used by the cooler box, as stated in equation (3), which can be found in previous references and studies [13],[14],[15]. In this study, air is used as the load in the cooler box cabin, so the cooling effect can be seen from the air temperature inside the cooler box cabin.

2.2 Experimental Procedure

Experimental testing was conducted using a data collection method for each type of heat sink on the hot side, namely testing heat sinks with fan heat sinks and heat sink-water cooler blocks (WCB) with dimensions of 40 mm x 80 mm and a thickness of 15 mm, using aluminium material. The DC current entering the thermoelectric device uses the PZEM-017 with a 1% margin of error, connected to the data acquisition system (NI 9274). Type K thermocouples were installed to measure all temperatures and connected to the data acquisition system (NI 9213). The thermocouple positions are indicated in Figures 2 and 3 with yellow dots, where temperatures are recorded using LabVIEW 2019 data acquisition software and stored on a desktop computer for each test. It is assumed that the air mass inside the box is constant without any transfer from the environment. The cooling load inside the box is water with a mass of 0.35 kg. The fan power in the cooling box is also calculated as a cooling load, assuming that the heat transfer generated by the fan motor is equal to the fan power (2.88 watts). The external cabin temperature is measured and serves as a free variable that can influence the heat loss through the box walls. The experimental scheme is presented in Figures 2 and 3.

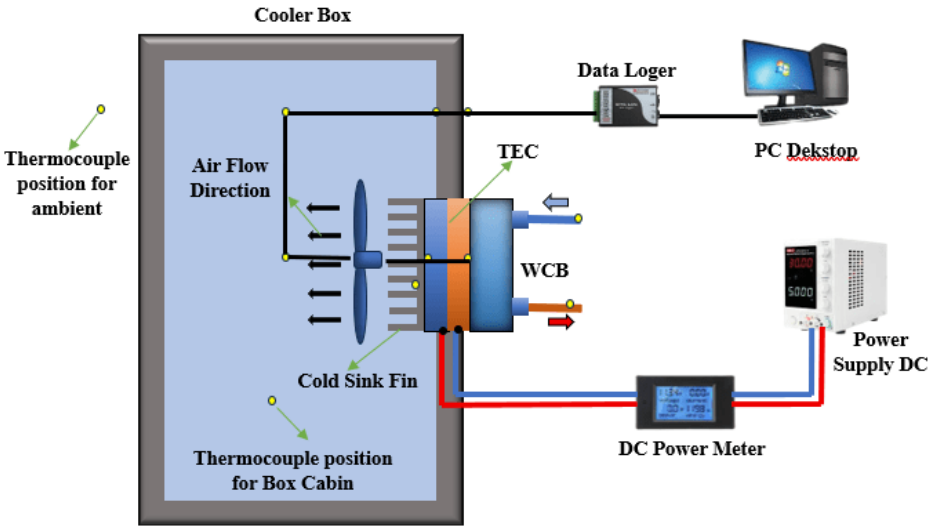

Figure 2. Experimental heat sink-WCB scheme

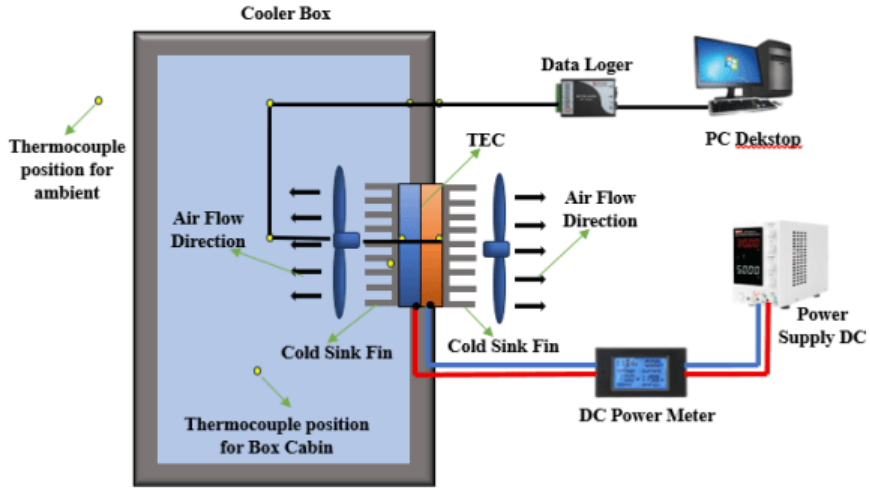

Figure 3. Heat sink-fan diagram

Experimental data collection was carried out for ± 180 minutes with a data collection interval of every 10 minutes. At this stage, the experimental data collection process was carried out twice.

3. RESULTS AND DISCUSSION

3.1 Temperature Comparison on Heat Sink

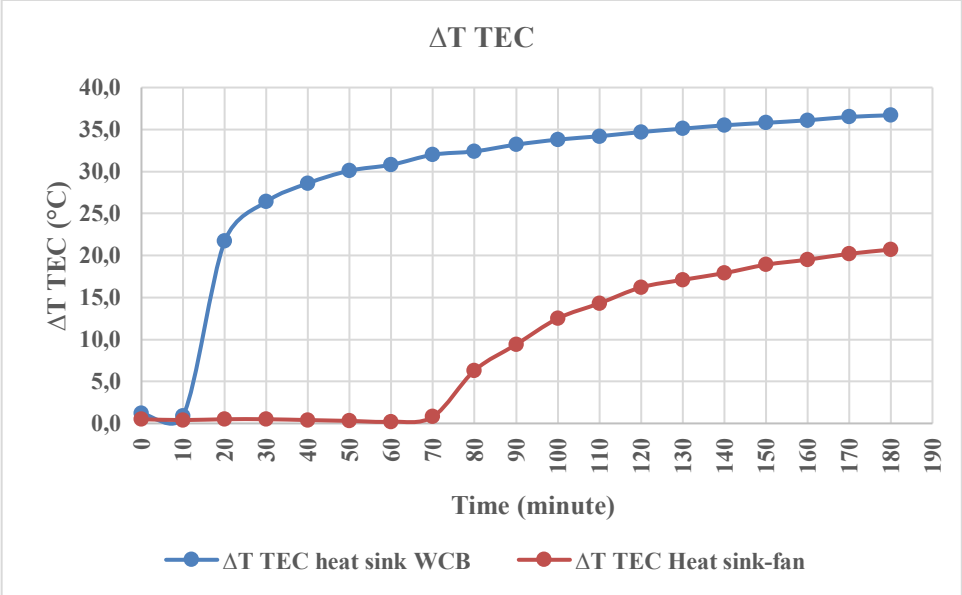

Figure 4. Temperature comparison on heat sink

The temperature difference between the hot side of the thermoelectric module is a key indicator in determining the efficiency of heat transfer from the TEC module to the environment. Figure 4. shows a graph comparing the thermoelectric ΔT against the test time between the hot side and the cold side for both types of TEC-fan and TEC-WCB tests. The blue lines and points indicate the test temperature of the TEC heat sink with WCB. The yellow lines and points indicate the temperature changes for the TEC heat sink test with a fan.

Based on the test results, the system using a heat sink-WCB showed a higher temperature increase of 36.7 °C. Significant changes began to occur at the 10-minute mark and continued gradually until the 180-minute test time. Meanwhile, the system using a heat sink-fan showed a stable temperature increase trend until the 70th minute, and then gradually increased until the 180-minute testing time with a final value of 20.7 °C. These results are consistent with those reported by Nugroho Tri Atmoko et al. [11], where the addition of WCB on the hot side of the TEC had a better effect. This is because heat transfer in the heat sink-fan system relies solely on forced convection by air, which has a relatively low specific heat capacity compared to water. In contrast, the heat sink with WCB can transfer heat more quickly through conduction and forced convection of water, and utilize a radiator

to dissipate heat more effectively into the environment.

This significant temperature difference shows that the WCB system has an advantage in keeping the hot side temperature low and stable. A lower hot side temperature will increase the temperature difference (ΔT) between the hot side and the cold side of the TEC module, thereby increasing the Peltier effect. This increase in ΔT directly impacts the cooling capacity of the module, as the heat transfer process from the cold side becomes more intensive. Additionally, the stability of the hot side temperature prevents overheating of the module, which can extend the overall lifespan of the TEC.

3.2 Temperature Inside the Cooler Box Cabin

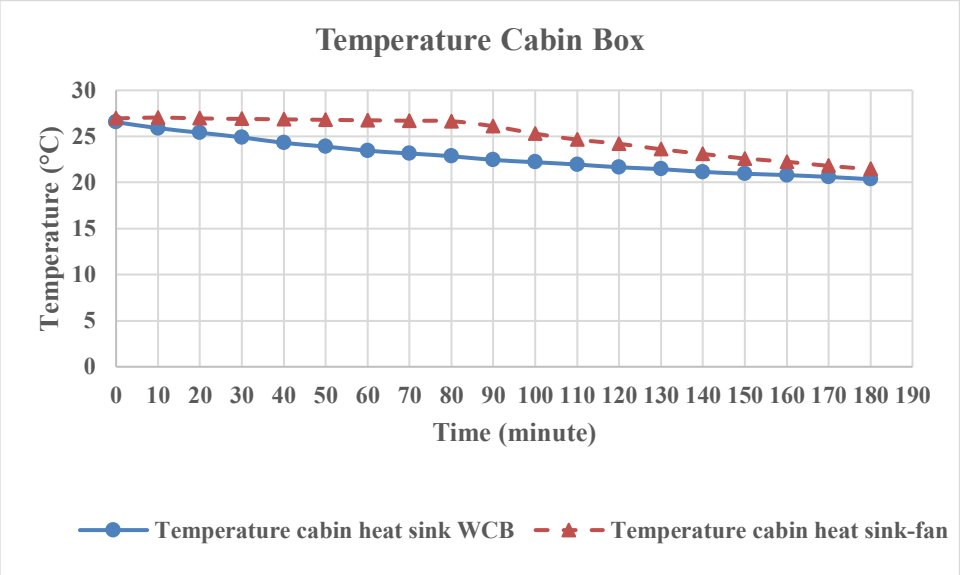

Figure 5. Comparison of temperatures inside the cooler box cabin

Figure 5 shows a graph comparing the temperature inside the cabin cooler box for the TEC-WCB test (blue line and dots) and the TEC-fan test (yellow line and dots). The experimental results show that the cooler box with the WCB system was able to achieve a lower temperature reduction of 20.35 °C within the 180-minute testing period. A significant temperature drop occurred in the first 60 minutes, indicating that the initial efficiency of the WCB system is very high in absorbing heat from the cabin air. In the heat sink fan system, the temperature drop tends to be slower and more stable. The cabin temperature began to drop at the 90-minute mark and gradually decreased until the 180-minute test, with a cabin temperature of 21.45 °C. This phenomenon is caused by the heat dissipation performance on the hot side of the TEC being influenced by the heat dissipation effect on the hot side of the TEC. With better heat dissipation in the WCB system, the cold side of the TEC module can achieve a lower temperature, and heat absorption from the load and cabin air becomes more effective and optimal, leading to thermal equilibrium. With the ability to lower cabin temperature faster and to a lower level, the WCB cooling system is highly suitable for applications requiring small-capacity cooling systems that need to achieve stable temperatures quickly, such as food storage, beverage storage, pharmaceuticals, or other sensitive materials.

3.3 Performance Comparison (COP)

To assess the energy efficiency of the cooling system, the Coefficient of Performance (COP) parameter is used, using equation (1), which is the ratio between the cooling load (Qtotal) and the total electrical power used (Ptotal). To determine the total cooling load on the cooler box, equation (2) is used. The total electrical power used can be calculated using equation (3).

Figure 6 shows the COP graph for each heat sink. The trend shows that the COP in the WCB system is consistently higher than in the system with a heat sink fan. The COP value remains relatively constant from the start of the test until the 180th minute, with an average COP value of 0.09687. Meanwhile, the COP values for the heat sink-fan system tend to be stable with an average value of 0.04718. This indicates that the WCB system is more efficient in converting electrical energy into cooling energy. This advantage arises because water, as the cooling medium in the WCB, is able to maintain the temperature of the hot side at a low level, ensuring that the TEC performance remains optimal without excessive heat load [10]. Meanwhile, in fan systems, heat accumulation on the hot side causes the TEC to operate in suboptimal thermal conditions, requiring more electrical energy to produce the same cooling effect. The increase in COP also indicates significant energy-saving potential if this system is applied on a large scale or for long-term operations. Thus, the thermoelectric cooler box system with WCB is not only superior in terms of cooling performance but also in energy efficiency.

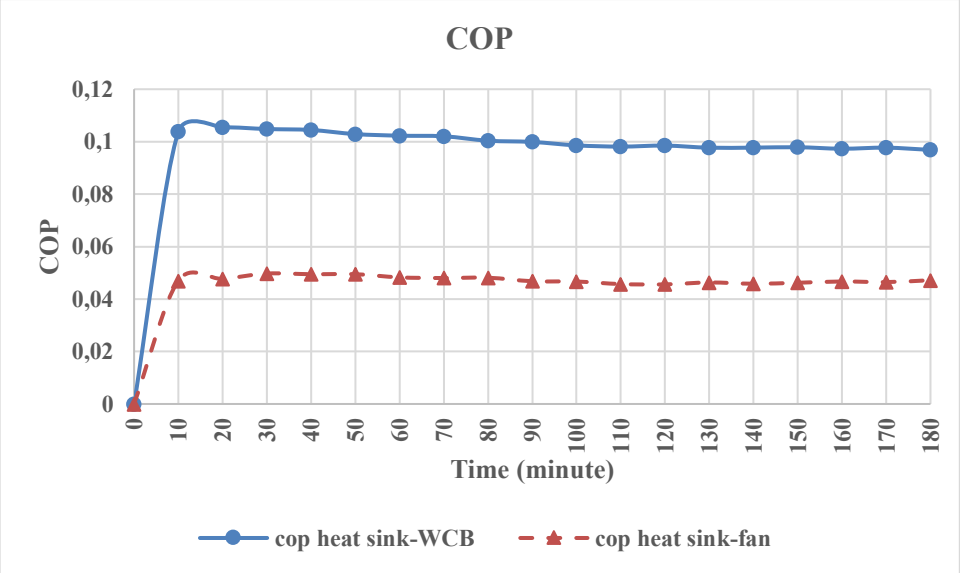

Figure 6. Performance Comparison (COP)

3. CONCLUSION

Experimental research has been conducted on thermoelectric cooler boxes with WCB heat sink cooling and heat sink fans, where water is used as the cooling medium on the hot side of the TEC-WCB and air is used as the cooling medium on the TEC-fan. The cooling load applied is water with a mass of 0.35 kg. Experimental data showed that the TEC ΔT value comparison for the heat sink with WCB reached a maximum of 36.7 °C at minute 180. The heat sink-fan had a TEC temperature comparison value was 20.7 °C at the 180th minute. The temperature drop data for the thermoelectric cabin cooler box with WCB reached a minimum temperature of 20.35 °C. This temperature achievement is better than the TEC-fan, which could only reach a cabin temperature of 21.45 °C during the 180-minute testing period. The experimental COP value of the system was found to have an average value of 0.09687 for TEC-WCB, while the TEC-fan had a value of 0.04718. From the three aspects observed, namely heat sink temperature, cabin temperature, and COP value, it can be concluded that the use of Water Cooling Block (WCB) provides a significant improvement in the performance of the thermoelectric cooling system. This system is not only able to dissipate heat more efficiently, but also improves cabin cooling capabilities and overall energy efficiency. These findings align with the research objective, which was to experimentally evaluate the impact of the WCB on the performance of the thermoelectric cooler box.

5. REFERENCES

[1] T. R. Buntu, "Analisis beban pendinginan produk makanan menggunakan cold box mesin pendingin LUCAS NULLE type RCC2," *J. Poros Tek. Mesin UNSRAT*, vol. 6, no. 1, 2017.
[2] U. Prayogi and R. Sugiono, "Analisis global warming potential (GWP) dan ozone depletion potential (ODP) pada refrigeran R32, R290, R407C, R410A sebagai pengganti R22," *J. Tek. Mesin*, vol. 11, Universitas Mercu Buana, Jakarta, 2022.
[3] K. Liang, Z. Li, M. Chen, and H. Jiang, "Comparisons between heat pipe, thermoelectric system, and vapour compression refrigeration system for electronics cooling," *Appl. Therm. Eng.*, vol. 146, pp. 260–267, 2019.
[4] B. P. A. Sedayu, "Aplikasi pendingin elektrik TEC1-12706 dengan water cooling pada cooler box berbasis semikonduktor," S1 Thesis, Dept. Teknik Mesin, Univ. Negeri Surabaya, 2022.
[5] D. Astrain and Á. Martínez, "Heat exchangers for thermoelectric devices," in *Heat Exchangers – Basics Design Applications*, J. Mitrovic, Ed. InTech, 2012, doi: 10.5772/33464. [Online]. Available: http://www.intechopen.com/books/heat-exchangers-basicsdesign-application/heat-exchangers-for-thermoelectric-devices
[6] M. Rautl, "Thermoelectric air cooling for cars," *Int. J. Eng. Sci. Technol.*, vol. 4, no. 5, pp. 2381–2394, 2012.
[7] F. Gandhi and Y. M. Meqorry, "Perancangan sistem pendingin air menggunakan elemen Peltier berbasis mikrokontroler ATmega8535," *J. Fisika Unand*, vol. 5, no. 1, pp. 35–41, 2016.
[8] H. Munnik, D. Yohannes, and Y. Bekti, "Pemanfaatan Peltier untuk cooler box mini," *J. Teknol. Ind.*, vol. 11, 2022.
[9] E. Yudiyanto, "Utilization of Peltier as a cooling system for medicine cooler box," D3 Thesis, Dept. Teknik Mesin, Politeknik Negeri Malang, 2020.

[10] E. Perdana, "Simulasi dan eksperimental variasi luasan heatsink pada termoelektrik generator," S1 Thesis, Institut Teknologi Indonesia, Tangerang Selatan, 2021.
[11] A. Aziz, "Aplikasi modul pendingin termoelektrik sebagai media pendingin kotak minuman," S1 Thesis, Dept. Teknik Mesin, Universitas Riau, 2013.
[12] N. T. Atmoko, "An experimental study of the TEG performance using cooling systems of waterblock and heatsink-fan," S1 Thesis, Dept. Mechanical Engineering, Sekolah Tinggi Teknologi Warga Surakarta, 2022.
[13] J. Vián and D. Astrain, "Development of a thermoelectric refrigerator with two-phase thermosyphons and capillary lift," *Appl. Therm. Eng.*, vol. 29, no. 10, pp. 1935–1940, 2009.
[14] S. Jugsujinda, A. Vora-ud, and T. Seetawan, "Analyzing of thermoelectric refrigerator performance," *Procedia Eng.*, vol. 8, pp. 154–159, 2011.
[15] Á. Martínez, D. Astrain, A. Rodríguez, and G. Pérez, "Reduction in the electric power consumption of a thermoelectric refrigerator by experimental optimization of the temperature controller," *J. Electron. Mater.*, vol. 42, no. 7, pp. 1499–1503, 2013.

LOGIC
Journal of Engineering Design and Technology
Vol. 25 No.2 July 2025; p. 100-106

p-ISSN : 1412-114X
e-ISSN : 2580-5649
http://ojs2.pnb.ac.id/index.php/LOGIC

THE EFFECT OF REINFORCEMENT SURFACE TREATMENT WITH CITRIC ACID ON THE FLEXURAL AND HARDNESS PROPERTIES OF EPOXY/WOOD SAWDUST COMPOSITES

I Wayan Padma Yogi Asana [1)*], Risa Nurin Baiti [1)], Komang Widhi Widantha [1)]

1) Department of Mechanical Engineering, Politeknik Negeri Bali

Corresponding email: iwpadmayogi@pnb.ac.id

Abstract. This study investigates the effect of citric acid surface treatment on wood sawdust used as reinforcement in epoxy-based composites by evaluating both bending strength and Brinell hardness. Wood sawdust was subjected to surface modification using citric acid and sodium hydroxide (NaOH) under equivalent molar concentrations. Bending strength tests showed that both citric acid and NaOH treatments significantly improved mechanical performance compared to untreated samples, with average strengths of 33.83 MPa and 32.82 MPa, respectively, versus 21.83 MPa for the untreated group. Statistical analysis was conducted to compare the two treatments. After confirming normal distribution but unequal variances, a Welch two-sample t-test was performed, yielding a p-value of 0.742 showed no significant difference between the two treatments. Brinell hardness measurements produced mean values of 9.56 HB, 9.01 HB, and 9.77 HB for citric acid-treated, NaOH-treated, and untreated composites, respectively. One-way ANOVA indicated no significant variation in hardness among these groups. These results demonstrate that citric acid treatment enhances flexural performance to the same extent as NaOH without altering surface hardness.

Keywords : ANOVA, Bending strength, Citric Acid, Composite, Hardness, Wood Sawdust.

1. INTRODUCTION

The increasing demand for sustainable materials has driven the development of composite materials derived from renewable natural resources. One such material with promising potential is wood sawdust waste, a byproduct generated from wood processing industries [1], [2]. The use of wood sawdust as a composite constituent enables the production of materials that can be tailored to meet specific performance criteria. Moreover, wood-based composites offer an opportunity to enhance the utility of low-quality wood by converting it into higher-value products [3].

However, one of the primary challenges in utilizing wood sawdust in polymer composites lies in the inherent incompatibility between the hydrophobic epoxy resin and the hydrophilic nature of wood particles. This mismatch leads to poor interfacial adhesion, which negatively affects the mechanical performance of the composite. To address this issue, surface treatment of the wood sawdust is essential for improving the compatibility and adhesion between the filler and the matrix [4].

Alkaline treatment using sodium hydroxide (NaOH) has been widely adopted to modify the surface of lignocellulosic materials, aiming to enhance the adhesion between wood fibers and polymer matrices in wood-plastic composites [5], [6], [7]. During this treatment, hydrogen bonds within the lignocellulosic matrix are disrupted, increasing the proportion of amorphous cellulose and surface roughness. While effective, the use of NaOH poses significant environmental hazards, creating a need for more eco-friendly and cost-effective surface

treatment alternatives [8].

Citric acid, a natural organic poly(carboxylic acid) with three carboxyl groups, has demonstrated potential as a cross-linking agent through esterification with hydroxyl groups, forming stable cross-linked networks [9]. Beyond its applications in the food, beverage, and pharmaceutical industries, citric acid has shown strong cross-linking capabilities with plant fibers, paper, wood, starch, and natural elastomers [8], [10], [11]. Although citric acid offers notable advantages in improving fiber adhesion, research on its use for surface treatment of wood sawdust in composite applications remains limited.

This study aims to investigate the effect of citric acid surface treatment on wood sawdust used in epoxy-based composites. The influence of this treatment will be evaluated through mechanical characterization, specifically flexural (bending) strength and Brinell hardness, and benchmarked against both untreated and NaOH-treated counterparts. Emphasis is placed on assessing whether citric acid can serve as a viable and environmentally friendly alternative to conventional alkali treatments.

2. METHODS

This research employed a laboratory-based experimental approach to evaluate the effect of citric acid surface treatment on the mechanical performance of epoxy composites reinforced with wood sawdust. The primary focus was to investigate bending strength using a three-point bending test and Brinell Hardness, as these properties are essential for evaluating the rigidity and surface resistance of composite materials. The composite matrix was composed of a commercially available clear epoxy resin and its corresponding hardener, mixed in a 2:1 weight ratio, ensuring a consistent and reliable polymer crosslinking process.

Wood sawdust, obtained as a byproduct from a local woodcraft production facility, served as the reinforcing filler. The raw sawdust was used without prior chemical treatment unless otherwise specified for comparison. Food-grade citric acid purchased from a local supermarket was used as the primary surface treatment agent without further purification due to its known ability to modify lignocellulosic surfaces. Sodium hydroxide (NaOH), a widely used alkaline modifier, was also used as a comparative treatment, prepared at the same molarity as the citric acid solution to ensure consistency in treatment conditions. Before treatment, wood sawdust was manually sieved using a 40-mesh screen to obtain uniform particle size distribution. The particles retained on the sieve were subjected to surface modification. These sawdust particles were immersed in either NaOH or citric acid solution, stirred continuously for 2 hours to enhance contact between the chemical agents and the sawdust surface, then rinsed thoroughly with distilled water and oven-dried at 60 °C to remove residual moisture. After drying, the treated sawdust was mixed into the epoxy resin at a weight ratio of 19%. The mixture was stirred manually until a homogeneous blend was achieved and then poured into pre-fabricated molds. The molds were left at room temperature for curing under ambient laboratory conditions. After curing, the composite plates were demolded and cut into test specimens with standardized dimensions of 100 mm × 16 mm × 5 mm (length × width × thickness), suitable for mechanical testing.

Three-point bending tests were conducted using a universal testing machine with an 80 mm support span in accordance with ASTM D790 standards. This test provided data on flexural strength and modulus. Brinell hardness was measured by applying a predetermined load to a 2.5 mm diameter steel ball indenter pressed into each specimen's surface. The resulting indentation was used to calculate hardness values based on ASTM E10 guidelines. The combination of these two tests enabled a comprehensive evaluation of the mechanical behavior of the developed composites under different surface treatment conditions.

3. RESULTS AND DISCUSSION

3.1 Effect of Surface Treatment on Flexural Bending Strength

The epoxy composites reinforced with NaOH and citric acid-treated wood sawdust exhibited substantially higher bending strength than the untreated control. Untreated specimens averaged is 21.83 MPa, whereas the NaOH-treated group averaged 32.82 MPa and the citric-acid-treated group 33.83 MPa. These values correspond to roughly 50–55% improvement over the untreated case as shown in Figure 1.

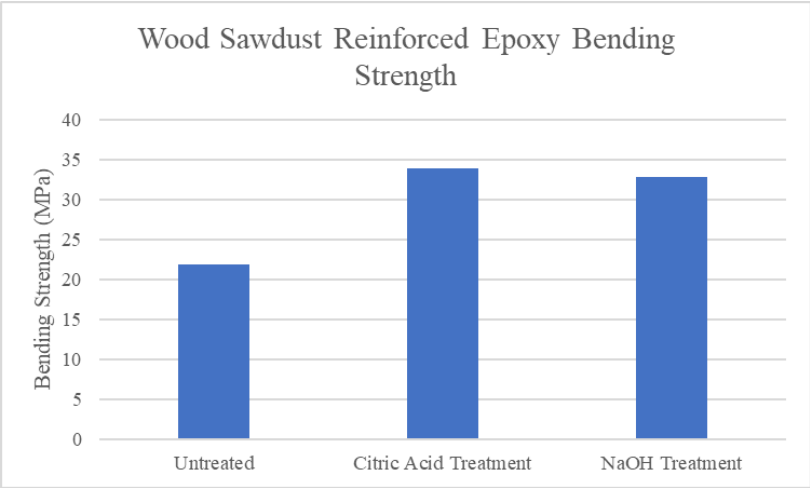

Figure 1. Wood sawdust reinforced epoxy bending strength comparison from different treatment

This level of enhancement is consistent with prior studies showing that chemical surface treatments of lignocellulosic fillers lead to stronger fiber–matrix bonding. For example, alkali (NaOH) treatment is known to remove lignin and other amorphous constituents from wood fibers, exposing cellulose and roughening the surface; this typically increases interfacial adhesion and flexural strength [12], [13]. Likewise, citric acid treatment promotes esterification between its carboxyl groups and fiber hydroxyls, improving fiber hydrophobicity and bonding with the polymer matrix [14]. In short, both treatments likely improved stress transfer across the interface, which accounts for the marked rise in bending strength [12], [14].

Due to high difference between treated sample and untreated sample, the statistical analysis was conducted only for the citric acid and NaOH treated group. First, the bending strength data for each group were assessed for normality using hypotheses H_0: data are normally distributed and H_1: data are not normally distributed. The test yielded p-values greater than the significance threshold for both citric acid and NaOH groups, indicating no significant departure from normality and thus failing to reject H_0 for either group as shown in Figure 2.

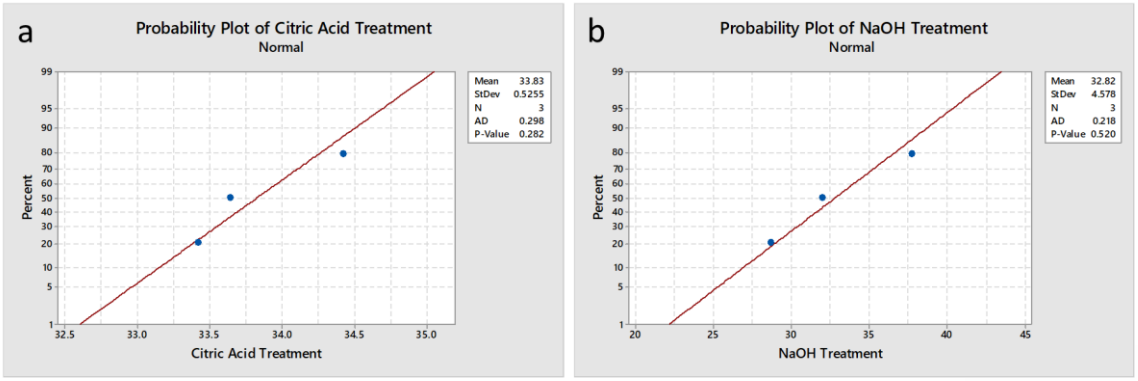

Figure 2. Normality test result for (a) Citric acid treatment and (b) NaOH treatment

Afterward, equal variances were evaluated with hypotheses H_0: group variances are equal; H_1: there is difference in variances. The equal variance test result in a statistically significant result which P value = 0.011 greater than significance level $\alpha = 0.05$ as shown in Figure 3, leading to rejection of H_0 and indicating unequal variance.

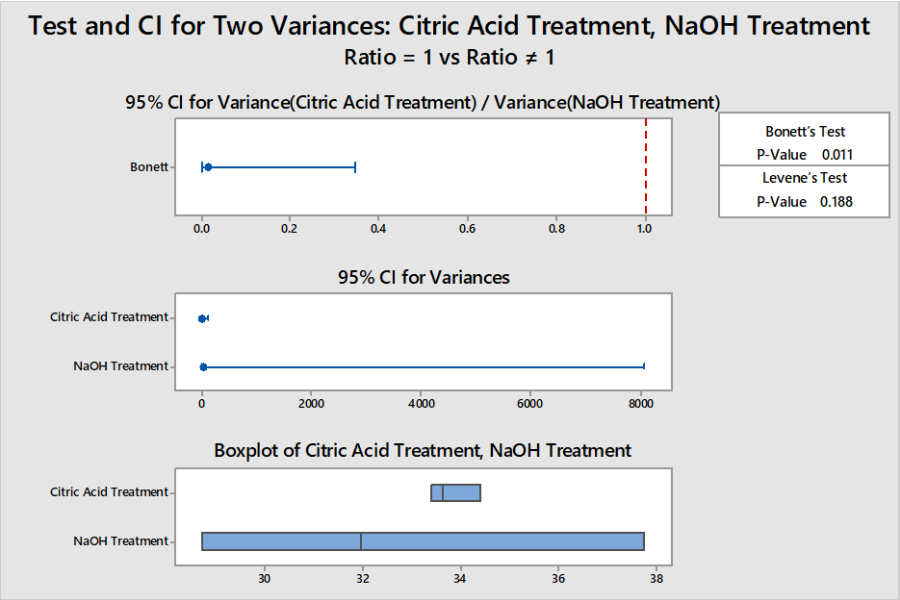

Figure 3. Test for equal variance of citric acid treatment and NaOH treatment

Due to the unequal variance, a Welch two-sample t-test is used to compare the group means. The hypotheses for the t-test are H_0: the mean bending strength is the same for both treatments, and H_1: the means is different. The result of the test is shown as Figure 4. The P value of 0.742 is greater than the significance level of $\alpha = 0.05$ and H_0 is not rejected, this indicates there is no significant difference in mean bending strength.

```
Two-sample T for Citric Acid Treatment vs NaOH Treatment

                        N    Mean  StDev  SE Mean
Citric Acid Treatment   3  33.827  0.525     0.30
NaOH Treatment          3   32.82   4.58      2.6


Difference = μ (Citric Acid Treatment) - μ (NaOH Treatment)
Estimate for difference:  1.01
95% CI for difference:  (-10.44, 12.45)
T-Test of difference = 0 (vs ≠): T-Value = 0.38  P-Value = 0.742  DF = 2
```

Figure 4. Welch two-sample t-test result

3.2. Effect of Surface Treatment on Hardness

The hardness value also evaluated through Brinell's hardness test with result shown as Figure 5. The mean hardness value for the epoxy, untreated, citric acid-treated, and NaOH-treated composites are 8.70 HB, 9.77 HB, 9.56 HB, and 9.01 HB respectively. These result indicate that incorporation of wood sawdust increase the surface hardness relative to epoxy.

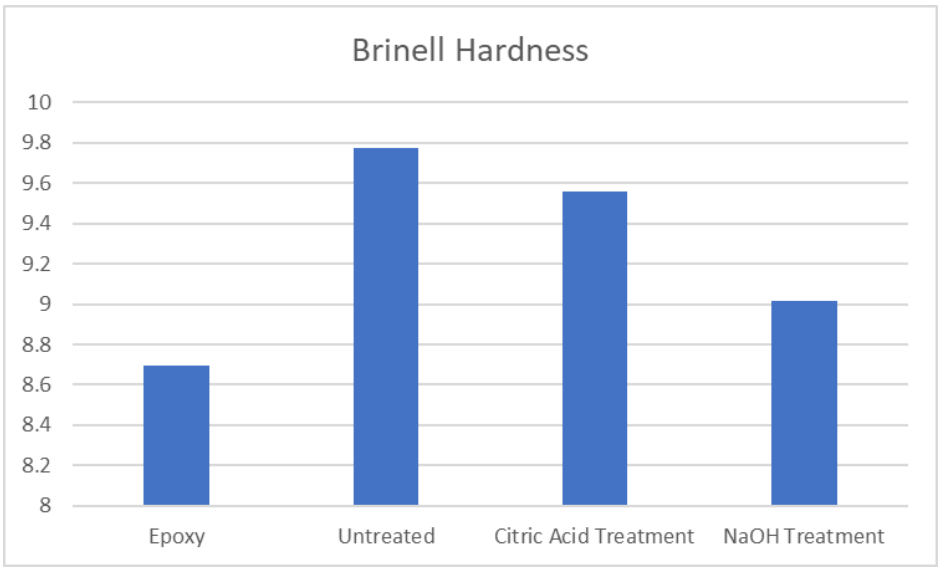

Figure 5. Brinell hardness

To determine wether these observed differences in hardness were statistically different, a one-way analysis of variance (ANOVA) was performed. The hypotheses are H_0: the mean Brinell hardness is the same for epoxy and all other treatments, and H_1: at least 1 mean is different resulting in a P value of 0.017 which is less than the significance level of $\alpha = 0.05$ and H_0 is rejected, indicating there is at least 1 mean is different as shown Figure 6.

Analysis of Variance

Source	DF	Adj SS	Adj MS	F-Value	P-Value
Treatment	3	2.1891	0.7297	6.33	0.017
Error	8	0.9221	0.1153		
Total	11	3.1112			

Figure 6. Analysis of variance of hardness value

To determine wether the difference between a pair of groups is statistically significant, the Tukey Pairwise Comparison is deployed. As shown in Figure 7., the grouping from each treatment including epoxy resulting in there is significant difference between epoxy and untreated wood sawdust composite's Brinell Hardness. The range of hardness value for each treatment and the confidence interval for the difference between the means of hardness are shown in Figure 8.a and b respectively.

Tukey Pairwise Comparisons

Grouping Information Using the Tukey Method and 95% Confidence

Treatment	N	Mean	Grouping
Untreated	3	9.773	A
Citric Acid	3	9.557	A B
NaOH	3	9.013	A B
Epoxy	3	8.697	B

Means that do not share a letter are significantly different.

Figure 7. Tukey pairwise comparisons result

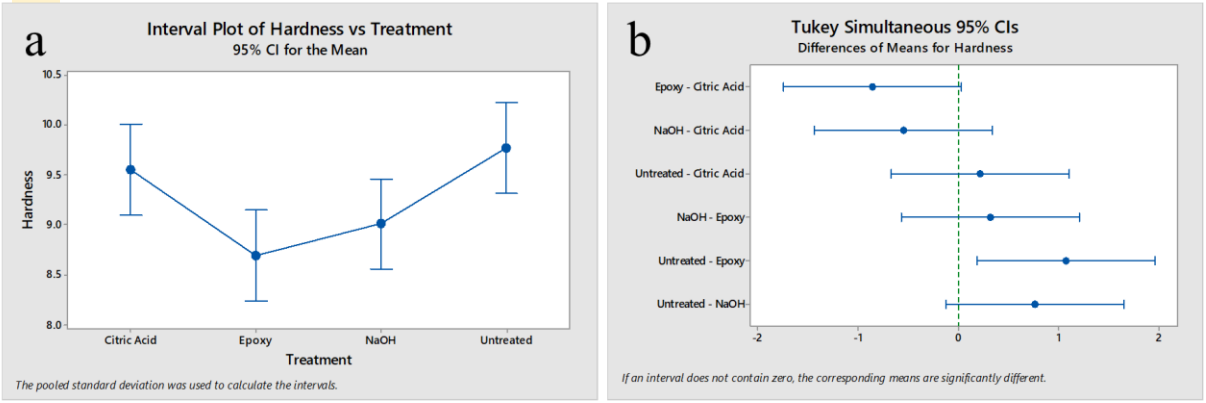

Figure 8. Interval plot of a) Hardness vs treatment; b) Difference of means for hardness

Figure 8.b show that the confidence interval for the difference between the means of untreated wood sawdust composite and epoxy does not include zero, which indicates that the difference between these means is significant. However, as shown in Figure 7. and 8.b, the hardness value for each composite of untreated wood sawdust, citric acid treated, and NaOH treated do not show any significant difference of means for hardness. These results indicate that both treatments enhanced fiber–matrix adhesion, leading to increased flexural strength without significantly affecting hardness. This aligns with prior studies showing that higher wood content generally increases hardness in wood–polymer composites [15]. However, since the wood sawdust content was constant across all specimens in this study, hardness remained unchanged. The elevated hardness values compared to pure epoxy further confirm the reinforcing effect of wood sawdust.

In summary, citric acid achieves the mechanical benefits of alkali treatment while being safer, renewable, and easy to implement. This makes citric acid surface treatment a practical alternative for producing high-strength, sustainable epoxy–wood composites, in line with trends in bio-composite research.

4. CONCLUSION

The citric acid surface treatment significantly enhanced the bending strength of the epoxy–sawdust composites compared with untreated sawdust. Statistical analysis using Welch's two-sample t-test showed no significant difference ($p = 0.742$) between the bending strengths of citric acid–treated and NaOH–treated composites, indicating that the two treatments are equivalently effective. In contrast, Brinell hardness testing revealed that wood sawdust reinforced composite achieved similar surface hardness regardless to the surface treatments, with one-way ANOVA indicating no significant difference among treatments. These results demonstrate that citric acid treatment enhances flexural performance to the same extent as NaOH without altering surface hardness. Due to its environmentally friendly characteristics, citric acid offers a viable and sustainable alternative to traditional alkaline treatments in natural fiber-reinforced composites.

5. ACKNOWLEDGEMENT

The authors wish to acknowledge the Material Testing Laboratory, Mechanical Engineering Department, Politeknik Negeri Bali for providing testing facilities for this research.

6. REFERENCES

[1] S. Shahani *et al.*, "Preparation and characterisation of sustainable wood plastic composites extracted from municipal solid waste," *Polymers (Basel)*, vol. 13, no. 21, Nov. 2021, doi: 10.3390/polym13213670.

[2] S. Vitolina, G. Shulga, B. Neiberte, J. Jaunslavietis, A. Verovkins, and T. Betkers, "Characteristics of the Waste Wood Biomass and Its Effect on the Properties of Wood Sanding Dust/Recycled PP Composite," *Polymers (Basel)*, vol. 14, no. 3, Feb. 2022, doi: 10.3390/polym14030468.

[3] K. C. Devendrappa and P. N. R., "Investigate Technical Viability to Fabricate Wood Polymer Composites Made of Waste Wood Powder and Epoxy Resin," *INTERANTIONAL JOURNAL OF SCIENTIFIC RESEARCH IN ENGINEERING AND MANAGEMENT*, vol. 08, no. 06, pp. 1–5, Jun. 2024, doi: 10.55041/ijsrem35976.

[4] N. Kharchi *et al.*, "Citric acid treatment: A new approach to improving Ampelodesma mauritanica fibers-poly-lactic acid composites," *Ind Crops Prod*, vol. 223, Jan. 2025, doi: 10.1016/j.indcrop.2024.120143.

[5] H. Al Abdallah, B. Abu-Jdayil, and M. Z. Iqbal, "The Effect of Alkaline Treatment on Poly(Lactic Acid)/Date Palm Wood Green Composites for Thermal Insulation," *Polymers (Basel)*, vol. 14, no. 6, Mar. 2022, doi: 10.3390/polym14061143.

[6] E. O. Olakanmi, E. A. Ogunesan, E. Vunain, R. A. Lafia-Araga, M. Doyoyo, and R. Meijboom, "Mechanism of fiber/matrix bond and properties of wood polymer composites produced from alkaline-treated *D aniella oliveri* wood flour," *Polym Compos*, vol. 37, no. 9, pp. 2657–2672, Sep. 2016, doi: 10.1002/pc.23460.

[7] X. Liu *et al.*, "Effects of alkali treatment on the properties of WF/PLA composites," *J Adhes Sci Technol*, vol. 31, no. 10, pp. 1151–1161, May 2017, doi: 10.1080/01694243.2016.1248703.

[8] J. De and R. N. Baxi, "Experimental Investigation and Analysis of Mercerized and Citric Acid Surface Treated Bamboo Fiber Reinforced Composite," in *IOP Conference Series: Materials Science and Engineering*, Institute of Physics Publishing, Sep. 2017. doi: 10.1088/1757-899X/225/1/012154.

[9] Q. Wu, K. Jiang, Y. Wang, Y. Chen, and D. Fan, "Cross-linked peach gum polysaccharide adhesive by citric acid to produce a fully bio-based wood fiber composite with high strength," *Int J Biol Macromol*, vol. 253, Dec. 2023, doi: 10.1016/j.ijbiomac.2023.127514.

[10] L. Cruz-Lopes, M. Sell, R. Lopes, and B. Esteves, "Enhancing Pinus pinaster Wood Durability Through Citric Acid Impregnation," *Sustainability (Switzerland)*, vol. 17, no. 5, Mar. 2025, doi: 10.3390/su17051979.

[11] M.-A. Berube, D. Schorr, R. J. Ball, V. Landry, and P. Blanchet, "Determination of In Situ Esterification Parameters of Citric Acid-Glycerol Based Polymers for Wood Impregnation," *J Polym Environ*, vol. 26, no. 3, pp. 970–979, Mar. 2018, doi: 10.1007/s10924-017-1011-8.

[12] F. Vilaseca, F. Serra-Parareda, E. Espinosa, A. Rodríguez, P. Mutjé, and M. Delgado-Aguilar, "Valorization of hemp core residues: Impact of NaOH treatment on the flexural strength of PP composites and intrinsic flexural strength of hemp core fibers," *Biomolecules*, vol. 10, no. 6, Jun. 2020, doi: 10.3390/biom10060823.

[13] N. Sienkiewicz, M. Dominic, and J. Parameswaranpillai, "Natural Fillers as Potential Modifying Agents for Epoxy Composition: A Review," Jan. 01, 2022, *MDPI*. doi: 10.3390/polym14020265.

[14] L. Simonini and A. Dorigato, "Surface Modification of Wood Fibers with Citric Acid as a Sustainable Approach to Developing Novel Polycaprolactone-Based Composites for Packaging Applications," *Journal of Composites Science*, vol. 9, no. 6, p. 274, May 2025, doi: 10.3390/jcs9060274.

[15] B. Jian *et al.*, "A Review on Flexural Properties of Wood-Plastic Composites," Oct. 01, 2022, *MDPI*. doi: 10.3390/polym14193942.

LOGIC
Journal of Engineering Design and Technology
Vol. 25 No.2 July 2025; p. 107 - 116

p-ISSN : 1412-114X
e-ISSN : 2580-5649
http://ojs2.pnb.ac.id/index.php/LOGIC

EXPERIMENTAL STUDY ON SOLAR DRYING OF ARABICA COFFEE BEANS: ACHIEVING STANDARD MOISTURE CONTENT USING A DRYING CHAMBER COLLECTOR

Hilman Mafazi [1)*], Selly Septianissa [1)], Ahmad Rajani [2)]

1) Department of Mechanical Engineering, Widyatama University, Bandung 40125, Indonesia
2) Research Centre for Energy Conversion and Conservation, BRIN, Indonesia

Correponding email: hilman.mafazi@widyatama.ac.id

Abstract. Drying technology plays a critical role in preserving and enhancing the quality of agricultural products, particularly in the post-harvest handling of Arabica coffee. In this experimental study, Arabica coffee beans were dried using a solar drying chamber equipped with a collector system to achieve standard moisture content. A total of 6000 grams of coffee beans were dried over 28 hours, with the system operating under an average chamber temperature of 40°C and a peak solar radiation intensity of 1122 W/m² occurring at 12:00 PM. The drying process utilized an air velocity of 9.2 m/s to enhance heat and mass transfer within the chamber. Among all trays tested, tray 2 produced the best quality beans with a final moisture content of 11.8%, aligning with the recommended standard for green coffee storage. These results demonstrate that integrating high air velocity and optimized collector design in a solar drying chamber can significantly reduce moisture content while maintaining bean quality, thereby offering an effective and sustainable alternative to conventional drying methods.

Keywords : Arabica Coffee, Air Velocity, Drying Chamber, Moisture Content, Solar Drying

1. INTRODUCTION

Coffee is one of the most widely traded agricultural commodities in the world and plays a crucial role in the economies of many developing countries [1–3]. In Indonesia, Arabica coffee is a prominent export product, especially from highland regions, where its unique flavor and aroma characteristics are preserved [4], [5]. Post-harvest processing is essential to maintain the quality of coffee beans, and among the various stages, drying is particularly influential [6–9]. The drying process not only determines the moisture content but also affects the physical appearance, biochemical composition, and storage stability of the beans[10–13].

Traditionally, coffee beans are dried using open sun drying methods [13], [14]. While this technique is cost-effective and accessible for smallholder farmers, it has several disadvantages: it is highly weather-dependent, requires large drying areas, and often results in uneven drying and potential contamination from dust, pests, and microbial activity [15], [16]. Under ideal conditions, sun drying may take 2 to 3 weeks to reduce the moisture content of coffee beans to the standard range of 11–12% wet basis, suitable for storage and export [17], [18] However, in practice, fluctuating environmental conditions frequently compromise efficiency and product quality [19]

To improve drying efficiency and consistency, solar dryers have been developed and classified into direct, indirect, and hybrid modes [20–23]. These systems aim to reduce drying time and enhance quality by creating controlled microclimates within drying chambers [24], [25]. Notably, the integration of solar collectors and forced air convection systems has emerged as a promising alternative to traditional methods [26], [27]. Forced convection can significantly improve heat and mass transfer by increasing the air velocity across the drying surface, accelerating moisture removal, and allowing for better control of drying parameters [26], [28].

Recent studies have demonstrated the importance of airflow variation in solar drying systems [29].

investigated the effect of different air velocities (1–3 m/s) on the drying performance and quality of Arabica coffee beans [29]. Their results showed that varying airflow had a significant impact on drying time and moisture content, with lower velocities yielding better moisture control while higher velocities slightly reduced efficiency [29]. Meanwhile, Kebede et al., evaluated a diminutive solar dryer with an integrated reflector and blower system in the Ethiopian highlands. Their study achieved a final moisture content of 10% in only two days, highlighting the effectiveness of optimized collector design and airflow control in maintaining coffee quality [30].

Building on this foundation, the present study focuses on an experimental evaluation of Arabica coffee drying using a solar drying chamber equipped with a collector system and operating at an air velocity of 9.2 m/s, substantially higher than in many previous studies. The research explores how collector orientation, surface material, and solar exposure time affect the internal temperature, humidity, and drying kinetics within the chamber. A batch of 6000 g of Arabica coffee beans was dried over 42 hours, and key performance indicators such as moisture content, drying rate, solar radiation, and chamber conditions were closely monitored. This study aims to contribute to the ongoing optimization of sustainable, off-grid drying technologies that enhance quality and efficiency in coffee processing, particularly in rural or electricity-scarce regions.

2. METHODS

2.1. Materials

The coffee beans used in this study were Arabica variety, sourced from Pangalengan, West Java. The cherries were harvested at optimal ripeness and underwent standard post-harvest processing, including de-pulping, washing, and an 8-hour fermentation period to remove mucilage. After fermentation, the beans were rinsed and prepared for drying. The beans were spread in a thin layer (0.5-1 cm thickness) on drying trays to ensure uniform exposure to hot air during the drying process.

2.2. Equipment

The drying system consisted of a single-unit solar coffee dryer, specifically designed to optimize heat transfer and air circulation. The main components are illustrated in Figure 1. The drying chamber measured approximately 900 × 800 × 1200 mm. The outer casing was constructed from aluminum sheets and insulated with glass wool to minimize heat loss. The interior walls were lined with aluminum foil to maintain cleanliness and prevent contamination of the coffee beans.

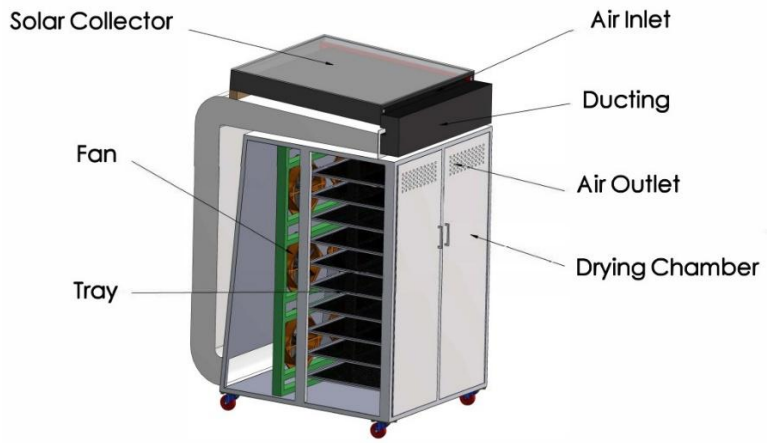

Figure 1. Coffee drying unit utilizing forced convection

The solar collector was built using a single layer of glass and a black-painted metal absorber plate designed to maximize solar energy capture. The collector was integrated into the drying system to ensure a continuous supply of heated air. An axial blower fan was installed to force hot air from the collector into the drying chamber at a velocity of 9.2 m/s. This setup was intended to enhance the convective drying process and ensure even moisture reduction across all trays. Temperature and relative humidity inside the drying chamber were monitored using thermocouples connected to a data logger. Solar radiation intensity was measured using a solar power meter, and bean moisture content was assessed periodically using a moisture analyzer.

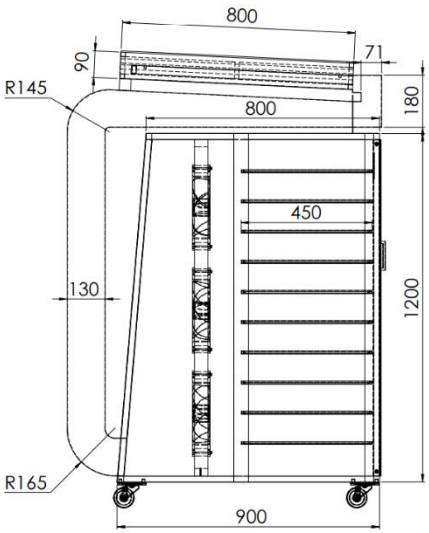

Figure 2. Assembly design of the solar-powered coffee drying unit

2.3. Experimental Procedure

The drying experiments were conducted daily from 08:00 a.m. to 03:00 p.m. to take advantage of peak solar irradiance with a temperature of 46.5°C. Each test involved drying 6000 grams of Arabica coffee beans in the chamber until they reached a target moisture content of approximately 11.8% wet basis, suitable for safe storage and quality preservation. The coffee beans were evenly distributed in a thin layer (0.5–1 cm) on the drying trays to ensure uniform exposure to the heated air circulating inside the chamber.

Throughout the drying process, key environmental and operational parameters such as chamber temperature, relative humidity, solar radiation intensity, and ambient conditions were recorded every 15 minutes using thermocouples and a data logger system. The experiment focused on evaluating the system's drying efficiency by monitoring moisture reduction rate, drying time, and the stability of chamber conditions, aiming to demonstrate the effectiveness of the solar dryer in producing high-quality coffee with improved energy efficiency.

3. RESULTS AND DISCUSSION

3.1 Thermal Performance of the Solar Drying System

The performance of the solar drying chamber was significantly influenced by daily solar radiation patterns. As shown in Figure 3, solar radiation exhibited a bell-shaped curve across all five days, with peak intensities occurring between 11:00 AM and 12:30 PM. Day 4 recorded the highest radiation intensity, peaking at 1122 W/m², while Day 1 exhibited the lowest values. These variations directly impacted the thermal response of the dryer components and ultimately affected the drying process efficiency.

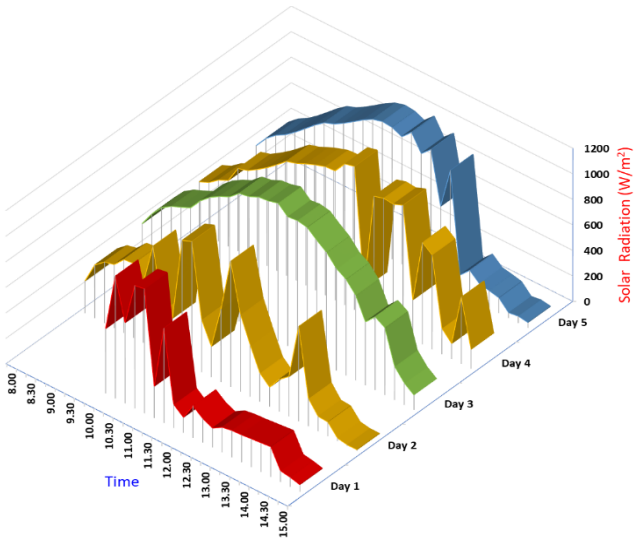

Figure 3. Daily solar radiation of the mobile solar dryer

Figure 4 presents the temperature distribution within the Phase Change Material (PCM) housing, which acts as a thermal energy buffer. PCM housing temperatures steadily increased during daylight hours and remained relatively stable in the afternoon, particularly on days 2 to 5. Peak PCM temperatures ranged from 60°C to 72.25°C, demonstrating the effectiveness of the PCM in storing and gradually releasing heat energy. This buffering capability helped mitigate temperature drops and extended the chamber's thermal activity beyond peak solar hours.

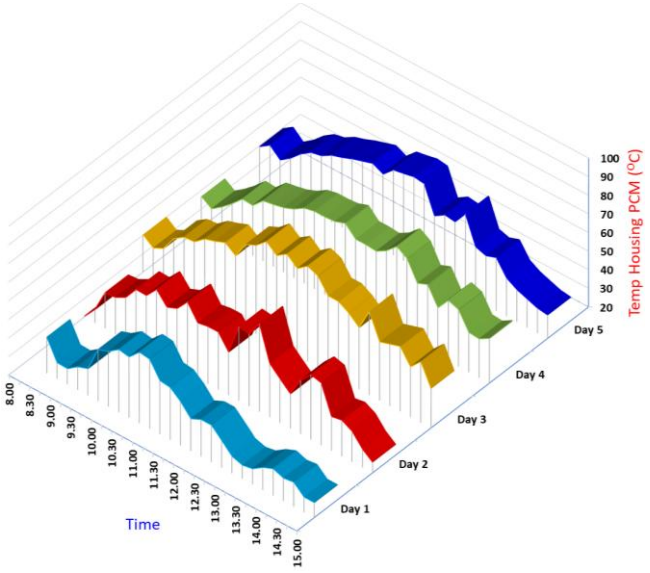

Figure 4. PCM (phase change material) housing temperature - mobile solar dryer

In parallel, Figure 5 highlights the performance of the aluminum absorber plate, which is crucial for converting solar radiation into heat. During Days 4 and 5, absorber plate temperatures consistently exceeded 72°C during midday hours, indicating a high absorption efficiency. This high-temperature gradient between the absorber and the drying air facilitated effective heat transfer into the chamber.

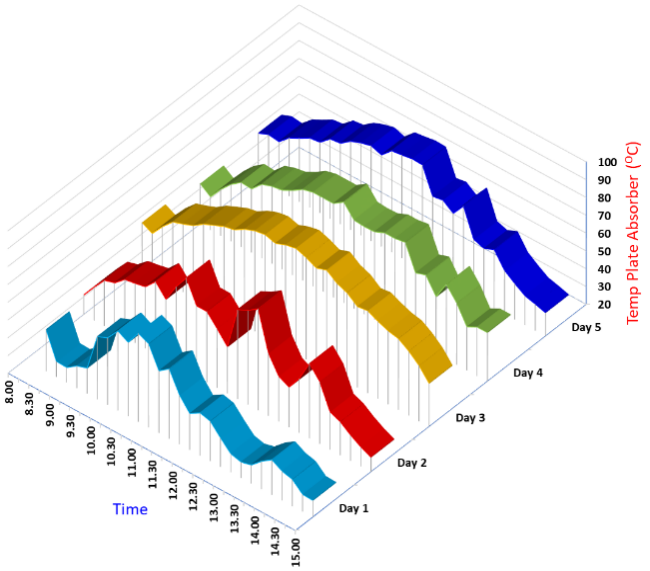

Figure 5. Aluminum absorber plate temperature - mobile solar dryer

The internal drying chamber temperatures, as illustrated in Figure 6, ranged from 40°C to 46.5°C, with an average peak of around 46.5°C. This temperature range is considered optimal for drying Arabica coffee, supporting both rapid moisture reduction and quality preservation. Notably, Days 3 through 5 maintained higher and more consistent chamber temperatures compared to the first two days, correlating with higher radiation intensity and improved absorber/PCM response.

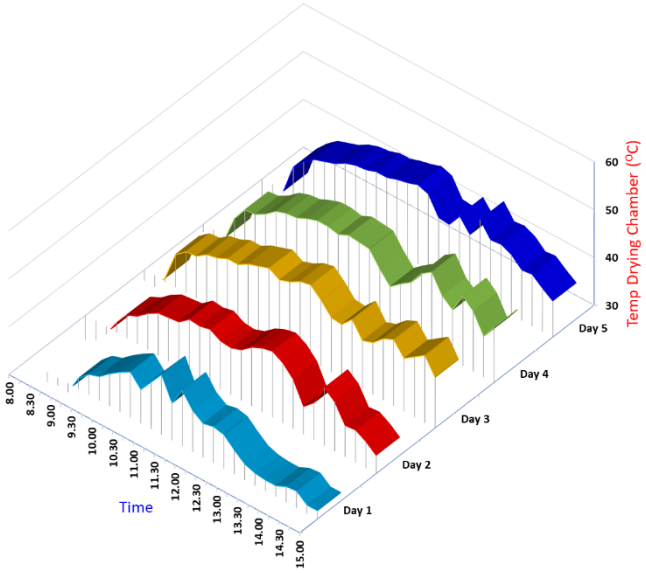

Figure 6. Drying chamber temperature

3.2. Drying Behavior and Process Efficiency

The combination of solar collector design, PCM integration, and forced air convection at 9.2 m/s contributed to efficient and uniform drying across all trays. The high air velocity improved heat and mass transfer inside the chamber, ensuring consistent exposure of beans to hot air and preventing uneven moisture removal. The drying chamber was equipped with 12 perforated trays, arranged vertically from Tray 1 (bottom) to Tray 12 (top). Tray 2, referred to in the results section, was positioned as the second-lowest tray. The vertical arrangement was used to evaluate the effect of airflow and temperature distribution on drying performance at different heights. Among all trays tested, tray 2 consistently produced beans with a final moisture content of 10%, aligning with storage standards for green coffee.

While Days 1 and 2 experienced slightly lower solar input, the drying system still managed to sustain chamber temperatures above 40°C, aided by the thermal insulation and latent heat release from the PCM. This resilience suggests that the system remains functional under moderate environmental conditions, making it suitable for variable tropical climates.

The experimental drying duration of 28 hours to reach 11.8% moisture content is notably shorter than traditional sun drying methods, which can take several weeks under fluctuating weather. This reduction in drying time not only enhances processing efficiency but also minimizes the risk of contamination and quality degradation due to prolonged exposure. To prevent rehydration or moisture absorption during non-drying periods (evenings and nights), the coffee beans were stored in a sealed, clean, and dry container each day after drying. The storage area was kept at room temperature and protected from ambient humidity exposure, ensuring that the drying progress remained stable across the entire process.

Overall, the results confirm that integrating solar energy with thermal storage and forced convection provides a reliable and energy-efficient solution for post-harvest coffee processing. For future development, additional studies may explore optimizing PCM volume, airflow direction, or collector surface treatment to further enhance system performance and potentially enable nighttime drying cycles.

3.3. Thermal Performance of the Solar Drying System

The performance of the solar dryer was strongly influenced by the daily pattern and intensity of solar radiation. During the four days of testing, solar radiation peaked between 11:00 AM and 1:30 PM, reaching a maximum of 1122 W/m² on day 4. Day 1 showed the most irregular radiation pattern, with abrupt drops likely caused by transient cloud cover, which impacted the heat gain of the system.

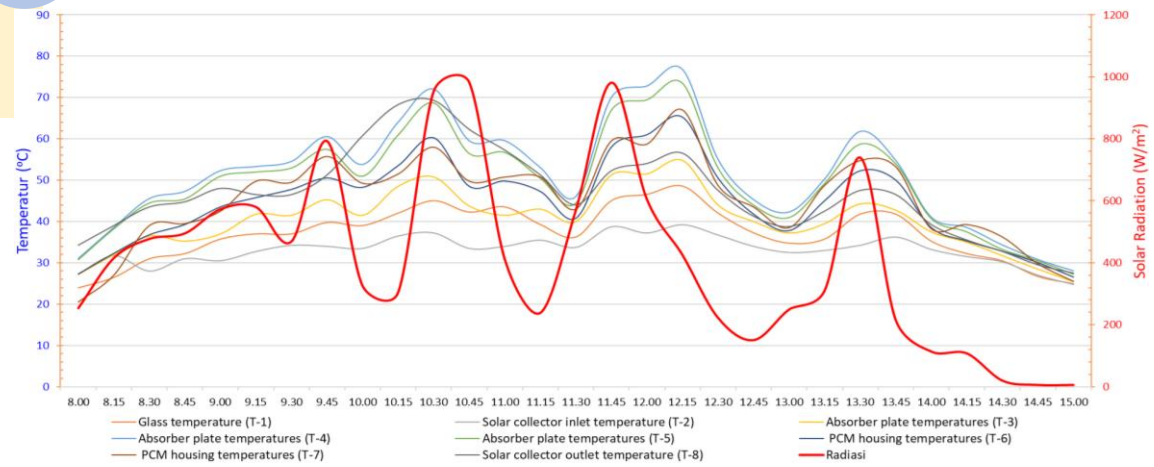

Figure 7. Graph of glass temperature, collector, absorber plate, pcm housing, and solar radiation (day 1)

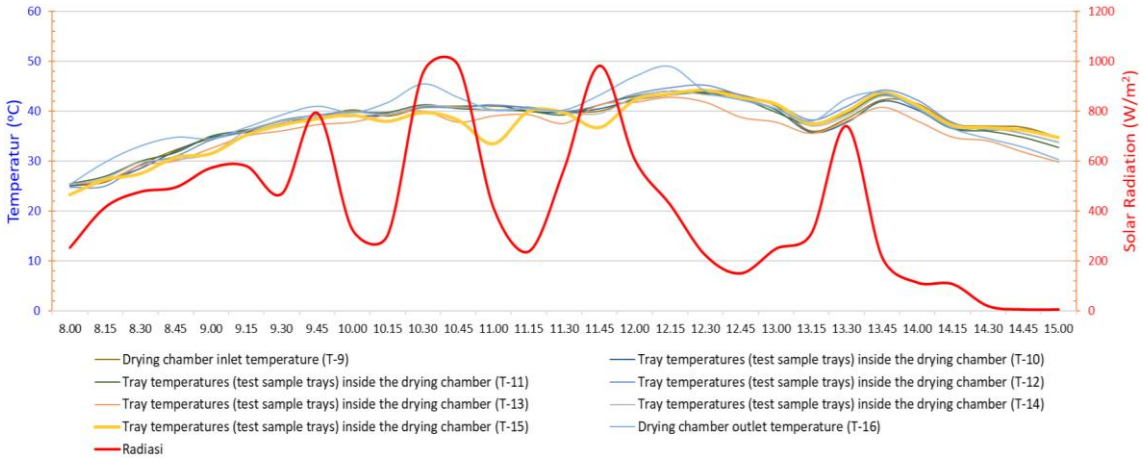

Figure 8. Graph of drying chamber temperature, tray temperature, and solar radiation (day 1)

The absorber plate responded quickly to changes in radiation, with maximum temperatures exceeding 75°C on Days 2 and 4. This confirms the effectiveness of the black-painted metal surface in absorbing solar energy and transferring it to the airflow. Meanwhile, the PCM housing exhibited a delayed yet stable rise in temperature, peaking at 72.25°C on day 3. This delayed thermal response highlights the role of PCM as a thermal buffer that stabilizes the drying environment during periods of fluctuating solar input.

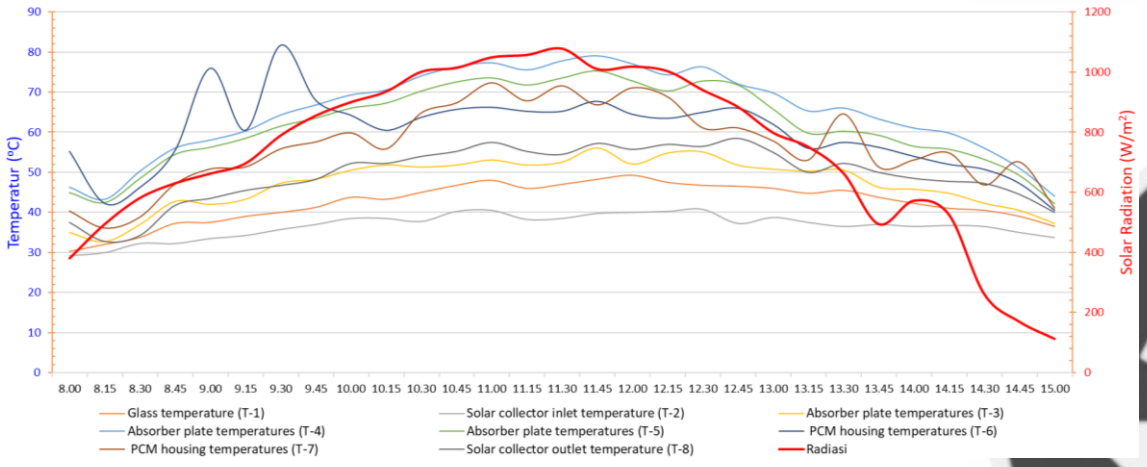

Figure 9. Graph of glass temperature, collector, absorber plate, pcm housing, and solar radiation (day 2)

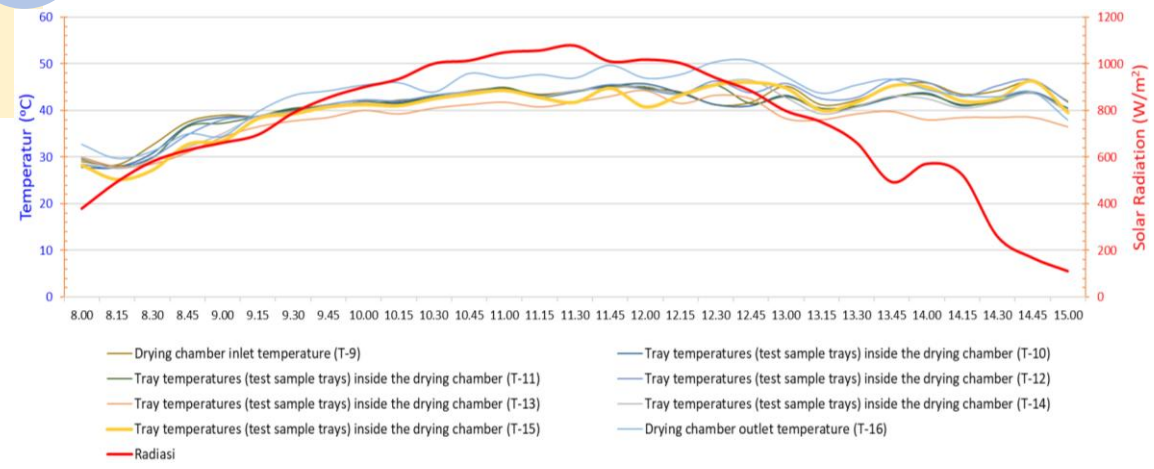

Figure 10. Graph of drying chamber temperature, tray temperature, and solar radiation (day 2)

Temperature differences between the collector inlet and outlet remained consistent at 30-55°C during peak radiation hours, indicating efficient heat transfer. Additionally, the drying chamber maintained average internal temperatures ranging from 40°C to 46.5°C, optimal for drying Arabica coffee while preserving quality.

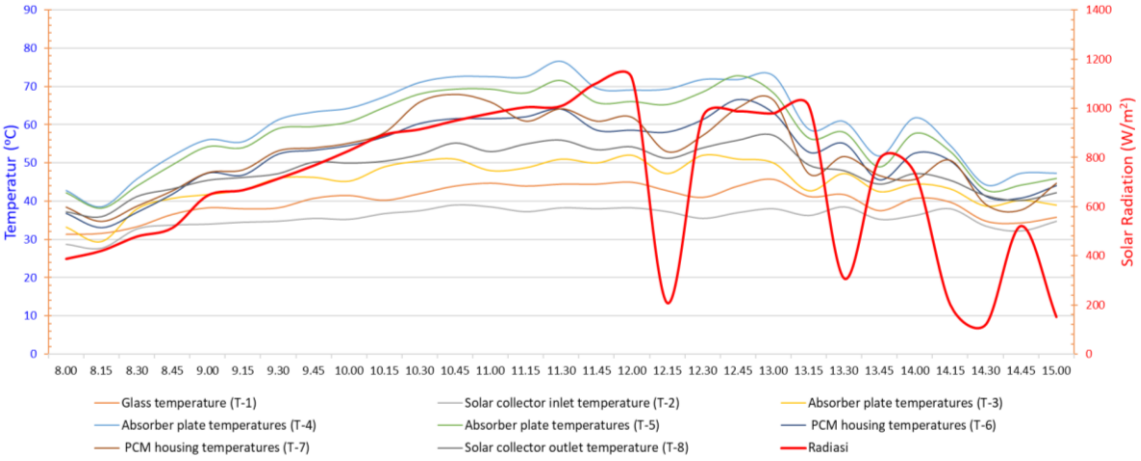

Figure 11. Graph of glass temperature, collector, absorber plate, pcm housing, and solar radiation (day 3)

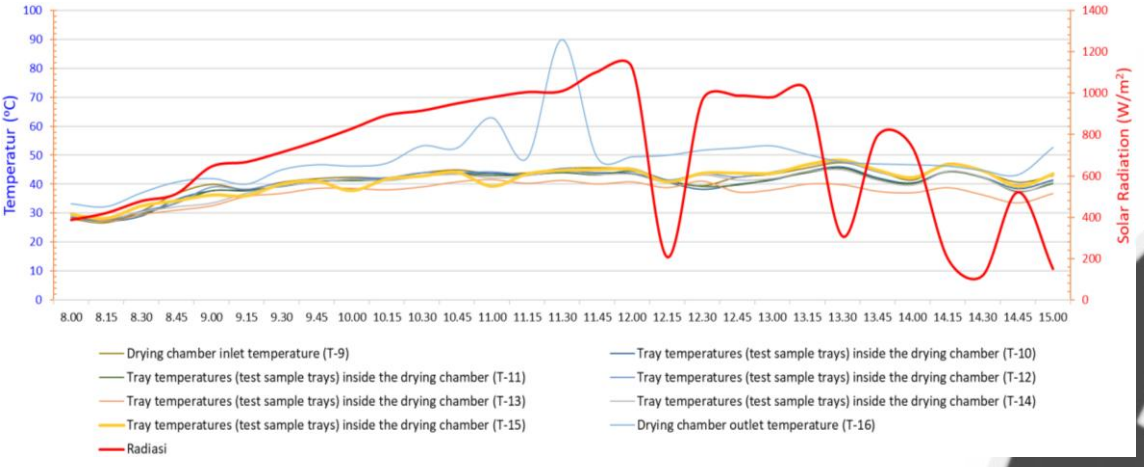

Figure 12. Graph of drying chamber temperature, tray temperature, and solar radiation (day 3)

Day 4 demonstrated the most stable thermal performance across all components, with minimal fluctuation in absorber plate and PCM temperatures. The combination of strong solar input, thermal insulation, and PCM heat storage contributed to this consistency, making the system reliable under varying climatic conditions.

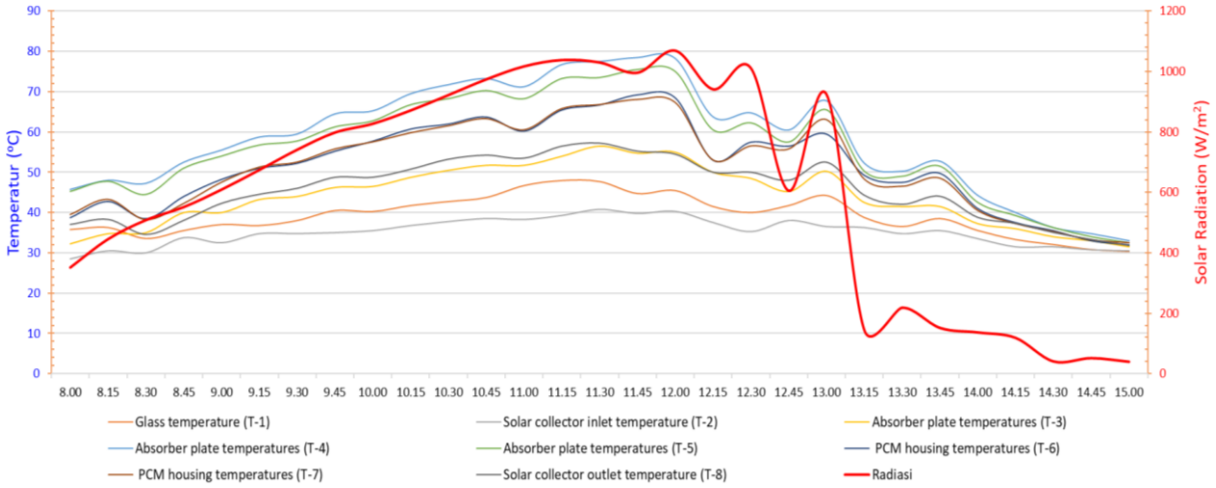

Figure 13. Graph of glass temperature, collector, absorber plate, pcm housing, and solar radiation (day 4)

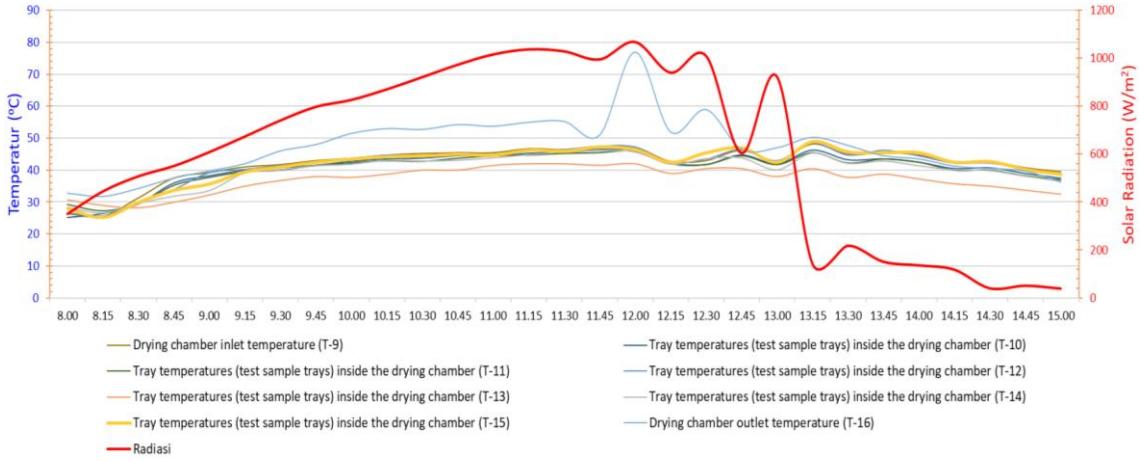

Figure 14. Graph of drying chamber temperature, tray temperature, and solar radiation (day 4)

3.4. Drying Behavior, Efficiency, and Implications

Temperature measurements at various trays inside the drying chamber (T-10 to T-15) showed a fairly uniform distribution, generally ranging between 40°C and 45°C. Slight variations in trays T-12 and T-14, which exhibited earlier temperature peaks, suggest minor positional effects related to airflow distribution. Nevertheless, the overall thermal uniformity ensured even drying across all trays.

These results indicate a vertical moisture gradient, where lower trays (Tray 1–4) generally achieved better drying performance compared to upper trays (Tray 9–12). This gradient can be attributed to the vertical upward flow of heated air inside the chamber, which loses temperature and velocity as it rises. Notably, tray 2 produced the lowest final moisture content (10.0%), representing the optimal tray position under the current system configuration. This superior result to the main heat source and air inlet, resulting in high and stable air temperatures.

In contrast, tray 1, although closest to the heat source, showed slightly higher moisture content (11.8%), possibly due to limited air circulation right at the chamber floor or heat being lost to the base. Trays in the upper part (Tray 10–12) performed less effectively due to reduced temperature and airflow intensity as the air rises and heat dissipates. These findings underline the importance of tray position optimization in vertical dryers and justify the need for improved airflow balancing or chamber redesign to reduce positional drying variation.

The correlation between radiation and temperature in system components was evident, particularly in absorber and collector outlet temperatures, which closely mirrored solar intensity patterns. However, the PCM helped mitigate abrupt temperature drops in the drying chamber such as those observed around noon on Day 1 and Day 4 by gradually releasing stored heat.

The 9.2 m/s forced air velocity played a key role in sustaining even temperature distribution. This high airflow rate enhanced convective heat and mass transfer, preventing hotspots or cold zones in the chamber. As a result, the drying process was efficient and consistent throughout the 28 hours total duration. Compared to traditional open-sun drying, which may take up to two weeks depending on the weather, the experimental dryer significantly reduced drying time while improving hygiene and quality control. The final moisture content of 11.8% especially consistent in Tray 2 meets the standard for green coffee storage and ensures better shelf life. These findings validate the integration of solar thermal collectors, PCM storage, and forced convection as an effective post-harvest drying solution. This design is particularly relevant for off-grid rural communities, providing a clean, low-cost, and scalable alternative for sustainable coffee processing.

Despite its promising performance, the current system relies heavily on consistent daytime solar radiation, which can be limiting during extended cloudy or rainy periods. The absence of nighttime drying capability also restricts throughput. Additionally, the system has not yet been tested with different crop types or under extreme humidity conditions, which could affect its generalizability. Future work should focus on developing hybrid energy inputs (e.g., integrating biomass or electric heaters), automated drying control systems, and exploring multi-layer PCM designs to improve energy retention. Field trials in diverse climatic zones are also recommended to validate scalability and robustness of the system.

4. CONCLUSION

This experimental study demonstrates the effectiveness of a solar drying chamber equipped with a collector system, phase change material (PCM), and high-velocity forced convection in reducing the moisture content of Arabica coffee beans to the desired level. The system successfully dried 6000 grams of coffee beans to a final moisture content of 11.8% within 28 hours, a significant improvement compared to traditional open-sun drying methods that may take several days. The use of a 9.2 m/s axial blower fan enhanced convective heat and mass transfer, ensuring uniform drying across trays and reducing the risk of quality degradation due to uneven moisture distribution.

The integration of thermal insulation, PCM heat storage, and solar radiation collection provided consistent thermal performance even under fluctuating environmental conditions. Tray 2 consistently yielded the highest quality beans, confirming the chamber's uniformity and design reliability. These findings support the adoption of solar-powered, energy-efficient drying systems for post-harvest coffee processing, especially in rural or off-grid areas. Future research may focus on optimizing PCM mass, improving airflow design, and extending system functionality to enable nighttime drying, further enhancing its sustainability and scalability.

5. ACKNOWLEDGEMENT

The authors would like to express their deepest gratitude to the Research Centre for Energy Conversion and Conservation, BRIN, for providing all the necessary equipment and instrumentation used in this study. The authors also sincerely thank the Department of Mechanical Engineering, Widyatama University, for providing access to laboratory facilities and research space that supported the experimental work.

6. REFERENCES

[1] J. Pancsira, “International coffee trade: a literature review,” *J. Agric. Informatics*, vol. 13, 2022, doi: 10.17700/jai.2022.13.1.654.
[2] J. Abrhám, M. Vošta, P. Čajka, and F. Rubáček, “The specifics of selected agricultural commodities in international trade,” *AgEcon Search*, vol. 7, pp. 5–19, 2021.
[3] J. Abafita and T. Tadesse, “Determinants of global coffee trade: Do RTAs matter? Gravity model analysis,” *Cogent Econ. Finance*, vol. 9, 2021, doi: 10.1080/23322039.2021.1892925.
[4] J. E. Loppies *et al*., “Physical quality and flavor profile of arabica coffee beans (Coffea arabica) from Seko, South Sulawesi as a specialty coffee,” *IOP Conf. Ser. Earth Environ. Sci.*, vol. 1338, p. 012048, 2024, doi: 10.1088/1755-1315/1338/1/012048.
[5] F. Ashardiono and A. Trihartono, “Optimizing the potential of Indonesian coffee: a dual market approach,” *Cogent Soc. Sci.*, vol. 10, 2024, doi: 10.1080/23311886.2024.2340206.
[6] D. J. M. de Abreu *et al*., “Influence of drying methods on the post-harvest quality of coffee: effects on physicochemical, sensory, and microbiological composition,” *Foods*, vol. 14, p. 1463, 2025, doi: 10.3390/foods14091463.

[7] C. S. da Silva *et al*., "Post-harvest of coffee: factors that influence the final quality of the beverage," *Rev. Eng. Agric.*, vol. 30, pp. 49–62, 2022, doi: 10.13083/reveng.v30i1.12639.
[8] S. Das, "Post-harvest processing of coffee: An overview," *Coffee Sci.*, vol. 16, pp. 1–7, 2021, doi: 10.25186/.v16i.1976.
[9] E. T. Cortés-Macías *et al*., "Impact of post-harvest treatments on physicochemical and sensory characteristics of coffee beans in Huila, Colombia," *Postharvest Biol. Technol.*, vol. 187, p. 111852, 2022, doi: 10.1016/j.postharvbio.2022.111852.
[10] I. Wainaina *et al*., "Thermal treatment of common beans (Phaseolus vulgaris L.): Factors determining cooking time and its consequences for sensory and nutritional quality," *Compr. Rev. Food Sci. Food Saf.*, vol. 20, pp. 3690–3718, 2021, doi: 10.1111/1541-4337.12770.
[11] S. Aravindakshan *et al*., "The impact of drying and rehydration on the structural properties and quality attributes of pre-cooked dried beans," *Foods*, vol. 10, p. 1665, 2021, doi: 10.3390/foods10071665.
[12] D. Shofinita *et al*., "Drying methods of coffee extracts and their effects on physicochemical properties: A review," *Food Bioproc. Technol.*, vol. 17, pp. 47–72, 2024, doi: 10.1007/s11947-023-03067-4.
[13] E. F. Eshetu *et al*., "Effect of processing and drying methods on biochemical composition of coffee (Coffea arabica L.) varieties in Jimma Zone, Southwestern Ethiopia," *Cogent Food Agric.*, vol. 8, 2022, doi: 10.1080/23311932.2022.2121203.
[14] E. Duque-Dussán and J. Banout, "Improving the drying performance of parchment coffee due to the newly redesigned drying chamber," *J. Food Process Eng.*, vol. 45, 2022, doi: 10.1111/jfpe.14161.
[15] B. Soeswanto, N. L. E. Wahyuni, and G. Prihandini, "The development of coffee bean drying process technology – a review," 2021, doi: 10.2991/aer.k.211106.026.
[16] E. Duque-Dussán, J. R. Sanz-Uribe, and J. Banout, "Design and evaluation of a hybrid solar dryer for postharvesting processing of parchment coffee," *Renew. Energy*, vol. 215, p. 118961, 2023, doi: 10.1016/j.renene.2023.118961.
[17] D. S. Ferreira *et al*., "Association of altitude and solar radiation to understand coffee quality," *Agronomy*, vol. 12, p. 1885, 2022, doi: 10.3390/agronomy12081885.
[18] S. Madhankumar *et al*., "A review on the latest developments in solar dryer technologies for food drying process," *Sustain. Energy Technol. Assess.*, vol. 58, p. 103298, 2023, doi: 10.1016/j.seta.2023.103298.
[19] A. E. Peñuela Martínez, J. R. Sanz Uribe, and R. D. Medina Rivera, "Influence of drying air temperature on coffee quality during storage," *Rev. Fac. Nac. Agron. Medellin*, vol. 76, pp. 10493–10503, 2023, doi: 10.15446/rfnam.v76n3.104115.
[20] G. Prasad, S. Sarkar, and L. N. Sethi, "Solar drying technology for agricultural products: A review," *Agric. Rev.*, 2024, doi: 10.18805/ag.R-2457.
[21] M. Yazici and R. Kose, "Energy, exergy and economic investigation of novel hybrid dryer, indirect solar dryer and traditional shade drying," *Therm. Sci. Eng. Prog.*, vol. 49, p. 102502, 2024, doi: 10.1016/j.tsep.2024.102502.
[22] G. D. Shekata, G. S. Tibba, and A. T. Baheta, "Recent advancements in indirect solar dryer performance and the associated thermal energy storage," *Results Eng.*, vol. 24, p. 102877, 2024, doi: 10.1016/j.rineng.2024.102877.
[23] W. Hao *et al*., "Research on the performance and life cycle assessment of photovoltaic/thermal hybrid solar dryer: Comparative analysis with direct and mixed-mode," *Appl. Therm. Eng.*, vol. 272, p. 126425, 2025, doi: 10.1016/j.applthermaleng.2025.126425.
[24] D. Kong, Y. Wang, M. Li, and J. Liang, "A comprehensive review of hybrid solar dryers integrated with auxiliary energy and units for agricultural products," *Energy*, vol. 293, p. 130640, 2024, doi: 10.1016/j.energy.2024.130640.
[25] A. H. Majeed, J. J. Faraj, and F. M. Hussien, "Enhancing solar drying efficiency through indirect solar dryers integrated with phase change materials," *Int. J. Heat Technol.*, vol. 42, pp. 121–131, 2024, doi: 10.18280/ijht.420113.
[26] H. Chouikhi and B. M. A. Amer, "Performance evaluation of an indirect-mode forced convection solar dryer equipped with a PV/T air collector for drying tomato slices," *Sustainability*, vol. 15, p. 5070, 2023, doi: 10.3390/su15065070.
[27] D. D. S. Garcia-Marquez *et al*., "Prototype of a solar collector with the recirculation of nanofluids for a convective dryer," *Int. J. Renew. Energy Dev.*, vol. 11, pp. 1124–1133, 2022, doi: 10.14710/ijred.2022.44221.
[28] N. Ouyang *et al*., "Improvement and development of physical field drying technology: Principles, models, optimizations and hybrids," *Food Eng. Rev.*, 2025, doi: 10.1007/s12393-025-09398-6.
[29] P. Siagian *et al*., "The effect of varying the air flow in a solar collector on the quality of Arabica coffee beans," *Fluids*, vol. 9, p. 75, 2024, doi: 10.3390/fluids9030075.
[30] A. Y. Kebede *et al*., "Performance evaluation of diminutive solar dryer for drying of green coffee beans: In Ethiopian highlands," *Case Stud. Therm. Eng.*, vol. 65, p. 105653, 2025, doi: 10.1016/j.csite.2024.105653.

LOGIC
Journal of Engineering Design and Technology
Vol. 25 No.2 July 2025 ; p. 117 - 125

p-ISSN : 1412-114X
e-ISSN : 2580-5649
http://ojs2.pnb.ac.id/index.php/LOGIC

ANALYSIS OF THE IMPACT TEST STRENGTH OF SQUID FIBRE-REINFORCED COMPOSITES

Fiky Firmansyah [1], Moh. Hartono [1]

1) Mechanical Engineering Departement, State Polytechnic of Malang, Jl Soekarno-Hatta 9, Malang, Indonesia

Correponding email [1] : moh.hartono@polinema.ac.id

Abstract. This study aims to determine the effect of volume fraction, fibre angle direction, and fibre length on the impact strength of squid fibre-reinforced composites. Squid fibre is a natural animal fibre that has excellent potential in the development of composite materials. The use of squid fibre as a composite reinforcement can be an alternative to reduce organic waste from marine products and produce new composite materials in sustainable manufacturing applications. The research method was conducted with quantitative experiments to determine the effect of fibre volume fraction with variations of 25%, 50%, and 75%; fibre angle direction with variations of 45° and 90°; and fibre length with variations of 20 mm, 30 mm, and 40 mm. This study used the Factorial DOE statistical data analysis method. The results showed that volume fraction and fibre length significantly affected the impact strength of the composite. The higher the volume fraction and fibre length, the higher the impact strength value of the composite. Meanwhile, the direction of fibre did not show a significant effect. The 75% volume fraction produced the highest impact strength of 0,0738 J/mm², and the 25% volume fraction produced the lowest value of 0,066 J/mm². The 45° fibre direction produced an impact strength value of 0,07098 J/mm², and the 90° fibre direction produced a value of 0,07097 J/mm². The 40 mm fibre length produced the highest impact strength value of 0,078 J/mm², and the 90° fibre direction produced a value of 0,07097 J/mm².

Keywords : Composite, Epoxy, Squid Fibre, Impact Test.

1. INTRODUCTION

Technological developments in the materials industry are proliferating, especially in composite materials. Composites have many advantages, including corrosion resistance, structural strength, environmental friendliness, and lightweight, so their utilisation must be maximized. Composites are materials formed by combining two or more separate components to achieve physical and mechanical qualities superior to those of the individual constituent components [1]. In composites, natural fibers are starting to be used as reinforcing materials. Natural fibers are fibers obtained from nature, both plants and animals. Plant-derived fibers are banana leaf, jute, pineapple, and bagasse fiber. Animal-derived fibers are fleece, leather, and squid fiber. Natural fibers have several advantages over synthetic fibers, such as being recyclable, renewable, safe for the environment and human health, having superior mechanical qualities, not causing tool abrasion, cheaper, and lower density [2].

Many natural resources in the sea can be processed to be useful. One of the abundant natural resources is squid, which has a part in the form of squid fiber or squid cranial bone. However, few people know that this animal contains fiber in its squid, which is usually discarded when squid meat is processed [3]. Squid fiber is organic waste, so it needs to be utilized to explore the use of organic waste as reinforcement material in composites. According to data from the Ministry of Maritime Affairs and Fisheries of the Republic of Indonesia, 0.82% of squid fiber is utilized in Indonesian waters [4]. Using squid fiber as a composite material can increase the use value of underutilized squid fiber, thus helping to reduce organic waste.

This study employs organic waste readily available in Indonesia, specifically squid fibre. Due to research restrictions, squid fibre is still infrequently used as a reinforcing material in composites. Squid fibre has not been extensively studied in materials engineering. Thus, its application is less common than natural fibres such as

coconut, hemp, or glass fibre. Furthermore, squid fibre's thin, transparent, and flexible nature needs particular treatment to work ideally as reinforcement in composite structures. Processing problems, such as alkalisation treatment, also limit its broad use. Squid fiber is often a waste problem if not utilized properly, so it is processed in a certain way to be used as a basis for composite material engineering. The central concept is converting worthless materials into high-value ones [5]. Several studies have been conducted related to research on composites using animal natural fibers. Fuady et al. [6] researched composites reinforced with rice field snail powder for drone frame applications. The results stated that the highest impact strength value was found in the 75% : 25% ratio of 2,0722 kj/m^2. Asmeati et al. [7] researched free-range chicken eggshell waste. The results explained the highest impact strength value in the 30% fraction of 19,163 kj/m^2. Nayiroh et al. [8] examined the effect of the volume fraction of green mussel shell particle filler on mechanical properties. The results of this study resulted in impact strength ranging from 0,190 to 0,317 J/mm^2, with the highest impact price at 10% filler volume fraction and the lowest at 40% filler volume fraction. Previous research has examined using organic waste such as rice field snail shells, native chicken eggshells, and green mussel shells as reinforcement for composite materials. The research focused on the variation of particle volume fraction and its effect on impact strength. Most studies used powder form as reinforcement material and did not use fibre form; fibre has mechanical characteristics different from particles. Thus, there is still a research gap in using fibres as reinforcement, especially natural fibres that have not been widely studied, such as squid fibres. As has been demonstrated in previous natural fibre-based composites, using squid fibre as a composite reinforcement is expected to boost the material's impact strength while also enhancing volume fraction, fibre length, and appropriate fibre orientation direction.

Research on composites is growing due to their sustainability, low environmental impact, and various possible uses. A common strategy is to use natural fibers, especially animal fibers, as fillers in composite materials. Natural fibers are the right choice to create lightweight, strong, environmentally friendly, cost-effective composite materials [9]. Composite materials from natural fibers are as strong as metal composites [10]. Using animal fibers as composite reinforcement is expected to produce composite materials that have good mechanical performance and help reduce the amount of waste produced. In this study, the authors used a method to test the mechanical properties of composites, namely the impact test. This impact test measures the energy a material absorbs until the material breaks, where the load comes suddenly and does not occur gradually. This energy absorption process produces material responses such as plastic deformation, inertial effects, friction, and hysteresis [11].

Based on these problems, a solution is needed to produce a strong material with good mechanical properties. Through impact testing, this research aims to analyse squid fibre-reinforced composite materials with variations in fibre volume fraction composition, fibre angle direction, and fibre length in an epoxy resin matrix. In quantitative research, it is necessary to formulate a hypothesis that aims to provide a clear direction from the beginning of the study. Hypotheses are formulated based on temporary conjectures to answer the problems raised. In this study, the hypothesis was formulated to examine the effect of squid fibre on composite strength, especially in impact strength testing.

2. METHODS

2.1 Research Methods

This research is experimental, namely, by making specimens and conducting tests with a type of quantitative research methodology, analysing the impact strength of the specimens using statistical software.

2.2 Research Concept Framework

The following is a conceptual research framework using an input-output diagram, as shown in Figure 1.

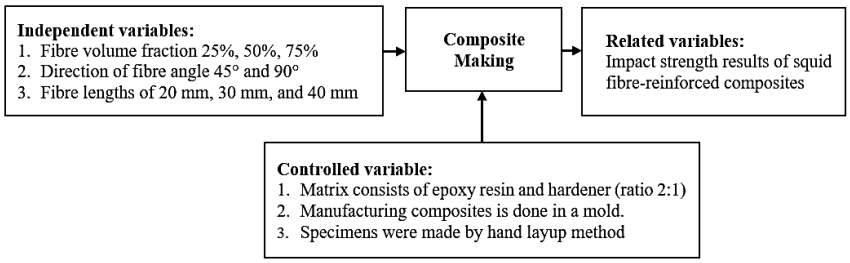

Figure 1. Research concept framework

The conceptual framework of this research describes the relationship between variables. It aims to determine the effect of fibre volume fraction, fibre angle direction, and fibre length on the impact strength of squid fibre-reinforced composites as the dependent variable. In this study, the composite manufacturing process becomes the intermediary, while the controlled variables to ensure the validity of the results are the matrix used with a ratio of 2:1 between resin and hardener, manufacturing in composite manufacturing, and making specimens by hand layup

method.

2.3 Specimen Making

Squid fiber used as composite reinforcement needs an alkali process. In this process, a 3 N NaOH solution was added to 100 g of squid fiber in a ratio of 1:10, stirred for one hour at 90°C, and then washed with distilled water [12]. Then, specimen molding was carried out; at this stage, the fibers were calculated and weighed according to the variables, and epoxy resin and hardener were mixed in a ratio of 2:1 for each fiber variable. Brush the mold with mirror glaze. The mold used Teflon material with dimensions of 60 mm long by 50 mm wide and 10 mm thick. The method used in making specimens is hand lay-up. Fibre embedding is done to arrange the fiber in the mold. After that, pour the mixture of epoxy resin and hardener into the surface of the mold until it is evenly distributed, as shown in Figure 2. The specimen is dried until it becomes hard. The next step is to remove the specimen from the mold, cut the specimen, and make notches according to ASTM E23 impact testing standards. The ASTM E23 impact testing standard has a specimen dimension of 55 mm long, 10 mm wide, and 10 mm high, a notch 2 mm deep, and a notch angle of 45°.

Figure 2. Specimen making

Impact testing is based on the absorption of potential energy from a pendulum load that swings from a certain height and strikes the test object, causing the test load to deform [13]. It is considered strong when a material can withstand high shock loads without being easily broken or distorted [14]. This study used the Charpy impact test method to determine the energy absorbed in testing specimens. This Charpy impact test method produces more accurate test values [15].

Figure 3. Impact testing machine

Figure 3 is a Charpy impact testing machine with specifications. It has a maximum capacity of 200 Joules of impact energy, a pendulum weighing 8,3 kg, and an arm length of 0,62 metres. The test is performed by starting the pendulum swing from an angle of 130°, which then strikes the specimen to measure the energy absorbed at fracture. It can be used to test various types of materials, including composites and metals. The impact energy can be calculated in equation 1, while the impact price can be calculated by equation 2 [16].

$$\boldsymbol{Energy\ impact = m.g.R\ (\cos\beta - \cos\alpha)} \quad (1)$$

$$\boldsymbol{Impact\ price = \frac{Energy\ impact}{A}} \quad (2)$$

E*impact* = Energy absorbed (Joules)
R = Radius of the center to the center of gravity of the pendulum (m)
m = Pendulum mass (kg)
g = Gravity (m/s^2)
β = Angle of swing breaking the test piece (°)
α = Angle of swing without test piece (°)

Impact price = Impact toughness (J/mm^2)
A = Cross-sectional area (mm^2)

3. RESULTS AND DISCUSSION

3.1 Research Results

Data collection in this study used Charpy impact test equipment at the Malang State Polytechnic Mechanical Engineering Material Testing Laboratory. The results of the research on the effect of volume fraction, angular direction, and fibre length on the impact strength of squid fibre-reinforced composites are as follows:

Table 1. Impact test results

No.	Volume Fraction	Fiber Direction	Fiber Length	Result (J/mm^2)			Average Impact Strength (J/mm^2)
				1	2	3	
1.	25%	45°	20 mm	0.0352	0.0692	0.0626	0.0556
			30 mm	0.0725	0.0714	0.0604	0.0681
			40 mm	0.0659	0.0714	0.0746	0.0706
		90°	20 mm	0.0506	0.0495	0.0439	0.0479
			30 mm	0.0735	0.0659	0.0823	0.0739
			40 mm	0.0746	0.0823	0.0779	0.0783
2.	50%	45°	20 mm	0.0549	0.0517	0.0648	0.0571
			30 mm	0.0658	0.0866	0.0757	0.076
			40 mm	0.0997	0.0714	0.0812	0.084
		90°	20 mm	0.0637	0.0692	0.0735	0.0688
			30 mm	0.0823	0.0659	0.0866	0.0783
			40 mm	0.0703	0.0768	0.0823	0.0764
3.	75%	45°	20 mm	0.0659	0.0899	0.0856	0.0804
			30 mm	0.0921	0.0703	0.0549	0.0724
			40 mm	0.0658	0.0757	0.0823	0.0746
		90°	20 mm	0.0692	0.0571	0.0615	0.0626
			30 mm	0.0626	0.0669	0.0681	0.0659
			40 mm	0.0964	0.0909	0.0724	0.0866

Based on the research results in, Table 1 shows that the composite with a variable volume fraction of 75% in the direction of 90° fibre angle and 40 mm length produces the highest impact strength of 0,0866 J/mm^2. Meanwhile, the 25% fraction with a fibre angle of 90° and a fibre length of 20 mm produced the lowest impact strength of 0,0479 J/mm^2.

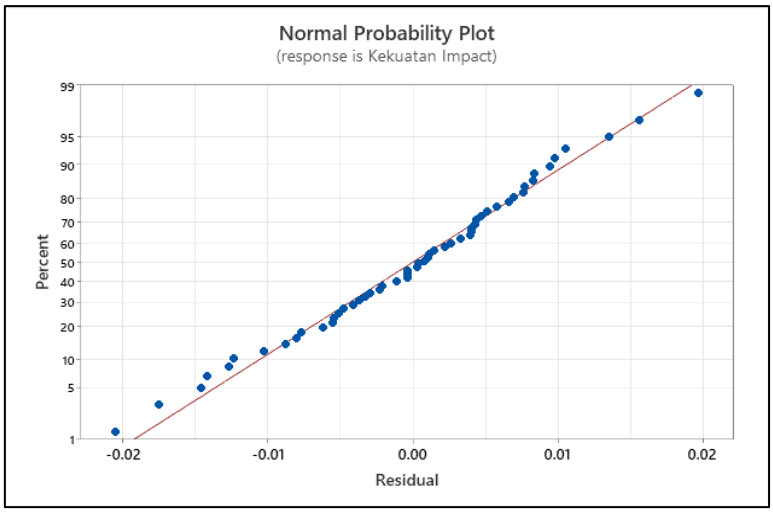

Figure 4. Graphic normal probability plot

Figure 4 normal probability plot graph shows the distribution of data based on the standard line drawn from the data on the replication of each variable. The graph results, which are close to the standard line, indicate the normal distribution of data. Figure 4 shows that the points on the graph are close to the diagonal line, so it can be stated that this data is usually distributed and fulfills the requirements for normal data distribution.

Table 2. Analysis of variance (ANOVA)

Analysis of Variance

Source	DF	Adj SS	Adj MS	F-Value	P-Value
Model	17	0.005263	0.000310	3.08	0.002
Linear	5	0.003196	0.000639	6.35	0.000
Volume Fraction	2	0.000740	0.000370	3.68	0.035
Fiber Direction	1	0.000000	0.000000	0.00	0.986
Fiber Length	2	0.002455	0.001228	12.20	0.000
2-Way Interactions	8	0.001067	0.000133	1.33	0.262
Volume Fraction*Fiber Direction	2	0.000114	0.000057	0.57	0.573
Volume Fraction*Fiber Length	4	0.000785	0.000196	1.95	0.123
Fiber Direction*Fiber Length	2	0.000169	0.000084	0.84	0.441
3-Way Interactions	4	0.001001	0.000250	2.49	0.061
Volume Fraction*Fiber Direction*Fiber Length	4	0.001001	0.000250	2.49	0.061
Error	36	0.003623	0.000101		
Total	53	0.008886			

To assess whether the research hypothesis is acceptable, the P-value analysis of the Analysis of Variance test is used. This study set a significance level (α) of 0,05 or 5%, which is the maximum acceptable error limit for an alternative hypothesis to be declared significant. Based on the results presented in Table 2, the fiber volume fraction variable has a P-value of 0,035, so it can be stated that the fiber volume fraction variable has a significant effect on impact strength. The fiber direction variable has a P-value of 0,986, so it can be noted that the fiber direction variable has no significant effect on impact strength. The fiber length variable has a P-value of 0,000, so it can be stated that the fiber length variable has a significant effect on impact strength. The interaction variable of volume fraction and fiber direction has a P-value of 0,573, so it can be stated that the interaction variable of volume fraction and fiber direction has no significant effect on impact strength. The interaction variable of volume fraction and fiber length has a P-value of 0,123, so it can be stated that the interaction variable of volume fraction and fiber length has no significant effect on impact strength. The interaction variable of fiber direction and fiber length has a P-value of 0,441, so it can be stated that the interaction variable of fiber direction and fiber length has no significant effect on impact strength. The interaction variable of volume fraction, fiber direction, and fiber length has a P-value of 0,061, so it can be stated that the interaction variable of volume fraction, fiber direction, and fiber length has no significant effect on impact strength.

Table 3. Model summary

Model Summary

S	R-sq	R-sq(adj)	R-sq(pred)
0.0100316	59.23%	39.98%	8.27%

Based on Table 3 shows that the coefficient of determination (R-sq) has a scale of 100%, if the coefficient of determination is closer to 100%, the more significant the influence between the independent variables on the dependent variable. In the results of data analysis obtained, the coefficient of determination R-sq has a value of 59,23%, which means that the independent variable affects the dependent variable or the strength of the impact is influenced and the rest is influenced by other factors.

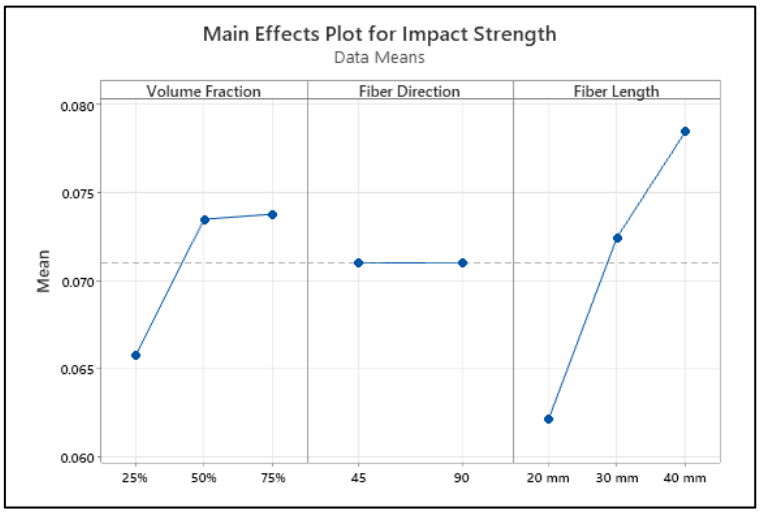

Figure 5. Main effects plot for impact strength

The graph has two main lines, horizontal and vertical; the horizontal line is the independent variable, and the vertical line is the dependent variable. Figure 5 shows that the variation of fibre volume fraction affects the impact strength linearly, and the impact strength increases as the fibre volume fraction increases. In the variation of fibre direction, the average value of impact strength is the same for both levels, so fibre direction does not significantly affect impact strength. The fiber length variation affects the impact strength linearly, and the impact strength increases as the fiber length increases.

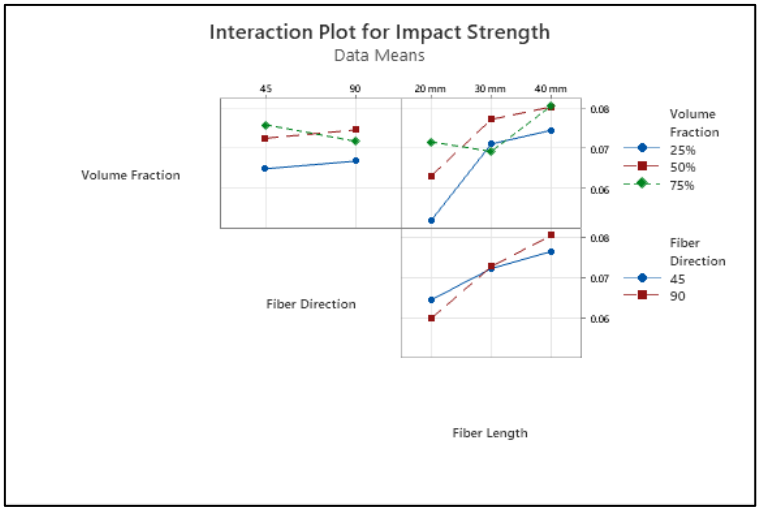

Figure 6. Interaction effect plot for impact strength

Based on Figure 6, it is known that the interaction graph of volume fraction and fibre angle direction has the highest impact strength value found in the 75% volume fraction and 45° fibre angle direction which is 0,0758 J/mm^2, at 25% volume fraction and 45° fibre angle direction has a low impact strength value of 0,0647 J/mm^2. In

the interaction between volume fraction and fibre length, the highest impact strength is found in the 75% volume fraction and 40 mm fibre length of 0,0806 J/mm^2, and the lowest impact strength in the interaction of volume fraction and fibre length is found in the 25% volume fraction and 20 mm length of 0,0517 J/mm^2. In the interaction between fibre direction and fibre length, the highest impact strength is found in the 90° fibre direction and 40 mm fibre length of 0,0804 J/mm^2. In comparison, the 90° fibre direction and 20 mm length have the lowest impact strength value of 0,0643 J/mm^2.

3.2. Discussion

Effect of fibre volume fraction on impact strength

Based on the results of data processing, the volume fraction variable has a significant effect on the dependent variable, namely impact strength. The results of the volume fraction variation show that the 75% fiber volume fraction with the composition (75% fiber and 25% resin) shows the highest impact strength. An increase in the volume fraction of squid fiber can increase the strength of the composite due to the increased bond between the fiber and the matrix; this occurs because a higher squid fiber composition produces more fiber bonds, thus increasing the strength of the composite when withstanding shock loads. While the composition of less fiber than the matrix makes the function of fiber as reinforcement in the composite less than optimal, if the larger matrix composition shows the rigid but brittle nature of the matrix obtained at 25% fiber volume fraction with a composition (25% fiber and 75% resin) shows a low impact strength value so that it does not require significant energy to break the composite. The relationship between increasing fiber volume fraction and impact strength is not always linear. Several factors, such as uneven fiber distribution and poor interaction between fiber and matrix, can cause this. The volume fraction of squid fibre in the composite increases along with the rise in the number of volume fractions, as supported by research conducted by Asmeati et al. (2024) [7] with the title "Analysis of Impact Test and Microstructure of Polyester Resin Matrix Composites Filled with Hometown Chicken Egg Shells" said that the more the volume fraction increases, the more the strength of the specimen increases, so that variations in the volume fraction of squid fibre affect the mechanical properties of the specimen.

Effect of fibre direction on impact strength

Based on data processing, the results show that the variable fiber angle direction does not have a significant influence on the dependent variable, namely impact strength. The variation of fiber angle direction shows that the 90° fiber angle direction shows the highest impact strength. This is because fibers arranged perpendicular to the direction of impact make a greater contribution to reducing energy. After all, the impact force directly hits the surface and fiber structure in parallel to absorb more energy before damage occurs. Meanwhile, the 45° angle direction, which has a fiber arrangement crossing or not parallel to the direction of impact loading, makes the fiber detached from the matrix and makes the load distribution less efficient because when given an impact load, it tends to experience interfacial shear failure. However, the 90° fiber angle direction variation showed the lowest impact strength results. So, it can be concluded that the variable fiber angle direction does not affect the impact strength because only the 90° angle direction affects the impact strength.

Squid fibres tend to have an amorphous structure that is not regularly arranged compared to synthetic fibres, such as carbon fibres, which are highly anisotropic. Anisotropic has different material properties in all directions at a point in the object [17]. Thus, when tested from various directions, anisotropic fibres show different mechanical properties (impact strength, tensile strength). The opposite of anisotropic isotropic is where isotropic has the same material properties in each direction. Based on the research results, the angular direction of squid fibre does not significantly affect the impact strength. Squid fibre does not show strong anisotropic in its mechanical properties, so the change in fibre angular direction does not produce significant differences in response to impact strength. So, it can be identified that the squid fibre is isotropic, where the properties of the fibre are the same in all directions. If the squid fibres are isotropic, then changing the fibre angle direction in the composite will not significantly change impact strength.

Effect of fibre length on impact strength

The results of the data analysis show that the composite fiber length variable significantly influences the dependent variable, impact strength. According to the impact test results, the 40 mm fiber length variation shows the highest impact strength, an average of 0,0784 J/mm^2. Fibers can absorb and distribute impact energy more effectively than short fibers. Long fibers allow for greater deformation before fracture so that impact energy can be adequately absorbed and does not immediately cause the composite to fracture. The increase in the length of squid fibers can increase the strength of the composite so that the impact force can be distributed evenly along the fibers. In composites, cracks tend to propagate through the matrix, so longer fibers inhibit crack propagation in the composite. Longer fibers require greater energy to be uprooted, thus absorbing more impact energy and providing greater structural stability to the composite. Meanwhile, On average, the 20 mm fiber length shows a low impact strength value of 0,062 J/mm^2. Short fibers tend to detach faster from the matrix when exposed to impact, so the energy is not spread evenly; the short fibers cause imperfect interface bonding, thus reducing the ability to

withstand impact loads. Short fibers do not have sufficient length to develop a strong and stable bond around the matrix, so when the composite receives an impact load, the stress from the matrix cannot be efficiently transferred to the fibers. Most of the load is borne by the matrix, which causes the matrix to become brittle. Shorter fibers are also less effective in inhibiting crack propagation, so cracks can easily pass through or cut through the fibers, causing failure. The variation of squid fibre length in the composite increases with increasing fibre length, as supported by research conducted by Maryanti et al. (2019) [15] with the title "Impact Strength Characteristics of Coconut Fiber Composites with Fiber Length Variations" said that fibre strength is significantly influenced by the matrix used when making composites, so that the longer the fibre, the higher the impact price. This is consistent with the research findings, which show that the impact price achieved increases along with the length of the fibre.

4. CONCLUSION

Based on the data analysis and discussion on the effect of volume fraction, fiber angle direction, and fiber length on the impact strength of squid fiber composites, it can be concluded that:

1. The volume fraction of squid fibre significantly influences the impact strength of the composite, where the 75% volume fraction produces the highest impact strength. In comparison, the 25% volume fraction produces the lowest impact strength. There is an increase in the bond between the fibre and the matrix as the fibre volume fraction increases, which contributes to the strength of the composite when withstanding shock loads. However, the relationship between fibre volume fraction and impact strength is not always linear, influenced by factors such as uneven fibre distribution and potential porosity due to imperfect composite manufacturing methods.
2. The angular direction of the fibres has no significant effect on the impact strength of the composite. Although the 90° angular direction shows the highest impact strength because fibres perpendicular to the direction of impact are more effective in reducing energy, the results show that changes in fibre angular direction do not produce significant differences in response to impact strength. This is due to the isotropic nature of squid fibres, where the mechanical properties are not significantly different in various directions, in contrast to synthetic fibres, which are anisotropic. Thus, it can be concluded that the squid fibre's angular direction does not significantly impact impact strength.
3. The fibre length significantly influences impact strength, where 40 mm fibre length produces the highest impact strength, and 20 mm fibre length produces the lowest impact strength. This is due to the ability of long fibres to absorb and distribute impact energy more effectively, as well as inhibiting crack propagation in the composite. This shows that the longer the fibre length, the higher the impact value. Thus, increasing fibre length can improve the structural stability and resistance of the composite to impact loads.

The application of squid fibre composites in this research is used as a drone frame, which has been reviewed in previous research. Using squid fibre composites as reinforcement produces higher mechanical properties than composites reinforced with rice snail powder used as drone frames. With the environmentally friendly nature of squid fibre, this material also supports sustainability in the manufacturing process.

5. ACKNOWLEDGEMENT

The author would like to thank Dr. Ir. Drs. Moh. Hartono, M.T., for their guidance in completing the journal, as well as both parents, siblings, and colleagues who have provided support to the author.

6. REFERENCES

[1] I. Kurniawan and V. A. Setyowati, "Effect of composite manufacturing method and artificial fibre variation on impact and tensile strengths," *J. Ilm.*, pp. 301–306, 2021.
[2] Y. Fu and X. Yao, "A review on manufacturing defects and their detection of fiber reinforced resin matrix composites," *Compos. Part C Open Access*, vol. 8, no. 2, pp. 2–7, 2022, doi: 10.1016/j.jcomc.2022.100276.
[3] Yulianis, M. Sanuddin, and N. Annisaq, "Making chitosan from chitin from bone waste in squid," *J. Healthc. Technol. Med.*, vol. 6, no. 1, pp. 62–69, 2020.
[4] Kementerian Kelautan dan Perikanan Republik Indonesia, "Estimation of potential, allowable catch, and utilisation rate of fish resources in the MPA WPPNRI," 2025. [Online]. Available: https://portaldata.kkp.go.id/portals/data-statistik/jtb-potensi-sdi/tbl-dinamis
[5] I. Mawardi, A. Azwar, and A. Rizal, "Assessment of coir fiber treatment on mechanical properties of coir fiber epoxy composites," *J. Polimesin*, vol. 15, no. 1, p. 22, 2017, doi: 10.30811/jpl.v15i1.369.
[6] S. H. A. I. Fuady and H. Saputra, "Impact test study on composites made from a mixture of rice snail powder for drone frames," in *Proc. Semin. Nas. Apl. Sains Teknol.*, no. 23, pp. 210–219, 2024.
[7] R. Asmeati, M. Y. Ali, and M. Syahrir, "Impact test analysis and microstructure of polyester resin matrix composites filled with chicken eggshells," *J. Sos. Teknol. Terap. AMATA*, vol. 3, no. 2, pp. 9–19, 2024.
[8] N. Nayiroh and K. Kusairi, "Study of the effect of filler volume fraction variation on the mechanical properties of polymer matrix composites (PMC) reinforced with green clam shells (*Perna viridis* L.)," *Wahana Fis.*, vol. 6, no. 1, pp. 48–58, 2021, doi: 10.17509/wafi.v6i1.33564.
[9] H. Sunardi, A. Zainuri, and A. D. Catur, "Effect of punching process stages and fibre direction on the tensile

strength of polyester–Pandan Wangi composite material," *Din. Tek. Mesin*, vol. 3, no. 1, pp. 1–9, 2013, doi: 10.29303/d.v3i1.82.
[10] A. Supriyatna and Y. Solihin, "Development of pineapple fibre reinforced epoxy composites for car interior applications," *Teknobiz J. Ilm.*, vol. 8, no. 2, pp. 88–93, 2018, doi: 10.35814/teknobiz.v8i2.900.
[11] F. Akbar, S. Sulardjaka, and N. Iskandar, "Effect of glycerol plasticiser and corn starch addition to gondorukem matrix on the impact strength of jute fibre reinforced composites," *J. Tek. Mesin*, vol. 11, no. 3, pp. 482–487, 2023. [Online].
[12] L. M. H. Nadia et al., "Antibacterial activity of chitosan from squid cartilage (*Loligo* sp.) against *Staphylococcus aureus* and *Escherichia coli* bacteria," *J. FishtecH*, vol. 10, no. 2, pp. 95–101, 2022, doi: 10.36706/fishtech.v10i2.14386.
[13] Safrijal, S. Ali, and H. Susanto, "Testing of composite boards reinforced with empty palm oil bunch fibre (TKKS) using Charpy impact test equipment," *J. Mekanova*, vol. 3, no. 5, pp. 1–10, 2017.
[14] B. Maryanti et al., "Impact strength characteristics of coconut fibre composites with varying fibre lengths," in *Proc. SENIATI*, vol. 5, no. 4, pp. 339–343, 2019.
[15] A. S. Wibowo, A. Wulansari, and R. Is, "Effect of variation in fibre direction and number of layers on tensile and impact tests of carbon fibre composites," *J. Teknol. Penerbangan*, vol. 7, no. 1, pp. 1–6, 2023.
[16] H. Wona, K. Boimau, and E. U. K. Maliwemu, "Effect of fiber volume fraction variation on bending and impact strength of Agave Cantula fibre reinforced polyester composites," *J. Tek. Mesin Lontar*, vol. 2, no. 1, pp. 39–50, 2015.
[17] R. M. Jones, *Mechanics of Composite Materials*. Philadelphia, PA, USA: Taylor & Francis, 1999, pp. 994–1006.

LOGIC
Journal of Engineering Design and Technology
Vol. 25 No.2 July 2025; p. 126-131

p-ISSN : 1412-114X
e-ISSN : 2580-5649
http://ojs2.pnb.ac.id/index.php/LOGIC

RECOMMENDATIONS FOR WORK SYSTEM ASSESSMENT OF SNI 9001: 2008 IMPLEMENTATION BASED ON MACRO ERGONOMICS AT PT SPU

Heri Setiawan [1)*], M. Yusuf[2)], Micheline Rinamuti [3)], Dominikus Budiarto [4)], Yohanes Dicka Pratama [5)], Achmad Alfian [6)]

[1,4,5,6)] Industrial Engineering Study Program, Musi Charitas Catholic University, Jl. Bangau No. 60 Palembang, South Sumatera, Indonesia
[2)] Mechanical Engineering, Politeknik Negeri Bali, Badung, Indonesia
[3)] Management Study Program, Musi Charitas Catholic University, Jl. Bangau No. 60 Palembang, South Sumatera, Indonesia

Corresponding email:
heri_setiawan@ukmc.ac.id

Abstract. The increasingly intense competition, the number of customer choice options and the more selective customers in choosing medical equipment products require PT SPU as one of the Indonesian National Medical Device (*Alkes*) industry engaged in the production process of medical devices and rehabilitation to always improve a better work system. To improve product quality PT SPU has implemented the SNI ISO 9001: 2008 Quality Management System which contains standard requirements used to measure the organization's ability to meet customer requirements and appropriate regulations. The purpose of this research is to identify and assess how much influence each component of the work system has on the satisfaction of customers, employees and leaders. The method used is Macro Ergonomics and data were collected through questionnaires and analyzed using regression analysis. The magnitude of the contribution of the work assessment process of SNI ISO 9001: 2008 implementation to the influence of significant macro ergonomic aspects on organizational conditions (52.45%), physical environment (37.37%), production processes (12.53%), infrastructure (9.69%), production process services (5.90%), and R&D activities (2.82%).(3) Proposed recommendations for improving organizational conditions by confirming the roles and responsibilities of each person so that there are no undisciplined employees between sections, improving communication. Physical work environment by rearranging the place and rejuvenating production process support tools that are not ergonomic and have been damaged, redesigning a conducive and comfortable work environment. Production process improvements including employees actively communicating with each other and development of standard operating procedures (SOPs) with legacy competencies through knowledge transfer. Improvements to Facilities and Infrastructure by adding air conditioning, such as blower/exhaust ventilators, and sufficient room ventilation. Improvements to R&D: by facilitating employee exchanges for R&D activities, training, technical guidance, and experience exchange; increasing access to cooperation with government and private organizations.

Keywords: Work system assesment, Macro Ergonomics, SNI 9001:2008, Medical device industry

1. INTRODUCTION

PT SPU Palembang, one of Indonesia's national medical device manufacturers, must continue to improve a better work system as a result of increasingly fierce competition and increasingly selective customers. One of the most important components in the progress of the organization is a good work system, which is the key to success in

increasing productivity and efficiency of the company and reduce the risk of work [1]-[3]. The work system consists of a series of different work systems that are combined to produce goods or services that generate value for the customer or profit for the company or organization [4][5].

It is essential that the worker, the work process, and the work environment fit together. This method is called the ergonomics approach. Ergonomics is the field that combines science, technology, and artistry to align tools, work methods, and surroundings with human strengths, capabilities, and restrictions. The goal is to develop workplaces and environments that are healthy, secure, pleasant, and productive [4][6][7]. Each component of the work system is increasingly complex due to advances in science and technology. Factors such as organization, technology, procedures and tasks, organization, physical, social, cultural, and behavioral environments, and regulation are some examples. Thus, micro ergonomics methods on the production floor are no longer relevant. In addition, researchers can assess such work systems by using a macro ergonomics approach, which is a top-down sociotechnical approach that aims to optimize the design of work systems and ensure that they function properly [8]-[11]. As a medical equipment manufacturing industry with many competitors, the main problem of PT SPU Palembang is whether the services provided are in accordance with customer expectations, because these customers are potential market consumers who will repeatedly purchase PT SPU medical equipment products repeatedly. Therefore, PT SPU Palembang should always provide good service by improving the performance of its employees for the satisfaction of its customers and make more potential consumers. This is what is called customer orientation. Organizations should have a good quality management system to improve the quality of their goods and services.

SNI ISO 9001:2008 is a globally recognized and internationally acclaimed quality management system standard. SNI ISO 9001:2008 has been adopted by BSN to become SNI for various business fields and improve the ability to compete. SNI ISO certification has many advantages, such as a better reputation, awareness of the importance of maintaining quality, procedures, and responsibilities become clearer and better documented, eliminate unnecessary work, audits become easier and easier to track, better service potential markets, increased customer and employee satisfaction, and continuous improvement. With the implementation of the SNI ISO 9001:2008 quality management system, services are better than ever. Every action is done systematically, recorded, and can be routinely analyzed. PT SPU will face many problems to fulfil their expectations and desires and increase customer satisfaction due to the demands, responsibilities, and elements of the work system itself [12]-[14]. Nonetheless, whether PT SPU has fulfilled the expectations and desires of customers by providing services in accordance with the service quality standards of SNI ISO 9001: 2008, and whether customer satisfaction has been met. Therefore, the influence of macro ergonomic elements on work system components on the level of customer satisfaction must be identified and evaluated. Organizational conditions, production processes, physical environment, business process services, research and development activities, adaptation facilities and infrastructure for the advancement of manufacturing technology and human resource development are macro ergonomic aspects of the work system in question. From the results of this assessment, the most important influence of macro ergonomic aspects on the work system will be identified and the work system components will be further analyzed.Unlike previous studies that focus on micro-level ergonomic interventions, this study adopts a macro ergonomics framework to assess organizational-level factors impacting ISO implementation. Although the SNI ISO 9001:2008 has been widely adopted in various industries, few studies have assessed its implementation through a macro ergonomics lens in the Indonesian medical device sector. Therefore, this study aims to identify which macro ergonomic components most influence work system effectiveness and stakeholder satisfaction at PT SPU.

2. METHODS

The object of the research is PT SPU Palembang customers who feel directly the results of the service on the implementation of work assessment based on macro ergonomics related to the implementation of SNI ISO 9001: 2008. There are 2 variables, namely the dependent variable is the level of customer satisfaction and the independent variable is the macro ergonomic elements of each component of the work system including organizational conditions, production processes, physical environment, business process services, R&D activities, as well as facilities and infrastructure adaptation for the advancement of manufacturing technology and human resource development [15]-[17].

The essential information is gathered from both primary and secondary sources, specifically: (1) primary data collected through firsthand observation and assessment of the research subject in the actual environment, which is: (a) preliminary observation by conducting direct observation of the real conditions in the work system related to customer satisfaction as the object of research and conducting interviews with PT SPU leaders, employees, and customers. (b) Macro ergonomic Organizational Questionnaire Survey (MOQS), a research questionnaire about the condition of the observed work system. The MOQS procedure includes; conceptualization,

namely determining the variables or components of the work system to be assessed, operationalization, namely determining the dimensions of the concept being assessed, and making a questionnaire consisting of: an open questionnaire to obtain indicators of macro ergonomic aspects to be studied, a preliminary closed questionnaire (tryout). The lattice that has been obtained is then compiled and developed into question items in a closed questionnaire, and a closed questionnaire (research). If the preliminary questionnaire data is declared valid and reliable, the questionnaire is suitable for use as an instrument for collecting actual research data, (2) secondary data, including: Data on the history, scope, structure, and management of the organization are included in the category of secondary data in this study, (3) data processing, analysis methods and discussion. The research flow chart is sequentially as follows; start-preliminary study & literature study-problem formulation and initial hypothesis-compiling & distributing open questionnaires-determining indicators and preparing grids-compiling & distributing closed questionnaires (tryout) SNI ISO 9001: 2008-tabulation of questionnaire data (tryout)-testing the validity and reliability of the instrument-results valid & reliable?, if not will be repeated back to the previous stage and if yes continue to the next stage-distribution of closed questionnaires-tabulation of questionnaire data-correlation and regression analysis-discussion analysis (proposed improvements based on macro ergonomics)-finished.

3. RESULTS AND DISCUSSION

Each indicator of the research variable was collected from the open-ended questionnaire. The question grid in the closed questionnaire can be determined by looking at the tabulation of the open questionnaire. The lattice was developed into question items with 5 answer options and an ordinal scale using a Likert scale of 1-5. These items are indicators of macro ergonomic elements of the work system that affect the level of employee satisfaction. The lattice of macro ergonomics aspects is presented in Table 1.

Table 1. Macro Ergonomics Aspect Grid

Variable	Indicators	Item Number
Organizational Conditions	Type of leadership	1,2
	Communication issues	3
	Rules and regulations	4,5
Production Process	Production process methods	7,8,12
	Extra production process activities	10, 11
	Workmanship of the production process	9
Production Services	Production service problems	14, 15, 16, 17, 18
Physical Environment	Conditions of physical environmental factors	20, 22
	Arrangement of production floor stations	21
Research Activities	Access to cooperation with outside parties	24, 25
Facilities and Infrastructure	Equipment condition	27, 28, 31, 33, 35
	Optimization of facilities and infrastructure	29, 30, 32, 34
Employee Satisfaction	Labor satisfaction level	6, 13, 19, 23, 26, 36

The alternative answers used are as follows:
SS (Strongly Agree): scored 5; S (Agree): scored 4; N (Neutral): scored 3; TS (Disagree): scored 2 STS (Strongly Disagree): scored 1.

The causal relationship of the research variables between macro ergonomics aspects of the conditions of the components of the work system at PT SPU Palembang to the level of satisfaction of customers, employees and leaders can be interpreted as follows: very strong relationship between (a) organizational conditions with processes at production floor stations, physical environment, (b) services with physical work environment, R&D activities, (c) physical environment with R&D, and (d) production processes with infrastructure facilities. The simultaneous contribution correlation shows the relationship or relationship between the conditions of all aspects of macro ergonomics on the components of the work system to customer satisfaction, employees and leaders of the correlation is very strong [2][4][5].

The influence of macro ergonomics aspects on the components of the work system on customer satisfaction, employees and leaders of PT SPU has a significant effect, namely; organizational conditions (52.45%), physical environment (37.37%), production processes (12.53%), infrastructure (9.69%), production process services (5.90%), and R&D activities (2.82%). (a) The organizational condition of the indicator is the form of interaction communication between leaders, employees and customers. Communication that is less harmonious and in line between the leadership, in this case the General Manager and the owner. General Manager and owner are sons-in-

law with in-laws not in line so that employees become confused about which one to follow and have an impact on the execution of the production process and service to customers [5][10]. (b) The physical work environment is an indicator that the layout of the production floor is not conducive, the room temperature still exceeds the threshold value by 35%, and exposure to dust and chemicals has not been eliminated with PPE that meets the requirements [9][11]. (c) Production process indicators are the lack of products returned by customers due to quality that has not been consistently maintained. (d) Infrastructure facilities indicators are still many tools and machinery that need to be upgraded to be more modern and more efficient. (e) Production process services are indicators that service access is slower and less friendly, does not provide a family atmosphere and is sometimes still based on individualism. And (f) R&D activities, the indicator is the absence of periodic training for employees to improve skills that follow the development of the production process and are more efficient [9][14].

Recommendations for improvement of organizational conditions are to improve communication harmonization, reinforce the role of the job description of each employee and leader, engage in thorough back-and-forth discussions focused on realizing the goals of the organization by setting aside personal pride. The second principle of quality management, which relates to leadership, emphasizes that leaders create and foster a cohesive direction and mission for the organization [12][16][17]. Consider the needs of all interested parties, including customers. Set challenging and socialized goals and targets and create and support values of togetherness, honesty and ethical task models at all levels of the organization. Physical environment with more ergonomic/comfortable production floor layouts and stations, improved air circulation. To meet the stipulations of ISO SNI 9001:2008 clause, it is essential to evaluate the workplace surroundings, which include physical elements, environmental conditions, and additional influences such as sound levels, temperature, moisture, illumination, and atmospheric conditions. Production process through a process orientation approach (principle 4), namely a desired result will be achieved efficiently, if the related activities and resources are managed as a process. Integration of sequential processes of people, materials, methods, machines, and equipment in an environment to produce value-added output for customers. Clause 6.1 of ISO SNI 9001:2008 on resource provision, where the organization must determine and provide the necessary resources [18]-[20].

The six recommendations related to the influence of the work system on customer satisfaction, employees and leaders of PT SPU, as mentioned earlier, exemplifies the application of quality management principles, specifically the concept of ongoing enhancement. The relentless pursuit of improving the organization's overall performance must be a constant objective of the entity. Ongoing enhancement entails methodical and cumulative actions that address the changing requirements and anticipations of customers, staff, and management, which will guarantee a vibrant development of the quality management framework, rooted in an ergonomic scientific methodology. Consistently implement the organization's approach through macro, micro, and total ergonomics for continuous performance improvement, provide and send employees for training/internships on continuous improvement methods and tools, implement continuous improvement on product, process and system objectives, and set goals and objectives as guidelines, and measure achievements for continuous improvement and reward and recognize improvements.

Theoretical Implications are this study contributes to the growing body of literature on macro ergonomics by demonstrating how a systems-based ergonomic approach can enhance the implementation of quality management standards such as SNI ISO 9001:2008. It reinforces the relevance of viewing work systems as sociotechnical structures in which organizational, physical, and process-level elements interact to affect employee and customer satisfaction [21]. The findings also validate the use of the Macro-ergonomic Organizational Questionnaire Survey (MOQS) as a diagnostic tool for evaluating ergonomic conditions in quality-focused manufacturing environments [22].

Practical implications; from a practical standpoint, the results provide actionable insights for managers and practitioners in the medical device industry, particularly those operating in developing economies. The identification of key ergonomic factors—especially organizational conditions and the physical work environment—offers a clear roadmap for targeted interventions. Companies can apply these findings to enhance internal communication, optimize workplace layout, and align standard operating procedures (SOPs) with ergonomic best practices. Moreover, the study supports integrating macro ergonomics with ISO-based quality improvement efforts to increase productivity, reduce errors, and improve employee well-being and customer satisfaction.

This study is limited to a single case study and self-reported data; future research could apply a comparative multi-site approach using mixed methods.

4. CONCLUSION

Based on the results of data processing and analysis that has been done, several things can be concluded, among others: (1) macro ergonomic aspects and indicators of customer, employee and leader satisfaction including organizational conditions, communication issues, applicable regulations, and leadership aspects. The physical

work environment is indicated by the condition of physical environmental factors and the layout of the workspace. The production process is indicated by the SOP method, additional activities outside the SOP, regeneration and competency transfer. Production process services are indicated by service problems at each work station. Infrastructure and facilities with indicators of equipment condition, optimization of facilities and infrastructure. R&D with metrics of access to cooperation with outside parties, training, technical guidance. (2) The influence of macro ergonomic aspects on the components of the work system on the satisfaction of customers, employees and leaders of PT SPU has a significant effect, on organizational conditions (52.45%), physical environment (37.37%), production processes (12.53%), infrastructure (9.69%), production process services (5.90%), and R&D activities (2.82%). (3) Proposed recommendations for improving Organizational Conditions are as follows: Affirm the roles and responsibilities of each person so that there is no undisciplined inter-section labor; improve communication. Recommendations for intensive two-way communication between company, factory, and section/department leaders and their employees. Reorganize the premises and rejuvenate the tools supporting the production process, especially for kits and equipment that are not ergonomic and have been damaged, to improve a conducive and comfortable working environment. Improvements to the production process included the workforce actively communicating with each other and the development of standard operating procedures (SOPs) with legacy competencies through knowledge transfer. Improvements to Facilities and Infrastructure are as follows: The presence of air conditioners, such as blower/exhaust ventilators, and sufficient ventilation, will make the workstation space less comfortable for the workforce. Recommendations for Improving Production Process Services: Labor is more friendly to customers and labor; Labor is more responsive to needs among labor and customers. Recommendations for R&D improvement: Facilitate labor exchange for research and development activities and experience exchange; increase access to cooperation with government and private organizations.

5. ACKNOWLEDGEMENT

The author would like to thank the staff of PT SPU Palembang for providing data support and observations, the academic community of lecturers of Industrial Engineering Study Program & Management Study Program, LPPM Musi Charitas Catholic University, and the Logic Journal Editor and Reviewer Team for publishing this article.

6. REFERENCES

[1] H. Setiawan and M. Rinamurti, "Recommendations of ergonomic checkpoints and total ergonomics intervention in the pempek kemplang palembang industry". *IOP Conf. Ser.: Mater. Sci. Eng.* 885 012057. Available at: https://doi.org/10.1088/1757-899X/885/1/012057, 2020.

[2] Setiawan, H., Susanto, S., Rinamurti, M., & Pratama, Y. D., "Implementation of A Total Ergonomics Approach to Improve the Quality of Life of Freight Workers In 16 Ilir Market, Palembang City, South Sumatera Province", *Journal of Medisci,* vol. 2, no. 3, pp.172–182. Available at: https://doi.org/10.62885/medisci.v2i3.596, 2024.

[3] Park, J.W. *et al.*, "Influence of coexposure to long working hours and ergonomic risk factors on musculoskeletal symptoms: an interaction analysis", *BMJ open*, vol. 12, no.5, p. e055186. Available at: https://doi.org/10.1136/bmjopen-2021-055186, 2022.

[4] Rinamurti, M., & Setiawan, H., "Industrial Ergonomic Work Design to Improve The Employee Quality of Life and Productivity at PT Cita Rasa Palembang", *AIP Conference Proceedings*, vol. 2680, no. 1, Available at: https://doi.org/10.1063/5.0127077, 2023.

[5] Setiawan, H., Susanto, S., Rinamurti, M., & Alfian, A., "Design and Implementation of Green Human Resource Management (Green HRM) in SMEs Palembang City", *Journal of Ekuisci*. 2(3), pp.188–198. Available at: https://doi.org/10.62885/ekuisci.v2i3.597, 2025.

[6] Graben, P.R. *et al.*, "Reliability Analysis of Observation-Based Exposure Assessment Tools for the Upper Extremities: A Systematic Review", *International Journal of Environmental Research and Public Health*, vol. 19, no.17, Available at: https://doi.org/10.3390/ijerph191710595, 2022.

[7] Kamala, V. and Robert, T.P., "Fuzzy-Logic-Based Ergonomic Assessment in an Automotive Industry", *South African Journal of Industrial Engineering*, vol. 33, no.4, pp. 109–125. Available at: https://doi.org/10.7166/33-4-2593, 2022.

[8] Setiawan, H., Susanto, S., Rinamurti, M., Alfian, A., Pratama, Y. D., & Budiarto, D., "Design of a Round Tofu Printer Using the Ergo-Product Design Method: (Case Study: Mr. Andi's Tofu Factory Palembang)", *Jurnal Improsci*, vol.2, no.4, pp.234–245. Available at: https://doi.org/10.62885/improsci.v2i4.614, 2025.

[9] Setiawan, H., *Keselamatan dan Kesehatan Kerja.* In A. dr. Agustiawan (Ed.), Book Chapter (1st ed., pp. 55–68). Indonesia: Media Sains Indonesia. 2022.

[10] Setiawan, H.,et al, *Psikologi ndustri dan Organisasi*: *Konsep dan Studi Kasus dalam Industri dan Organisasi*. In C. Nanny Mayasari, S.Pd., M.Pd. (Ed.). Book Chapter (1st ed., pp. 149–163). Indonesia: Get Press, 2023.
[11] Setiawan, H.,et al, *Sistem Lingkungan Industri*. In M. S.: Mila Sari, S.ST. (Ed.), Book Chapter (1st ed., pp. 103–121). Indonesia: Get Press, 2023.
[12] Setiawan, H., Susanto, S., Rinamurti, M., Pratama, "Implementation of Ergo-Tourism and Local Wisdom to Design Tourism Village Governance Based on Balinese Cultur in Darma Buana, Belitang II South Sumatera Province", *Jurnal Toursci*, vol.*2, no.*3, pp.237–247. Available at: https://doi.org/10.62885/toursci.v2i3.618, 2025.
[13] Setiawan, H., Rinamurti, M., Kusmindari, C. D., & Alfian, A., "Ergonomic Hazard Measurement, Evaluation and Controlling in the Pempek Palembang Home Industry Based on SNI 9011: 2021". International Journal of Innovative Science and Research Technology, vol. 8, issue 6. Available at: https://www.ijisrt.com/volume-8-2023_issue. 2023.
[14] Setiawan, H., Susanto, S., Budiarto, D., Pratama, Y. D,. & Alfian, A., "Recommendations for Sustainable Waste Management Technology in Palembang City", *Jurnal Agrosci*, vol.2, no.4, pp.254–266. Available at: https://doi.org/10.62885/agrosci.v2i4.641. 2025.
[15] Hari, A., & Setiawan, H., "Perancangan Alat Bantu Memasukkan Gabah Ergonomis ke Dalam Karung - Studi Kasus di Penggilingan Padi Pak Santo", *The Indonesian Journal of Ergonomics.* Vol. 06, no. 01, pp.37–44. Available at: https://doi.org/10.24843/JEI.2020.v06.i01.p05. 2020.
[16] H Setiawan & M Rinamurti, "Pemberdayaan Masyarakat Melalui Pelatihan Ergo-Entrepreneurship Untuk Meningkatkan Kualitas Hidup dan Sikap Kewirausahaan Karyawan Pembuat Pempek PT Cita Rasa Palembang", J*urnal Pengabdian kepada Masyarakat Universitas Bina Darma*, vol.1, no. 1, pp. 1-12, Available at: https://doi.org/10.33557/pengabdian.v1i1.1338, 2021.
[17] Setiawan, H., Susanto, S., Rinamurti, M., Alfian, A., Pratama, Y. D., & Budiarto, D., Clara. C., "Ergo-Technopreneurship Training to Improve Knowledge and Attitude of Technology Entrepreneurs Palembang Local Culinary Traders", *Journal Ekuisci*, 2(4), pp.226–236. Available at: https://doi.org/10.62885/ekuisci.v2i4.633, 2025.
[18] Celal Gungor and Mustafa Fikret Oguz, "Manual material handling risk assessment in furniture industry: REBA method", *World Journal of Advanced Research and Reviews*, vol. 21, no.3, pp. 1760–1765. Available at: https://doi.org/10.30574/wjarr.2024.21.3.0934, 2024.
[19] Hawari, N.M. *et al.*, "Musculoskeletal Discomfort Evaluation using Rapid Entire Body Assessment (REBA) and Quick Exposure Check (QEC) among Woodworking Workers in Selangor, Malaysia", *Asian Journal of Applied Sciences*, vol.10, no.5, pp. 407–416. Available at: https://doi.org/10.24203/ajas.v10i5.7047, 2022.
[20] Setiawan, H., et al, *Pengantar Teknik Industri*: In Ansarullah Lawi (Ed.), Book Chapter (1st ed., pp. 261-275). Indonesia: Widina Media Utama. 2023.
[21] M. Yusuf, I Ketut Gde Juli Suarbawa, and I Made Anom Santiana, "Analysis of potential ergonomic hazards in metal craft welding workers," Int. J. Occup. Saf. Heal., vol. 15, no. 2 SE-Original Articles, pp. 165–172, Apr. 2025, doi: 10.3126/ijosh.v15i2.66529.
[22] I. Super, L. Zhang, B. Wang, and O. Asan, "The impact of psychological factors on interprofessional team collaboration in the ICU: A macro-ergonomic case study," Appl. Ergon., vol. 128, p. 104535, Oct. 2025, doi: 10.1016/j.apergo.2025.104535.

LOGIC
Journal of Engineering Design and Technology
Vol. 25 No.2 July 2025; p. 132-139

p-ISSN : 1412-114X
e-ISSN : 2580-5649
http://ojs2.pnb.ac.id/index.php/LOGIC

ANALYSIS OF THE EFFECTIVENESS OF WATERWHEELS AS WATER PUMP DRIVERS

Anak Agung Gede Pradnyana Diputa [1)], I Made Anom Adiaksa [1)], Made Agus Putrawan [1)], I Wayan Suma Wibawa [1)], Made Ardikosa Satrya Wibawa [1)]

1) Mechanical Engineering Department, Politeknik Negeri Bali, Bukit Jimbaran, Kuta Selatan, Badung, Indonesia

Corresponding email [1)] : agungpradnya@pnb.ac.id

Abstract. A pump is a device used to move liquids from one location to another through a pipeline, typically by increasing fluid pressure using electrical power. This increase in pressure helps overcome various types of flow resistance, such as pressure differences, elevation changes, or frictional losses. Transporting fluids from lowland to highland areas is not a simple task, particularly in remote regions where access to electricity is limited. This research was conducted at Pura Beji, Tanah Lot, Beraban Village, Tabanan Regency—an area that has abundant clean water resources in the lowlands compared to the highlands. The study focuses on the process of transferring clean water using water wheels as mechanical drivers in a system known as PATA Technology (Pompa Air Tenaga Air). Therefore, the objective of this research is to analyze the mechanical power generated by the water wheels and the resulting pumping performance of the water pump. This study investigates the effectiveness of waterwheels as mechanical drivers for water pumps in rural areas with limited electricity access, using the PATA (Pompa Air Tenaga Air) system. According to the research result, it was found that for mass flowrate of water wheel 75.5 kg/s then for the mass flowrate of water pump 14.7 kg/s. The efficiency for the waterwheels against the water pump obtained >40%. The water wheels act as the main drive of the water pump through rotation axle gear mechanism which is transmitted to the housing pump with average power water wheel 650 kg.m/s^2.

Keywords : PATA, Fluid, Water pump, Water wheel.

1. INTRODUCTION

Water is a fundamental natural resource that sustains all forms of life and supports a wide array of human activities[1], including drinking, bathing, cooking, sanitation, agriculture, and industry. Access to clean and sufficient water is not only essential for daily survival but also for economic development and public health. In many parts of the world, especially in developing countries, the challenge of water accessibility is exacerbated by population growth, climate change, pollution, and unequal infrastructure distribution [2]. These issues are particularly pronounced in rural and remote areas where centralized water systems and electricity supply are limited or even non-existent[3]. To fulfill daily water needs, people commonly rely on water pumps to transport water from sources such as rivers, wells, or reservoirs to locations of use [4]. A water pump is a mechanical device that functions by increasing fluid pressure to move water through pipes [5],[6],[7] enabling it to overcome various forms of resistance, including elevation and frictional losses [8].

Most modern pumps are electrically powered, and while this is effective in urban environments with a stable electricity grid, it becomes problematic in areas where electricity is inaccessible or unreliable. The cost of installation and dependence on electrical infrastructure presents significant barriers to rural water access, often leaving communities without practical solutions for basic water supply [9]. In response to this problem, there is a growing interest in exploring alternative, renewable energy-based water pumping systems that are affordable,

environmentally friendly, and independent of the electrical grid. One such solution is the use of water wheels, a time-tested technology that harnesses the kinetic or potential energy of flowing or falling water to perform mechanical work. Historically, water wheels have played an important role in traditional industries such as milling, sawing, and even early electricity generation [10]. Today, their utility can be reimagined to meet modern sustainability needs, particularly for water pumping in off-grid locations. Building upon this concept, the development of PATA Technology (Pompa Air Tenaga Air) represents a significant step toward sustainable water access[11][12]. PATA utilizes a water wheel to drive a mechanical pump, transferring water from lower to higher elevations without relying on electrical energy [12]. This system is especially advantageous in regions where natural water flow is abundant but limited technological infrastructure. By converting the natural motion of water into rotational energy, the water wheel becomes a clean and renewable power source that can meet the daily water needs of remote communities.

Water access in remote, off-grid regions remains a major development challenge, particularly where electricity is limited or unreliable. Although water-wheel-driven pumps present a promising off-grid alternative, earlier studies show significant limitations in efficiency and flow rate. For example, Gunarto et al. (2023) reported an undershot water wheel system with only 16.5% efficiency and a flow rate of 0.32 L/min, insufficient for community needs [13]. Taweewithyakarn and Setthapun (2018) developed a hybrid water pumping system that reached 10–14 L/min flow with 13–14 m head[14]. Poudel et al. (2021) introduced a hydro-powered turbine pump for irrigation, demonstrating better scalability and sustainability [15]. These studies suggest significant untapped potential in water-wheel systems for rural development. The current study addresses this gap through the development of PATA Technology (Pompa Air Tenaga Air), a water-wheel-powered mechanical pump. Designed for areas with abundant natural water flow but lacking electricity, PATA prioritizes simplicity, low cost, and ease of maintenance using local materials.

The implementation of PATA Technology is planned at Pura Beji, located in the Tanah Lot area of Beraban Village, Tabanan Regency, Bali. This sacred temple site is characterized by its abundant water resources in the lowlands and the need to deliver water to higher ground for ritual and communal purposes. This area's natural topography and water availability make it an ideal location for testing and applying a sustainable water-lifting system powered entirely by the environment. Furthermore, by leveraging local resources and simple mechanical principles, this solution promotes community self-sufficiency and resilience in the face of energy-related challenges contrast, the PATA system is designed to be low-cost, mechanically simple, and operable with minimal training. This research study aims to evaluate the mechanical performance and efficiency of the waterwheel-powered pumping system (PATA) installed in Pura Beji. The successful implementation of PATA Technology at Pura Beji could serve as a model for other villages across Indonesia and beyond, especially those situated in hilly or mountainous terrain with access to flowing water. As water scarcity, energy poverty, and climate resilience become increasingly pressing global concerns, locally adapted systems like PATA can offer scalable, replicable, and impactful pathways toward sustainable development.

2. METHODS

This research provides a comprehensive analysis of the effectiveness of water wheels as mechanical drivers for water pumps by thoroughly evaluating the operational performance of a water wheel-powered pumping system. The study focuses on critical technical parameters such as energy transfer efficiency, hydraulic power output, rotational power input, and overall system responsiveness under real-world conditions. A key aspect of this research is to measure and compare the input energy derived from flowing water with the actual volume and pressure of water delivered by the pump, in order to assess the energy efficiency and mechanical viability of the PATA system. Understanding these performance metrics is essential, especially for rural communities where reliable and sustainable access to clean water is vital for daily life. Efficiency in this context does not only refer to mechanical performance but also to the system's ability to function consistently with minimal maintenance and without reliance on electricity. Thus, the findings are expected to inform future implementations of environmentally friendly, off-grid water supply systems in other locations with similar geographical and infrastructural challenges.

The research was conducted at Pura Beji Kangin, located in Banjar Pakedungan, Beraban Village, Kediri District, Tabanan Regency, Bali. This site was selected due to its abundance of natural flowing water in the lowlands and the cultural importance of water in temple rituals and community activities. The research was conducted using quantitative data from various testing phase involved a systematic collection of operational data, including wheel rotation speed, water discharge rate, and head height, among others then analyzed by statistical analysis to show as table and figure. These parameters were carefully measured under varying flow conditions to simulate different environmental scenarios. Additionally, the study incorporates both theoretical modeling and empirical validation to ensure that the outcomes are technically sound and applicable beyond the case study location. By integrating design principles with field experimentation, the research aims to bridge the gap between conceptual engineering and community-level implementation. The interaction between the wheel's mechanical energy and the pump's hydraulic function is at the core of this investigation, as it determines the feasibility of

PATA as a practical solution for decentralized water pumping. Ultimately, this research not only highlights the performance of the system but also contributes to the growing body of knowledge surrounding appropriate technologies for rural water infrastructure. The study's outcomes may serve as a reference for engineers, development planners, and policymakers seeking sustainable, replicable, and low-impact technologies for rural development. A schematic representation of the PATA technology installation is illustrated in Figure 1, providing a visual overview of the system configuration and layout used during field testing.

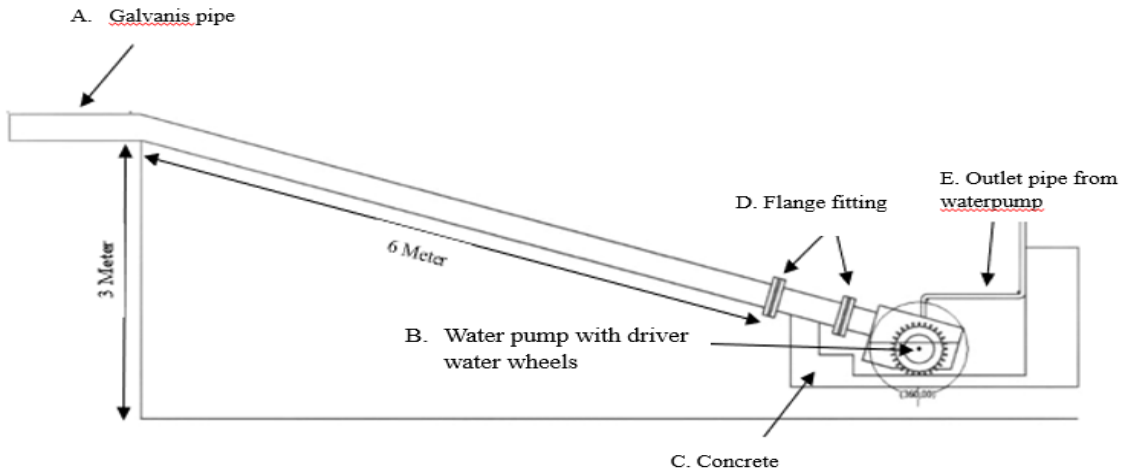

Figure 1. Schematic of water wheels installation against water pump (PATA)

From Figure 1, it can be observed that the water wheel-driven pump system is designed to utilize gravitational water flow as a renewable source of mechanical energy. The system begins with the entry of water through a 3-inch galvanized iron pipe (A), which functions as the intake conduit. This pipe collects water from a source located at a height of approximately 3 meters, enabling a consistent flow with sufficient pressure head to drive the mechanical system. The water exits the pipe with enough velocity to strike the paddles or blades of the water wheel (B), initiating rotational motion. The wheel is directly connected to the water pump via a flange coupling (D), allowing rotational torque to be transferred efficiently to the pump's drive mechanism. As the wheel spins under the force of the falling water, it provides continuous mechanical input to the pump, which begins to draw water from the source and push it through the system. This conversion of gravitational potential energy into mechanical energy forms the core principle behind the PATA (Pompa Air Tenaga Air) system. To maintain structural integrity, the system is firmly supported by a foundation bracket (C), which anchors the pipe and wheel assembly to a fixed base. The bracket is positioned precisely between the two flange fittings (D) to ensure stability and prevent misalignment or vibration during operation. This structural component is crucial for maintaining the correct axis of rotation and minimizing energy loss due to mechanical friction or imbalance. Once the pump is activated, it delivers water through a half-inch PVC pipe (E), which serves as the distribution line. This pipe directs the pumped water to a height of 1.2 meters, supplying it to a nearby fountain or water reservoir.

Despite the relatively modest size of the system, it successfully lifts water against gravity using only the kinetic energy of a naturally flowing stream, without relying on electricity or fossil fuels. This system exemplifies a sustainable water pumping solution for remote or rural areas where conventional energy sources are scarce or unreliable. By leveraging the natural topography and local water availability, it eliminates the need for electric motors and reduces both environmental impact and long-term operational costs. Furthermore, the simplicity of its design makes it easy to install, maintain, and replicate in various settings, from agricultural irrigation to community water supply.

The complete system configuration, including water intake, transmission components, structural support, and water outlet, is illustrated in Figure 2. This diagram provides a clear overview of the mechanical interactions and spatial layout of the PATA technology. The figure also emphasizes the modularity of the system, showing how each part can be adapted or scaled according to site-specific requirements, such as flow rate, lift height, or terrain conditions. In summary, this setup not only demonstrates the practical use of water wheel technology in modern rural engineering applications but also serves as a model for integrating renewable mechanical energy into small-scale infrastructure. It contributes to ongoing efforts in sustainable development, particularly in enhancing access to clean water through locally appropriate and energy-independent solutions.

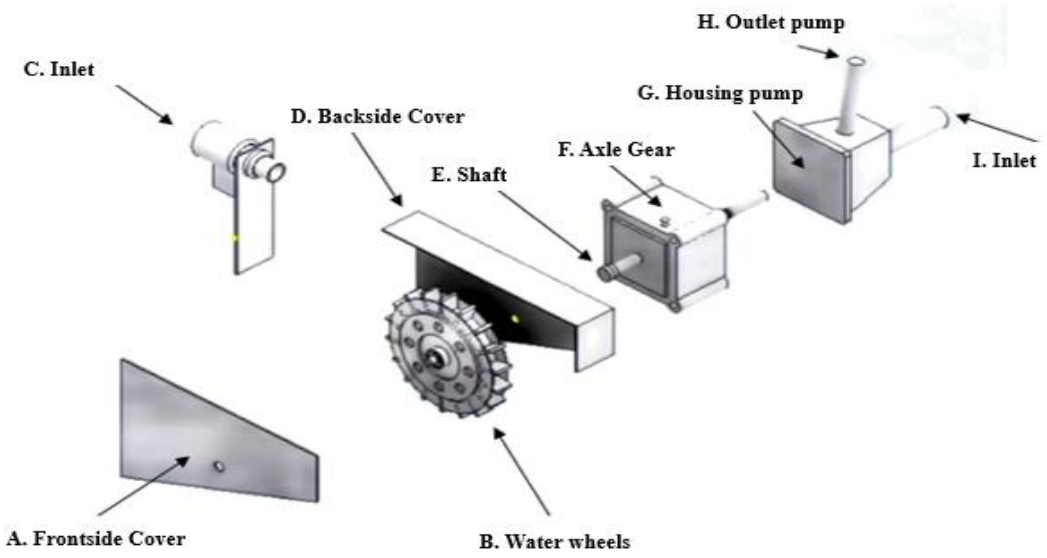

Figure 2. Design configuration devices

From Figure 2, the working principle of the water-powered pumping system can be described as a continuous and integrated mechanical process that begins when water enters through an inlet pipe and is directed toward the inlet nozzle (C), where the flow is concentrated and channeled under gravity and pressure to strike the blades of the water wheel (B). This flow generates torque that causes the wheel to rotate, with the resulting mechanical energy transmitted through a horizontal shaft (E) connected directly to the central hub of the wheel. The rear cover (D) not only serves as a mechanical enclosure protecting internal components from environmental factors and splashing water, but also functions as a bearing support that ensures alignment and reduces friction along the shaft during continuous operation. At the same time, the front cover (A) provides structural support and acts as a water guide, focusing the jet stream efficiently onto the blades to optimize rotation.

The rotational energy generated by the water wheel is then transmitted to a secondary drivetrain in the form of a 2016 Honda Beat axle gear (F), a repurposed motorcycle component that acts as a mechanical gear reducer and speed increaser. This gear assembly plays a crucial role in adjusting the rotational output from the relatively low RPM of the water wheel to a higher RPM more suitable for driving the pump system efficiently. The gear system then drives the Shimizu PC-260 Bit Jet Pump (G), a domestic centrifugal jet pump capable of lifting and pressurizing water for household or agricultural use. Clean water sourced from the Beji spring is drawn into the pump through its suction inlet (I), where it is pulled into the impeller chamber due to the rotational motion generated by the gear system. Once inside, the water is pressurized and discharged through the outlet pipe (H), allowing for vertical or horizontal distribution as needed.

This self-contained, gravity-driven system demonstrates the ability to convert the kinetic energy of naturally flowing water into usable mechanical energy for water pumping applications without requiring external electricity or fuel, making it an ideal solution for remote or off-grid rural environments. The entire setup exemplifies not only the creative integration of locally available components—such as repurposed vehicle parts and standard household pumps—but also the potential for community-scale implementation of sustainable, renewable technology. Furthermore, due to its simple construction and modularity, the system is easy to maintain, repair, and adapt to various flow rates or terrain conditions, offering practical value for rural water management, agricultural irrigation, or community water supply. Its design reflects both functional efficiency and innovative thinking, promoting a model of appropriate technology that bridges traditional mechanical engineering with local resource utilization to achieve energy independence and environmental sustainability.

3. RESULTS AND DISCUSSION

According to research results, the required data has been obtained through experiments and calculation were carried out to obtain the power of the water wheel and pump and the efficiency of the PATA implementation. In the test of waterwheel pump, the pump uses a waterwheel with an overshoot concept, water enters and pushes the blades with an input section with a pipe head height of 3 meters and using 42° inclination angle. The results are shown in the Table 1.

Table 1. Data results of waterwheel input flow rate and water pump output flow rate during running test

No	Date	Flow rate waterwheels, Pin (m^3/s)	Rotation (rpm)	Flow rate Waterpump, Pout (m^3/s)	Remarks
1	Saturday, 26-03-2022	0.0025	456	0.0005	Stable rivers flow
2	Sunday, 27-03-2022	0.0025	442	0.0005	Stable rivers flow
3	Monday,28-03-2022	0.0025	467	0.0005	Stable rivers flow
4	Thursday,14-04-2022	0.0025	451	0.0005	Stable rivers flow
5	Friday, 15-04-2022	0.0028	512	0.0007	Fast rivers flow
6	Friday, 15-04-2022	0.0026	519	0.0007	Fast rivers flow
7	Sunday, 01-05-2022	0.0025	486	0.0005	Stable rivers flow
8	Sunday, 01-05-2022	0.0025	471	0.0005	Stable rivers flow
9	Sunday, 01-05-2022	0.0025	452	0.0005	Stable rivers flow
10	Monday, 02-05-2022	0.0025	493	0.0005	Stable rivers flow

Measurement conducted from morning to afternoon, while keeping remarks on the river's flow condition. Based on the data produced with stable river flow conditions, the results of the discharge on the waterwheels and discharge out on the water pump, as well as rpm, are optimal enough to supply water, especially with fast river flow conditions, causing the discharge and rpm to increase proportionally. Based on the data in Table 1 above, the discharge from the waterwheel and water pump can be compared based on their RPM, which is illustrated in Figure 3.

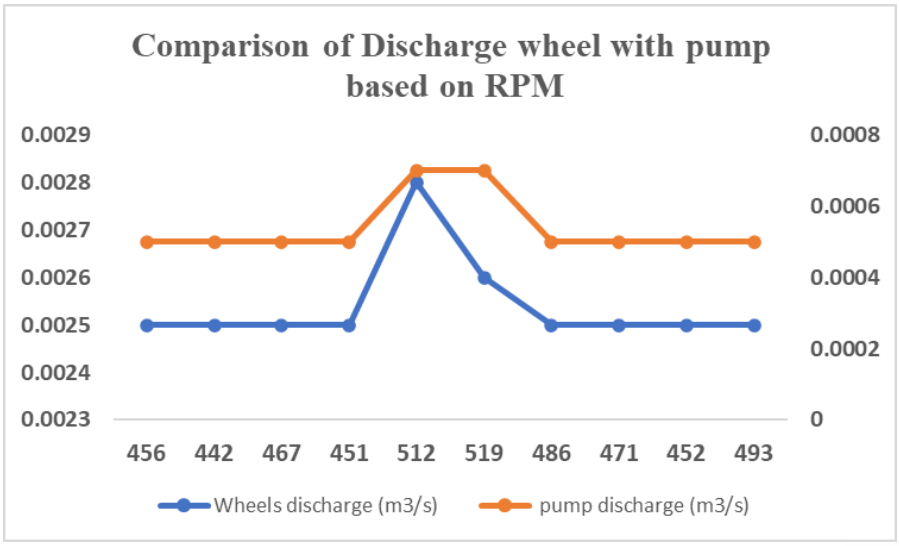

Figure 3. Comparison of the discharge of waterwheels and water pumps

From Figure 3, it can be explained that if the discharge from the water wheels is greater, then the water discharge produced by the pump will also be greater[16],[17]. This is because the water supply to the waterwheel increases its rotational speed[18][19], which in turn affects the suction and discharge power of the pump[20][21], resulting in a higher output[22]. Conversely, a lower water supply leads to a reduced output

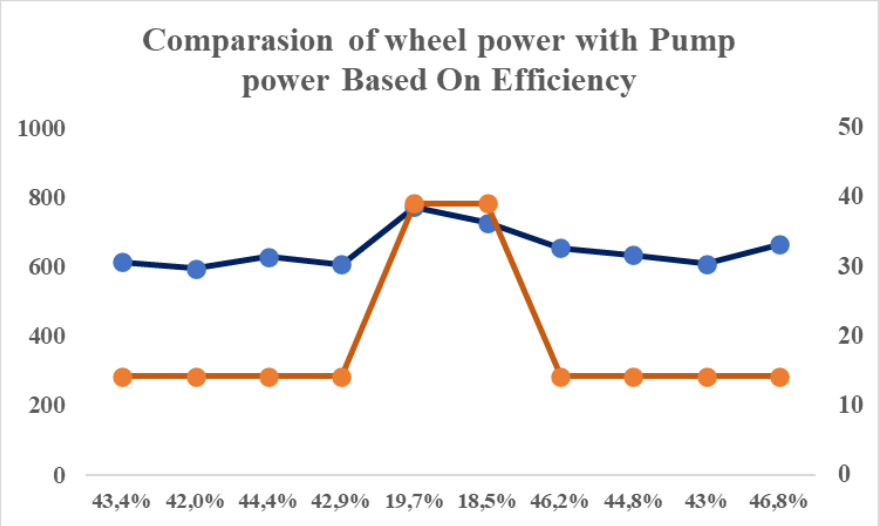

Figure 4. Comparison of power waterwheels and water pumps based on PATA efficiency

The power generated by the water wheel will increase if the height of the pipe inlet is raised above the current height of 3 meters. A higher inlet height will result in greater wheel power, which in turn will increase the water flow produced by the pump[23],[16], [24]. The overall efficiency of the system can also be improved by using materials that are waterproof, temperature-resistant, rustproof, and corrosion-resistant to protect against water leakage, which leads to a reduction in the generated energy[25]. Efficiency is a key aspect of the system, and ensures maximum conversion of running energy from water flow into energy to drive the water pump. Research from Koondhaar (2024) related to waterwheel design obtained an efficiency of 55-69% [12]. From Figure 2, it can be explained that the average efficiency value produced is 40%. Based on the available data results, implementation of PATA technology could be implemented, although the efficiency is less than optimal, which fluctuates based on flow rate and rpm of the waterwheels and pumps. Optimization of efficiency is possible by modifying the number and width of the blades in the water wheel [26]. In addition, if you want to increase efficiency can be done by modifying the nozzle line and waterway canal [26].

3.2. Equations

In processing the data obtained during the research, several equations were applied to analyze hydraulic performance and derive results aligned with the research objectives. The power of the pump was calculated using Equation (1) [24]:

$$P = g \times \rho \times Q \times H \quad (1)$$

Where: P = pump power (W),
g = gravitational acceleration (9.8 m/s²),
ρ = water density (kg/m³),
Q = volumetric flow rate (m³/s),
H = head or height (m).

The flow velocity was determined using Equation (2) [24]:

$$V = \frac{Q}{A} \quad (2)$$

where: V = flow velocity (m/s),
Q = flow rate (m³/s),
A = cross-sectional area of flow (m²).

To estimate the hydraulic power delivered by the flow, Equation (3) [27] was used:

$$Pa = \frac{1}{2}\rho Qv3 \quad (3)$$

where: Pa = available water power (kg/m),
ρ = water density (kg/m³),
Q = flow rate (m³/s),
V = flow velocity (m/s).

For waterwheel torque calculations, the power input from water flow was applied to Equation (4):

$$T = Pin.r^2 \quad (4)$$

where: T = torque (N·m),
Pin = input power to the waterwheel (kg/s),
r = radius of the waterwheel (m).

4. CONCLUSION

The water wheel, in this configuration, serves as the main driving element, converting the linear kinetic energy of water flow into rotational energy through a mechanical linkage. The average power generated by the system through this mechanism is approximately 650 kg·m/s², indicating a significant energy transfer from the water source to the pump. Based on performance analysis, the mass flow rate at the water wheel reaches 75.5 kg/s, while the water pump achieves a discharge mass flow rate of 14.7 kg/s, resulting in an overall system efficiency of 40%. This level of efficiency demonstrates the potential of the system for small-scale water lifting applications, particularly in rural or off-grid environments where access to electricity is limited. The combination of locally available components, simple mechanical design, and respectable performance metrics positions this system as a viable solution for sustainable and low-maintenance water pumping, promoting renewable energy utilization and supporting water resource management in remote areas. In conclusion, the water wheel-powered pump system not only offers a functional and environmentally friendly alternative to conventional electrically powered pumps, but also highlights the practical benefits of adapting mechanical engineering principles with repurposed components for community-scale renewable solutions. Its ease of construction, minimal operational cost, and independence from the electrical grid make it an ideal technology for supporting local water access and advancing energy resilience in developing regions.

5. ACKNOWLEDGEMENT

The authors would like to express their deepest gratitude to the residents surrounding Pura Beji in Braban Village for their invaluable support, hospitality, and cooperation throughout the implementation of this research. Their willingness to engage, assist in field activities, and share local insights played a vital role in facilitating the research process. The openness and enthusiasm of the community not only ensured the smooth installation and testing of the system but also added significant cultural and contextual value to the outcomes of this study. The authors are also profoundly thankful to Politeknik Negeri Bali (PNB) for the unwavering institutional support extended throughout the duration of the project. From the initial proposal development to technical planning, field deployment, data analysis, and eventual publication in JURNAL LOGIC, the institution provided essential resources, facilities, and mentorship that greatly contributed to the academic quality and integrity of this work. The encouragement from the academic leadership, administrative staff, and research supervisors at PNB was instrumental in overcoming challenges and maintaining focus during all phases of the project.

6. REFERENCES

[1] M. F. Chaplin, “Water: its importance to life,” *Biochem. Mol. Biol. Educ.*, vol. 29, no. 2, pp. 54–59, 2001, doi: 10.1111/j.1539-3429.2001.tb00070.x.
[2] A. Bassen, J. E. Drewes, M. Fischer, A.-K. Hornidge, and K. Pittel, *Water in a heated world: The Council Members*, 2024. [Online]. Available: https://www.wbgu.de/de/publikationen/publikation/wasser
[3] D. F. Barnes, R. Van Der Plas, and W. Floor, “Tackling the rural energy problem in developing countries,” *Finance Dev.*, vol. 34, no. 2, pp. 11–15, 1997.
[4] S. I. Yannopoulos et al., “Evolution of water lifting devices (pumps) over the centuries worldwide,” *Water (Switzerland)*, vol. 7, no. 9, pp. 5031–5060, 2015, doi: 10.3390/w7095031.
[5] J. P. Guyer, “Introduction to pumping stations for water supply systems,” *Cont. Educ. Dev.*, vol. 9, no. 877, p. 42, 2012.
[6] A. Emiliawati, “A study of water pump efficiency for household water demand at Lubuklinggau,” *AIP Conf. Proc.*, vol. 1903, no. 1, 2017, doi: 10.1063/1.5011613.
[7] J. B. Evett and C. Liu, Fundamentals of Fluid Mechanics. New York, NY, USA: McGraw-Hill College, 1987.
[8] X. Changxiang, “Pressure energy, resistance and reactance in fluid leak & flow,” *Int. J. Energy Power Eng.*, vol. 5, no. 4, p. 22, 2016, doi: 10.11648/j.ijepe.s.2016050401.13.
[9] D. Trisna et al., *The Challenges of Infrastructure Development in Indonesia*, vol. 1, 2023. [Online]. Available: https://www.bps.go.id/indicator/17/51/1/
[10] P. L. Viollet, “From the water wheel to turbines and hydroelectricity: Technological evolution and revolutions,” *Comptes Rendus Mec.*, vol. 345, no. 8, pp. 570–580, 2017, doi: 10.1016/j.crme.2017.05.016.
[11] R. Salim, “Rancang bangun pompa air dengan tenaga penggerak kincir air,” Diploma thesis, Politeknik Negeri Jember

[12] M. A. Koondhar et al., "Eco-friendly energy from flowing water: A review of floating waterwheel power generation," *IEEE Access*, vol. 12, pp. 90181–90203, 2024, doi: 10.1109/ACCESS.2024.3419019.
[13] Gunarto, D. Irawan, and E. Julianto, "Design and construction of a turbine pump as laboratory scale micro hydro electricity learning media," *J. Sains Teknol.*, vol. 12, no. 2, pp. 415–422, 2023, doi: 10.23887/jstundiksha.v12i2.46065.
[14] T. Taweewithyakarn and W. Setthapun, "Hybrid water pumping system for natural water resources," Res. Mod. Sci. Util. Technol. Innov. J. (RMUTI J.), vol. 11, no. 1, pp. 17–32, 2018.
[15] S. Poudel et al., "Design and analysis of a hydro-powered water turbine pump: A sustainable irrigation infrastructure," *Aqua Water Infrastruct. Ecosyst. Soc.*, vol. 70, no. 8, pp. 1231–1247, 2021, doi: 10.2166/aqua.2021.082.
[16] R. Kuang, Z. Zhang, S. Wang, and X. Chen, "Effect of hub inclination angle on internal and external characteristics of centrifugal pump impellers," *AIP Adv.*, vol. 11, no. 2, 2021, doi: 10.1063/5.0038109.
[17] J. Štigler, "Overshot water wheel efficiency measurements for low heads and low flowrates," *EPJ Web Conf.*, vol. 269, p. 01058, 2022, doi: 10.1051/epjconf/202226901058.
[18] A. Syuriadi et al., "Identifying the influence of blade number and angle of attack on a breastshot type waterwheel micro hydroelectric power generator using ANOVA," *East.-Eur. J. Enterp. Technol.*, vol. 4, no. 8(124), pp. 26–31, 2023, doi: 10.15587/1729-4061.2023.286040.
[19] L. Jasa, I. R. Agung, I. P. Ardana, A. Priyadi, and M. H. Purnomo, "An experimental to investigate the effect of nozzle angle and position of water turbine for obtaining highest rotation," Transport, vol. 1, no. 2, p. 3, 2013.
[20] Syafriyudin, B. Fajar, S. H. Winoto, and M. Facta, "Early analysis of jumping water effect on breastshot waterwheel for microhydro power plant," *J. Phys. Conf. Ser.*, vol. 953, no. 1, 2018, doi: 10.1088/1742-6596/953/1/012039.
[21] Kamalkant and J. Sinha, "Development and testing of a spiral tube water wheel pumping system," *J. Soil Water Conserv.*, vol. 20, no. 4, pp. 455–461, 2021, doi: 10.5958/2455-7145.2021.00057.6.
[22] H. L. Liu et al., "Investigation on performance in water jet pump under turning conditions," *Adv. Mech. Eng.*, vol. 13, no. 12, pp. 1–12, 2021, doi: 10.1177/16878140211067329.
[23] R. K. Tyagi, "The effect of an angle on the impact and flow quantity on output power of an impulse water wheel model," *J. Energy South. Afr.*, vol. 26, no. 3, pp. 100–104, 2015, doi: 10.17159/2413-3051/2015/v26i3a2146.
[24] A. Muliawan and A. Yani, "Analysis of power and efficiency of kinetic water turbine due to changes in runner rotation," *Sainstek J. Sains Teknol.*, vol. 8, no. 1, p. 1, 2017, doi: 10.31958/js.v8i1.434.
[25] D. R. Carruthers, P. Carruthers, and R. Wade, "A new, more efficient waterwheel design for very-low-head hydropower schemes," *Proc. Inst. Civ. Eng. Civ. Eng.*, vol. 171, no. 3, pp. 129–134, 2018, doi: 10.1680/jcien.17.00051.
[26] A. R. S. Pohan, D. Mugisidi, Z. Nurfadillah, and O. Heriyani, "Comparative analysis of waterwheel efficiency using nozzle and open canal on waterway," *SINTEK J. Ilm. Tek. Mesin*, vol. 17, no. 2, p. 143, 2023, doi: 10.24853/sintek.17.2.143-150.
[27] M. Darwis, "Analysis of the effect of valve opening on water turbine performance," *Knowl. J. Inov. Has. Penelit. Pengemb.*, vol. 3, no. 4, pp. 365–376, 2024, doi: 10.51878/knowledge.v3i4.2672.